Scuola di Dottorato di Ricerca
High Mechanics and Automotive Design And Technology
(Meccanica Avanzata e Tecnica del Veicolo)
XXV Ciclo

Experimental and analytical investigation of downdraft stratified gasifiers

Tutore scientifico
Chiar.mo Prof. Ing. Paolo Tartarini
Co-Tutore scientifico
Dott. Ing. Alberto Muscio
Coordinatore della scuola di dottorato
Chiar.mo Prof. Ing. Paolo Tartarini

Candidato
Dott. Ing. Giulio Allesina

Università degli Studi di Modena e Reggio Emilia
Anno Accademico 2011-2012

'Yake-ato nani yara saite iru'

[There
where the fire was
something is blooming]
T.Santoka

Sommario in lingua italiana

La ricerca scientifica mirata allo sviluppo e valutazione di soluzioni innovative nel campo delle biomasse destinate alla produzione di energia, ha assunto ormai un ruolo cardine nello scenario energetico mondiale. Di fatto, il costante aumento della domanda di energia primaria, cosí come il suo costo, sta portando alla creazione di complesse strategie di sviluppo ed incentivazione sia a livello nazionale sia internazionale. Questo lavoro di tesi nasce con lo scopo di analizzare l'impiego di biomasse legnose all'interno di gassificatori downdraft stratificati per la produzione di energia elettrica. Anzitutto sono state confrontate le diverse tecnologie attualmente adottate per la conversione in energia di biomasse ligno-cellulosiche. Definiti i parametri fondamentali per l'individuazione di un punto di ottimo, sono stati presentati i vantaggi termodinamici legati all'adozione di gassificatori, indicandone i principi di funzionamento e ponendo particolare attenzione ai reattori a letto fisso di tipo downdraft stratificati. Sono stati studiati ed instrumentati reattori di diversa taglia, dal lab-scale all'impianto industriale, al fine di acquisirne i principali parametri termo-chimici. Diverse metodologie di misura sono state adottate in funzione della taglia del reattore e della sua destinazione d'uso. I gassificatori cosí analizzati sono stati modellati matematicamente seguendo diversi approcci: dai bilanci energetici e di massa fino a modelli di cinetica chimica. Durante la campagna sperimentale é stata posta particolare attenzione nello sviluppo di metodi di analisi del contento di catrami e della composizione del gas tramite metodi basati sulla calorimetria. Scalando le equazioni utilizzate per la modellazione dei reattori é stato possibile individuarne un aspetto peculiare: il diametro del gassificatore non é considerato parametro influente sulle performance del reattore. Questo risultato é in contrasto con quanto ottenuto sperimentalmente, pertanto si é posta l'attenzione su questo aspetto, permettendo di distinguere cause reologiche e termodinamiche che intervengono nel processo di scala. I risultati ottenuti in questo lavoro hanno evidenziato la capacitá di questi reattori di essere impiegati in una molteplicitá di situazioni, anche ove altri gassificatori hanno evidenti limiti operativi. I vantaggi e gli svantaggi legati alla tecnologia studiata sono stati esposti e discussi, presentando infine alcune soluzioni innovative per l'impiego di questi reattori, specie per l'utilizzo di gassificatori di piccola taglia.

Contents

Chapter 1

Introduction

1.1 Abstract

Research on the utilization of biomasses for energy purposes is playing a key role for the assessment and the development of new solutions for the world energy scenario. In fact, the demand and price of primary energy are constantly increasing, along with the development of new national and international strategies providing incentives and development policies for renewable technologies. This work aims to investigate the biomass gasification in downdraft stratified reactors used for energy production. First, in Chapter 2 different solutions for the production of electrical energy starting from woodsy biomasses are discussed, pointing out the major parameters involved in the pursuit of an optimal solution. Then, the technologies and principles of gasification are explained focusing on downdraft stratified reactors. Different reactors are analyzed. Chapters 2-4 investigate full-scale power-plant, while the next chapters examine pilot scale and lab-scale stratified gasifiers. The main thermochemical parameters have been acquired adopting different methods and instruments depending on the reactor scale and ultimate aim. The reactors are modeled using different approaches: from energy and mass balances to kinetic chemical modeling. During the experimental campaigns, particular attention was paid to the development of innovative approaches for tar content evaluation and gas composition calculation, reported here in Chapters 5 and 6. The scaling of the equations set used in the stratified reactors modeling highlights a distinctive feature of this approach: the diameter of the gasifier seems to have no influence on the reactor performance, despite experimental data acquired during this work provided different results. For this reason, in Chapter 8 the influence of the diameter on the behavior of the gasifiers is investigated and its correlation with thermal and rheological parameters is discussed. Results show the capability of these reactors to be used under several operating conditions, even where other gasifiers have running difficulties. Advantages and disadvantages of this technology are discussed, some new solutions for downdraft reactors are proposed, with an emphasis on micro-scale application reported in Chapter 7.

1.2 From biomasses to energy

There are two possible ways to convert biomasses into energy or a suitable fuel for power generation: thermal conversion or biochemical conversion. The first group includes di-

rect combustion, pyrolysis and gasification; the second group is composed of anaerobic digestion, fermentation and trans-esterification for biogas, bio-ethanol or bio-diesel production respectively. This thesis is focused on the gasification. Only Chapter 7 considers the biodiesel production as integration of the on-field exploitation of oleaginous culture. The thermal conversion group consist of a group of processes where the heat is the key for biomass degradation, conversion and combustion. Depending on the desired effect on biomass the thermochemical process are dived in:

- Torrefaction: torrefaction is considered a pre-treatment process more than a biomass to energy conversion. Its main goal is to improve different characteristics of the processed biomass. Through torrefaction it is possible to increase the energy density (gravimetric heating value), chemical stability and hydrophobicity [1, 2].
- Pyrolysis: pyrolysis transforms biomass into gaseous and liquid compounds, the process can be obtained directly with under-stoichiometric combustion of biomass or indirectly if the heat is supplied externally instead of being generated from partial combustion of the fuel. The process temperatures are commonly set between 400 and 800^o C [3, 4]. The Pyrolysis process can be divided into different branches depending on velocities and temperatures, like slow, fast or flash pyrolysis [5]. The products of the pyrolysis can be directly sent to an engine or used as basis for bio-fuel production. Pyrolysis is also a fundamental part of the gasification process.
- Gasification: gasification is a thermal process that occurs at peak temperatures between 800-1000^o C. The gasification process is dived into different phases such as drying, pyrolysis, combustion and reduction [6]. The sequence of these phases depends on the reactor design. The gas produced through gasification can be used as engine fuel [7], for synthesis of more complex fuels [8, 9] or burned in order to produce high temperature heat.
- Combustion: the main product of biomass combustion is heat, in this process the biomass is completely oxidized. Biomass combustion is commonly used for heating, i.e. in stoves, boilers and district heating plants; but it can also be used for power generation in external combustion engine.

This thesis is focused on biomass gasification. Combustion has been considered in Chapter 2 as comparison in order to define and discuss the proper approach to biomass power plant design.

1.3 Gasification

As introduced in the previous section, gasification is a thermochemical process that allows the conversion of a solid fuel into an energy vector. The process takes place tanks to high temperatures (over 700^o C) and the presence of a gaseous medium that can cause partial oxidation of the solid fuel or can be used for biomass bed and gas moving only. Depending on the reactor typology and scale, the most used mediums are: nitrogen, air, oxygen, steam or carbon dioxide [8]. The solid fuel can be coal, various types of wood biomasses or waste. This thesis focuses on the gasification of wood biomasses like wood chips, wood blocks or by-products of wood industries (i.e. sawdust, cherry pits). The gas created through gasification has been named depending on gasifier fuel (carbon, coke or

biomass), design and period of construction: syngas, water gas, blue gas or producer gas [10, 11, 7]. Depending on the process used to produce the gas, its composition can change, and the gas heating value ranges from 4 to 14 MJ/Nm^3 [8, 12, 9].

When air is used as a gasification agent (air-blown gasifiers), gasifiers fed with biomass produce a gas with a heating value of 4-5 MJ/Nm^3 [6, 9], and the gas is always composed of CO, H_2, CO_2, CH_4, N_2 and H_2O. Usually a kilogram of wood is converted with air gasification into 2-3 cubic meters of gas [3].

The first attempt to use this gas for power generation was done in 1881, because the engine was drawing the gas from the gasifier, the gas was called 'suction gas' [13, 8] and the gasifier, linked to the rear of a car was called 'modern portable gas-producer'. It is odd how old the 'energy resources issue' is: the article 'The modern portable gas-producer', where the studies previously mentioned are reported, has been published in the 1939. It begins with: [Proven oil reserves are sufficient to meet the 1935 consumption for the next 35 years]. Fortunately the paper was wrong, nevertheless the research on renewable energy and fuel resources was carried on during all these years, with more strength in periods where the energy costs where increasing, like the Second World War, the '73 oil crisis and nowadays [14].

The commercial spread of gasifiers has been limited during all these years by several causes: the low price of other fuels, and the complexity of these systems never justified mass production, moreover gasifiers have the main issue of tar production. Tar, together with char, is one of the by-products of gasification; Chapters 2, 5 discussed how the tar content affects the gasification efficiency and how it can make engine applications became incompatible.

1.3.1 Gasification reactions

Unlike the complete combustion of biomasses, where all the carbon and the hydrogen is oxidized to carbon dioxide and water, gasification is based on incomplete combustion reactions and reduction processes [15]. In auto thermal gasification (where the heat is supplied by partial combustion of the fuel) only part of the solid fuel undergoes complete oxidation. Both the reactions ruling the complete and incomplete combustion of carbon are exothermic:

$$C + O_2 = CO_2 + 393kJ/mol \tag{1.3.1}$$

$$C + 1/2O_2 = CO + 123.1kJ/mol \tag{1.3.2}$$

The main equations of gasification are the water-gas 1.3.3 and the Bodouard 1.3.4, both these equations are endothermic and occur between a gaseous component (carbon dioxide or vapor) and the carbon content in the biomass:

$$C + H_2O = CO + H_2 - 118.5kJ/mol \tag{1.3.3}$$

$$C + CO_2 = 2CO - 159.9kJ/mol \tag{1.3.4}$$

Other equations that occur in the reduction zone are the water shift (1.3.5) and the methanisation (1.3.6):

$$CO_2 + H_2 = CO + H_2O - 40.9kJ/mol \tag{1.3.5}$$

$$C + 2H_2 = CH_4 + 87.5kJ/mol \tag{1.3.6}$$

Moreover, there are equations that need to be controlled because they can negatively affect the performance of the reactor, in fact the following equations consume part of the gas components responsible for the heating value of syngas:

$$CO + 1/2O_2 = CO_2 + 283.9kJ/mol \tag{1.3.7}$$

$$H_2 + 1/2O_2 = H_2O + 285.9kJ/mol \tag{1.3.8}$$

1.3.2 Gasification parameters

Cold gas efficiency

The first parameter used for gasifier performance monitoring is the gasifier efficiency, it is used for technical and economic feasibility of a gasifier system.

$$\eta_{g,cold} = \frac{\text{chemical energy of gas}}{\text{chemical energy content in the biomass}} = \frac{\dot{V}_g HHV_g}{\dot{m}_{bio} HHV_{bio}} \tag{1.3.9}$$

It represents the amount of energy converted into gaseous fuel divided by the chemical energy content of the biomass. In literature, there are many works that use the gasifier efficiency as the main parameter for reactor monitoring [16, 7, 6, 17, 18]. In this thesis, the gasifier efficiency has been discussed in different Chapters 2, 3, 4 as monitoring parameter; while, in Chapter 5, a set of equations define the gasification efficiency as a function of the tar content in the produced gas.

Equivalence Ratio

The second parameter that classifies the auto-thermal gasifiers is the equivalence ratio, ER, here indicated as ϕ_{bio} is defined as the ratio between the actual fuel/air ratio to the stoichiometric fuel/air ratio [9, 19].

$$\phi_{bio} = \frac{\text{oxygen used}}{\text{oxygen necessary for complete combustion}} \tag{1.3.10}$$

Literature reviews show that, depending on the gasifier, ϕ_{bio} normally range from 0.2 to 0.35. Higher equivalence ratio result in lower concentrations of H_2 and CO, decreasing the heating value of the gas. Lower equivalence ratio brings to higher tar content [6, 9, 20, 21, 8]. The ER of the reactors analyzed in this thesis have been set to 0.3 as suggested by [6].

Superficial Velocity and Hearth Load

Superficial velocity or hearth load is the ratio between the gas volumetric flow rate and the cross section area. In literature it is possible to find a different definition that uses the biomass consumption rate instead of the gas flow rate [7].

$$SV = \frac{\text{Gas Production Rate}}{\text{Cross Sectional Area}} = \frac{\frac{m^3}{s}}{m^2} = m/s \tag{1.3.11}$$

It is the function of the gas flow and the geometric properties of the gasifier. It is representative of the rate at which air, then gas, passes through the reactor [22, 6, 7]. A

low SV means slow pyrolysis and high charcoal and tar production. On the other hand, high SV causes very fast pyrolysis, low heating gas and few char production [23, 24].

Tar and particulate content

As previously reported, gasifiers have two major by products (tars and char). The amount of these products need to be monitored because the higher the tar content, the less energy is converted into gas, moreover the high tar content does not allow the use of the produced syngas with IC engines or gas turbines [25]. Hasler and Nussbaumer in 1999 proposed the results reported in Table 1.1 about the different tar and particulate content in fixed and fluidized bed gasifiers:

Table 1.1: Gas quality of raw producer gas from atmospheric, air blown biomass gasifiers [26]

Component	Unit	Fixed-bed co-current	Fixed-bed countercurrent	CFB gasifier
Fuel moisture	%mf	6-25	Nd	13-20
Particles	mg/Nm^3	100-8000	100-3000	8000-100000
Tar	mg/Nm^3	10-6000	10000-150000	2000-30000

Depending on the application, there are maximum levels of tar and particulate content that need to be taken into account, some of these limits are summarized in Table 1.2. To exceed these value means endangering the system operating with raw syngas.

Table 1.2: Gas quality limits [25]

Component	Unit	IC Engines	Gas Turbine	Methanol synthesis
Particles	mg/Nm^3	< 50	< 30	< 0.02
Particle size	μm	< 10	< 5	/
Tar	mg/Nm^3	< 100	/	< 0.1

1.3.3 Gas cleaning

Tar control in gasification systems is obtained by adopting primary and/or secondary methods [20]. Primary methods are all the thermal or catalytic treatments that occur inside the reactor, while the hot gas cleaning processes belongs to the secondary methods. There are cases in which it is easier and cheaper to produce a tar rich gas, proceeding then with thermal or catalytic tar cracking [20, 27, 12]. If the tar content is not too high, but it exceeds the limit for a specific application, the easier solution consists of gas cleaning processes. The first step for hot gas cleaning process is to force the gas to pass into one or more cyclones. The cyclones separate the dust and char from the gas but, in order to avoid local condensation, it is fundamental to keep the cyclones as close as possible to the reactor. Moreover, in some cases it is necessary to cover the cyclones with insulating material or heating tapes [7, 10, 28]. If the syngas speed is not too high and the particles size is over 1 μm, it is possible to use gravitational methods, such as sedimentation tanks instead of cyclone separators. These separators occupy a higher volume and are not highly efficient, for this reason they are not common in industrial power plants [29].

The 'dry methods' discussed above are only able to separate solid particles with a defined size. For tar and small particle separation it is possible to use electrostatic filters or a scrubber working with water or oil [8, 30]. Some gasifiers use bio-filters with the main advantage of gasificability of the filtering bed material once it needs to be changed, but on the other hand there are many issues related with these filters: the gas temperature needs to be controlled in order to prevent biofilter pyrolysis, moreover the filtering effectiveness change sduring the life span of the filtering bed [31, 32, 33]. A complete review of the filtering matter can be found in [34, 30].

1.4 Gasifier classification

The gasifier reactors can be classified following different methods, the gasification agent and heat source, reactor design, purpose of the produced gas and reactors scale:

1.4.1 Gasification agent and heat source

- Air-blown gasifiers: air as a gasification agent presents two major advantages: it is costless and constantly available. It usually generates a gas with low energy content and the reactors work with temperatures around 800-1000 ^{o} C [8, 12, 6, 35, 36]. This technology is commonly coupled with fixed bed gasifiers in order to create simple units, but in literature bubbling or fluidized bed gasifiers using air as well can be found [37, 38, 39].
- Oxygen gasifiers: gasifiers operating with pure oxygen produce a gas with a heating value higher than the air-blown one, in fact it can reach 12-25 MJ/Nm^3 [40, 6, 35, 9]. Oxygen is highly reactive and is able to process, through high temperature gasification, a wide range of materials. Oxygen-blown gasifiers were also used for pure carbon monoxide production from coke [41]. The CO and hydrogen content in an oxygen blown gasifier can reach the 90% [35]. There are cases of study where it is sufficient to add oxygen to air in order to increase the gasifier performance [42, 43, 44].
- Steam gasifiers: this process creates a rich gas but the reactions that take place are strongly endothermic. On the other hand it doesn't need an oxygen generator that is complex and energy consuming. Before entering the reactor, water passes through a steam generator that consist basically in a pressurized boiler [9, 35, 45, 46]. Due to the costs and the characteristics of the produced gas, steam gasification is used for synthesis of methanol and other chemicals [47, 48, 49]

Differences in terms of heating values of the gas produced by gasification with various mediums are reported in Table 1.3.

Table 1.3: Heating Values for Product Gas Based on Gasifying Medium [9]

Medium	Heating Value (MJ/Nm^3)
Air	4 - 7
Steam	10 -18
Oxygen	12 - 28

1. Auto-thermal (direct) gasifiers: in auto thermal gasifiers, somewhere in the reaction bed, the heat necessary for the whole system section is produced, according to [8] the heat can be obtained by:
   (a) Combustion of part of the produced gas and vapors
   (b) Combustion of produced char
   (c) Combustion of part of the feed material
2. Allo-thermal (indirect) gasifiers: the heat is supplied externally, it can be produced by the external combustion of the matters reported in the auto-thermal section [50, 51] or by heating tapes, heat pipes or heated gases that pass through the biomass bed [52]. Some gasifiers, fluid bed in particular the start-up/warm-up period is obtained by allo-thermal heating through heating tapes or heated gas [53, 54].

1.4.2 Reactor design

The reactor design influences the gasification process. There are three major types of gasifiers: fixed (moving) bed, fluid (fluidized) bed and entrained flow (not taken into account in this thesis).

- Fixed bed: also called moving bed, these gasifiers have been developed in many different designs and sizes, most of them are used to gasify coal waste or biomasses with particle size medium-big like wood chips, wood blocks, nut shells, corn cobs, wood pellet or briquettes [6, 7]. In these gasifiers biomass flows from top to the bottom where it is discharged as char and ashes. In literature fixed bed reactors are classified as a function of the direction of gas flow:
  - Updraft gasifiers: are considered the simplest type of gasifiers [8], biomass enter from the top while the air intake is situated at the bottom of the reactor, this solution creates a distribution of different layers as reported in Figure 1.1. This reactor is simple and has been built in many size, from small power plant [55] to many MW plants [56, 57, 58, 59]. The fuel is dried using the sensible heat of the gas flowing up in the reactor, this creates a syngas with low temperature but high tar and moisture content (up to 60% wb). The amount of tar and moisture in the produced gas makes this reactor more suitable for heat production instead of power, but in literature it is possible to find few plants working with updraft gasifier coupled with a robust gas cleaning apparatus [60, 61].
  - Downdraft gasifiers: in these reactors air and biomass flow in the same direction, depending on geometry and air intake position, these reactors can be further subdivided into:
    * Single and double throat gasifiers: these gasifiers became common during WWII for automotive applications, the Imbert industries were so famous that now many manuals and articles refer to this type of gasifier as Imbert [62, 63, 64]. This reactor has the air intake situated in an intermediate height, below the throat as sketched in Figure 1.1. The throat is the core feature of these gasifiers, it accelerate the flow, increasing the hearth load and creates a uniform combustion zone. Increasing the dimension of the

reactor means higher air speed and a higher number of nozzles necessary to create a combustion zone uniform enough. The same concept can be applied to the reduction of bed material size, the smaller the fuel size the harder it is for air to spread properly inside the biomass bed. For this reason reactors designed to operate with small fuels have a narrow throat and a long cone with high slope in order to prevent bed bridging [65], but different manuals in literature advise against this reactor design for sawdust or fine fuel processing [66, 67, 6, 35].

* Open core: these reactors represent the main topic discussed in this thesis. The open core reactor tries, with design simplification, to reduce the problem related to fuel size limitations reported in the Imbert gasifiers discussion. This gasifier, known also as 'open top' is basically a cylindrical reactor, air and biomass enter from the top and uniformly move down to the bottom, where char and ashes are discharged and syngas is drawn. Because all the biomass particles move uniformly down, the reactor presents a stratification of the different zones, therefore these reactors are also known as 'downdraft stratified'. Because the air enters from the top is less of the stoichiometric amount required for complete combustion of the fuel, the flame that is created in the top layer of the gasifier (sometimes covered by a drying zone) is called 'flaming pyrolysis'. This zone generates the major part of the gases of the gasification process, these gases are then forced to pass in the char reduction zone, where volatile tars can be cracked and CO_2 and H_2O gases can be reduced thanks to the superficial reaction of high temperature char. The gasification reactions subtract sensible heat to the gases, and continue until the temperature is too low (about 600 ^{o} C) then it stops. The rest of the gasifier is composed of inert char that wait to be discharged form the bottom of the reactor. This zone acts as a buffer for reactions and temperature fluctuations in the zones above. This reactor design presents different advantages if compared with the Imbert:

  1. The stratified reactor is more simple than the Imbert one, there are no nozzles or throats.
  2. The open top is a perfect point for measurements and monitoring of the reactor. Imbert gasifiers, when working in depression (because gas is drawn from the bottom) needs to be properly sealed in order to prevent combustion zone rising.
  3. This reactor is more flexible to fuel size variations

  On the other hand there are many disadvantages that have limited the spread of this kind of reactor, some of them are investigated in Chapter 8.

Because in all the downdraft gasifier the pyrolysis zone is situated before the oxidation one (in the stratified reactor the two zones coexist in the flaming pyrolysis one), the tar content is lower as reported in Table 1.4. This feature makes downdraft gasifiers more suitable for engine applications. On the other hand, the proximity of the combustion zone to the gas exit in the single or double throat gasifiers creates a gas with more particles and high temperature.

– Crossdraft gasifiers: these gasifiers were first designed for charcoal gasification, they can operate in a very small scale but they have different high-temperature-

related issues. If a good quality charcoal is used, small gasifiers can be suitable for micro-power production due to the clean gas produced that needa a cyclone and a packed filter only [68, 69, 70].

A comparison between different fixed bed gasifiers is reported in Table 1.4, while design differences are reported in Figure 1.1 .

Table 1.4: Comparison between fixed bed gasifiers [8]

Parameter	Downdraft	Updraft	Crossdraft (charcoal)	Open top
Fuel moisture (% wb)	12 (max 25)	43 (max 60)	10-20	7-15
Fuel ash content (% db)	0.5 (max 6)	1.4 (max 25)	0.5-1.0	1-2 (max 20)
Fuel size (mm)	20-100	5-100	5-20	1-5
Gas exit temperature (^{o}C)	700	200-400	1250	250-500
Tars (g/Nm^3)	0.015-0.5	30-150	0.01-0.1	2-10

- Fluid bed gasifiers: the development of fluid bed gasifiers starts from the discussion of fixed (moving) bed gasifiers limits [8, 71]:

  1. Fuels with high ash content may create slags due to hot spots inside the reactor
  2. Bridging and channeling phenomena of the biomass in the reactor
  3. Scale-up limitations
  4. Not suitable for small size biomasses

  To overcome these limitations the fluid bed gasifiers were imported from coal gasification to biomass applications [72, 35]. The gasification agent is blown from the bottom through a bed of solid particles at a sufficient velocity to keep them in a state of partial (bubbling bed) or total suspension (circulating fluidized bed). The reactor is prepared by filling it with sand and then pre-heated. In this way, when the biomass is introduced it can mix really fast with the heated bed material. Heat is transferred quickly with high efficiency from the bed material to the biomass. The bed material can be chosen looking at its thermal and catalytic properties, increasing the gasification efficiency [73, 74, 75]. Due to the heat transfer efficiency, this gasifiers result compact with a uniform temperature distribution in the reactor, on the other hand the reactors are complex, the tar and the particulate content in the gas is pretty high [71, 76]. A comparison between fluid bed gasifiers design is reported in Figure 1.2, differences between fluid bed and fixed bed are reported in Table 1.5. In this thesis a bubbling bed gasifier is used for tar measurements in Chapter 6, the rest of the thesis focuses on downdraft fixed bed gasifiers.

Table 1.5: Comparison between fixed bed and fluid bed gasifiers [8]

Parameter	Downdraft	Updraft	Bubbling bed	Circulating bed
T (^{o}C)	700-1200	700-900	< 900	< 900
Tars	low	high	moderate	moderate
Control	easy	very easy	moderate	moderate
Scale (MW$_{th}$)	< 5	< 20	10-100	>20

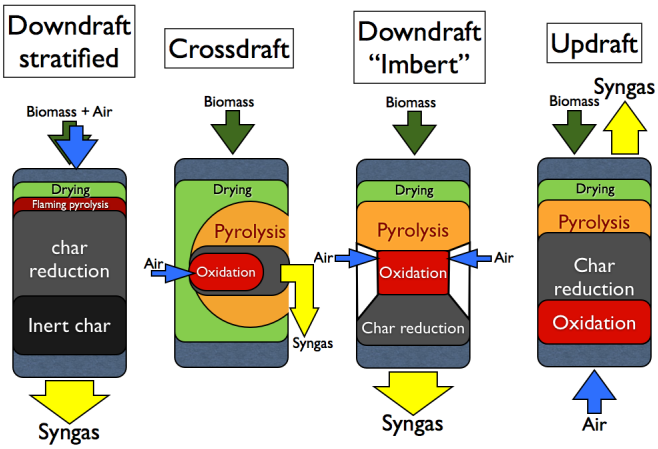

Figure 1.1: Fixed bed gasifiers

1.4.3 Gas purpose

Continuing with the classifications proposed by Knoef [8, 12], the gasifiers can be classified depending on the gas purpose. The syngas can be used for heat production i.e. in a furnace or used as engine fuel for power production. It is important to underline that there are some external combustion power systems that make this classification difficult to set properly.

- Heat gasifiers: if the main purpose of the produced gas consists in high temperature heat generation, nevertheless the reactor scale, there are different rules that need to be followed: the gas cleaning process is not necessary whenever a perfectly clean combustion is required. In fact, the tar content on the syngas may affect positively the heating value of the gaseous fuel. The heat produced by syngas combustion can be used for district heating or industrial process [77, 78, 79]. In Chapter 5 a calorimetric approach to gas analysis is proposed and differences between clean and raw gas combustion are discussed.

- Power gasifiers: the power production through gasification can be obtained in different ways, first of all the gas can be burnt in an IC engine, in literature it is possible to find a great number of studies, starting from Swedish experience [10, 7] to recent applications in high performance engines [80, 81, 82, 83]. Syngas can also be used as fuel in gas turbines, but the gas needs to be considerably clean for these applications [84, 85, 86]. In recent years, the market has proposed several applications of gasifiers designed to generate heat coupled with external combustion engines. For large scale use these engines basically are steam turbines, but for medium and small applications ORC power plant are a good solution [87, 88]. Other external combustion systems are the EFGT (external fired gas turbine) [84, 89] and the Stirling engines [90, 91, 55]. These external combustion systems hardly reach high level of energy conversion efficiency, but they are characterized by the major advantage of simple gas cleaning process and, most of the time, they require less maintenance when compared with gasifier-IC engine systems [92, 93].

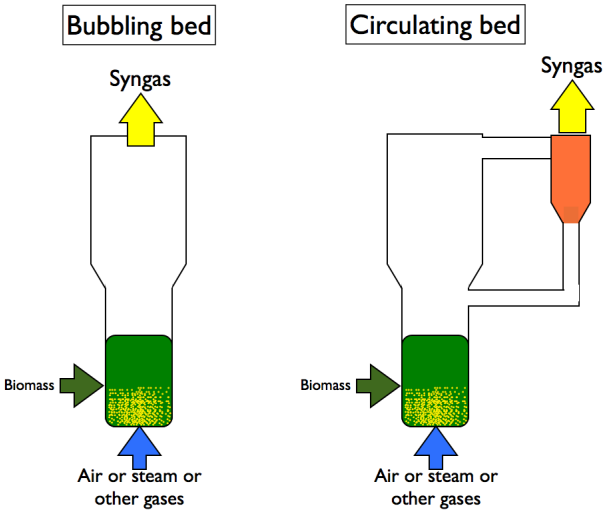

Figure 1.2: Fluid (fluidized) bed gasifiers

- Chemicals synthesis plant: coal, coke and biomass gasifiers are used for methanol synthesis since the first researche on gasification [94, 95]. The CO and H_2 in the syngas are the basic bricks for complex molecules synthesis, moreover, the recent successes in catalytic design for cracking a synthesis is leading to the biomass-to-liquid and biofuels concepts. The main goal is to create synthetic fuels or fuel components similar or compatible to those of current fossil-derived [96, 97, 98].

In this thesis the gasifiers studied are used for engine applications, except for Chapter 7 where an innovative method for biodiesel production through biomass to methanol synthesis is proposed and discussed.

1.4.4 Reactor scale

- Large and medium scale gasifiers: these plants were first designed for coal gasification [99, 6], during the last decades different attempts to design or convert big installation for power production were made [100, 101, 102, 103]. The power is generated with a steam ranking cycle or a gas turbine for large application, in some cases the presence of a second fuel for co-firing is reported [12, 104]. installation with power output of about 1-5 MW can work with IC engines [105, 106, 107, 108] or ORC turbines [109, 110, 111].

- Small and micro scale gasifiers: once market and research abandoned the industrial production of micro-scale gasifiers for automotive design, the focus seemed to move to large scale plants [8]. Recent years, with the increasing in fossil fuel cost and increasing energy demand even in underdeveloped countries, the development of simple reactors with a power output of about 10-50 kW has been increasing [33, 112, 113, 114, 115, 116]. Small fluidize or bubbling bed reactor are used mostly for research purposes [117, 118, 119]. Power output of 100-500 kW present very different reactor designs and engines, from fixed bed to fluid bed, working with engines, Stirling or ORC.

- Lab scale gasifiers: for the comprehension of kinetics, the effect of different parameters on gasification outputs and effectiveness of hypothesis for reactor design, it is possible to use lab scale gasifiers where there is optimum control on the process [120, 121]. It is fundamental to understand the limits of this approach, were the down-scaling effect is ruled by equations and hypothesis [122, 123, 22].

1.5 Gasifier modeling

Modeling and design guidelines for gasifiers of every type and size have been developed during the years working on two different approaches: the technical and the research one. This distinction is not always true, but it is necessary to understand the two major forces that have pushed the development of more refined models and design guidelines: On one hand there is basic research, since the first studies on gasifiers, chemists, physicists and engineers have investigated the gasification phenomena developing equations and models for there comprehension [35, 10, 6, 124, 125, 126, 127]. On the other hand, many studies have been carried out in order to guarantee the adequate performance of gasifier plants during the design and planning operations. These power plants represent a big investment: it is necessary to properly set all the supply chain and ensure an annual number of hours high enough to justify the initial investment. These necessities result in a series of technical report, hints and models for the proper design of a power plant [128, 129, 130].

In literature it is possible to find several works about gasification models. Because the great number of reactor typologies and variations it is possible to find specific models on a particular gasifier, fixed bed or fluid bed, or genetical models that tries to predict the behavior of a type or group of gasifiers [65, 131, 132, 133, 134, 135, 136].

There are also commercial models or features of chemical engineering software like ASPENplus [137, 138, 139]. This software was only used in this work for biodiesel modeling in Chapter 7. Moreover in the gasifiers models it is important to distinguish models that treat only a part of the reactor, such as char reduction [140, 141, 142, 143] or pyrolysis [144, 145, 146], or models that investigates the fluid dynamic of reactors and the multiphase flow in fluidized and bubble bed gasifiers [147, 148, 149, 150].

1.5.1 Downdraft stratified reactor modeling

Many works can be found in literature about the mathematical modeling of gasifiers, but stratified open core downdraft gasifiers raise less interest if compared to other reactors, this lack of interest has resulted in fewer works published on chemical and thermal modeling about this configuration. The first author that needs to be cited is Thomas Reed. He represents the major landmark for stratified reactors, during his work different models have been developed [125, 126, 120]. These models proposed are 'black box' approach to gasification modeling. Other equilibrium models are the Altafini at all model proposed in 2003 [151]. A very effective model, that takes into account the kinetic of reduction reactions, is proposed by Wang and Kinoshita [124]. This model is able to predict the char reduction zone using a kinetic approach where reactions between char particles surfaces and gas are modeled. More complex models for char reduction have beed proposed by Chen, [152, 153]. His model is divided into two part with the main goal of creating a tool for gasification zone design. Other char reduction models, focused on stratified reactors are [140, 143]. More complex works are the equilibrium model proposed by Di Blasi [133, 154].

In this thesis both black box and kinetic modeling approaches are reported: the work discussed in Chapter 4 is based on literature review as a basis for the development of a model that couples the two approaches previously proposed in order to give an analytical explanation of the channeling phenomenon in large stratified gasifiers.

Chapter 2

Comparison between gasification and combustion for industrial power production

As introduced in Chapter 1, gasification is only one of the many technologies available for thermochemical conversion of lignocellulosic biomasses [3], but since the first industrial applications [8], many research institutes and industries have considered gasification as one of the most promising technologies of the market. This Chapter discusses on a scientific basis the process behind the choice and consumption calculation for these kind of power plants. The equations reported here can be scaled for any size of plant, they are useful for anyone that wants to evaluate the annual biomass consumption variation changing the conversion technology.

This work is based on energy balances and efficiency variations for different solutions proposed, during the development of the equations necessary for energy balances, a relation between heat of combustion of clean and raw gas (uncleaned syngas) was necessary. For this reason equation 2.1.5 has been defined. The same equation has been used as a basis for what is reported in Chapter 5, where the equation has been developed in order to set a calorimetric analysis of gasifier reactors.

In the introduction the gasification advantages, if compared with combustion, have been thoroughly discussed, [6, 8, 12, 9]. They can be summed up as follows: the gaseous product of the process can be burned resulting in high temperature gases, these temperatures increase the Carnot efficiency of the process chosen for heat conversion. This advantage, together with heat recovery form the exhaust gases at the end of heat conversion system, can balance part of the losses of characteristic of the gasification process: part of the chemical energy of the biomass is not converted in syngas, because it is left as charcoal and tars or lost in the partial combustion of the biomass [155, 9]. Moreover, gasification produces less NO_x than biomass combustion. Even in the case of high char disposal, there would be some advantages, this carbon, if it is not burned in a second stage of the reactor [8], can be considered sequestered from the carbon cycle. As previously discussed in the introduction, if this carbon has particular properties can be considered biochar [156, 157].

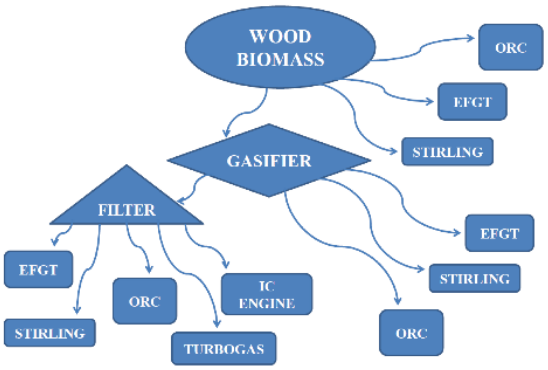

Figure 2.1: Synoptic scheme of wood to energy conversions

2.1 Electrical energy production through gasification or combustion: an energy based comparison

Different technologies for energy production can be compared: The first technology here proposed for wood biomass conversion into a suitable energy vector is gasification [6]. Gasification can efficiently convert a solid fuel into syngas that can be burned in internal and external thermal engines [6, 7]. An internal combustion (IC) engine can not be coupled with the gasifier if the syngas is not adequately cleaned [6, 7]. However, this filtering process decreases the heating value of the syngas due to the reduction of its tar content. For this purpose a downdraft gasifier is the best choice due to the low tar and oil content in the produced syngas [6, 7]. Moreover, the cold gas efficiency of the gasification process is about 75% [158], because part of the chemical energy of the biomass is lost due to reactor thermal dispersions or is disposed as char and tar. The direct combustion also avoids problems related to the char and tar disposal from the gasification plant. The thermal energy obtained in such a way will be easily exploited in an ORC plant, in an external firing gas turbine, in a Stirling engine, in a turbogas plant [159, 160, 161, 162]. In an Organic Rankine Cycle (ORC), heat is supplied externally to a closed cycle, the cycle uses organic siloxanes as working fluid, which operates between lower temperature heat sources if compared with the conventional steam Rankine cycle [159]. A modified version of the Brayton cycle is the external firing gas turbine (EFGT), which expands a hot air flow that is heated in a radiant boiler [160]. The Stirling engine is an external combustion reciprocating engine with a higher ideal thermodynamic efficiency; however, thermal and mechanical losses decrease its performance [161]. On the other hand, Stirling engines require less maintenance if compared to internal combustion engines [162]. In this Chapter, various scenarios have been analyzed in order to identify the best plant solutions for the energetic use of wood biomass. One of the first topics addressed was the gasification: this technology is needed in plants that work only with syngas, such as IC engines with diesel cycle or turbogas. Different scenarios of a hypothetical 250 kWel power plant have been evaluated from the synoptic depicted in Fig. 2.1 In this scheme, solutions that can use both raw biomass and synthesis gas, such as the ORC turbines or Stirling engines, have been considered.

A comparison with experimental data of an IC engine - downdraft gasifier plant of 250 kWel is also reported in order to estimate the difference between calculated and experimen-

tal input and output flows. In order to make this comparison, beside the bibliographical study of the involved technologies, some analysis were carried out on different wood biomass and on the waste products from the gasification process.

2.1.1 Modeling

Gasification modeling

This section describes the mathematics of the gasifier system in terms of annual biomass and waste production. The annual biomass consumption and the annual waste mass products have been calculated in two different operation modes depending on the presence or not of the gas cleaning process. In the clean gas operation, imposing a constant gasifier cold efficiency "$\eta_{gas,clean}$", clean syngas higher heating value $HHV_{syngas,clean}$, biomass higher heating value HHV_{bio}, char to wood mass ratio x_{char} and tar to wood mass ratio x_{tar}, the annual biomass consumption as well as the annual char and tar productions have been calculated by the following equation:

$$m_{bio} = \frac{HHV_{syngas,clean} V_{syngas}}{\eta_{gas,clean} HHV_{bio}} \tag{2.1.1}$$

Equation (2.1.1) defines the annual amount of biomass (m_{bio}) consumed through gasification. This equation is derived from the gasification efficiency as reported in [7] as function of the annual gas flow amount V_{syngas}.

$$m_{char} = m_{bio} x_{char} \tag{2.1.2}$$

Equation (2.1.2) defines the mass of char produced as function of the biomass consumed and the char to wood ratio. For fixed operating conditions, this ratio is constant and is a characteristic of a specific gasifier.

$$m_{tar} = m_{bio} x_{tar} \tag{2.1.3}$$

Equation (2.1.3) defines the mass of tar produced as function of the biomass consumed and the tar to wood ratio. The tar is separated from the gas stream through gas cleaning process, because in the raw gas the tar is diluted in the gas stream. This can be considered a fixed parameter, characteristic of a specific reactor.

In the untreated gas operation, the syngas can be sent directly to a burner without cleaning it in order to increase its high heating value, moreover this solution, decreases the plant complexity and no tar production needs to be considered. In this case the following equations for the gasifier modeling have been adopted:

$$m_{bio} = \frac{HHV_{syngas,raw} V_{syngas}}{\eta_{gas,raw} HHV_{bio}} \tag{2.1.4}$$

Equation (2.1.4) is similar to 2.1.1 and defines the biomass consumed for raw gas production through unfiltered gasification.

$$HHV_{syngas,raw} = HHV_{syngas,clean} + \frac{x_{tar} m_{bio} HHV_{tar}}{\eta_{gas,clean} HHV_{bio}} \tag{2.1.5}$$

Equation (2.1.5) had been created in order to define the heating value of the raw gas as function of the gasifier and tar properties. The major assumption behind this formula

is that the tar is a suspension of particles in the gas stream, tar does not increase the gas volumetric flow but only affects its heating value. A more accurate discussion of this approach can be found in Chapter5.

$$\eta_{syngas,raw} = \eta_{syngas,clean} \frac{HHV_{syngas,raw}}{HHV_{syngas,cleaned}} \tag{2.1.6}$$

Equation 2.1.4 can be reversed in order to obtain a formulation of the cold raw gas efficiency as reported in eq 2.1.6.

$$m_{char,rawgas} = m_{char,cleangas} = m_{bio} x_{char} \tag{2.1.7}$$

Because the raw or clean gas production only changes the end use of tars, equation (2.1.7) underline that the char production remains the same in the two cases.

ORC, EFGT and Stirling engines modeling

The mathematical modeling of these systems depends only on the fuel used and the efficiencies of the different parts that compose any of the power generation methods here proposed. All the system here described use the heat coming from the combustion of syngas or biomass.

In case the heat is supplied externally burning the untreated syngas, the annual volume of syngas has been calculated as follows:

$$V_{raw-syngas,ORC} = \frac{3.6 P_{el} t_{work}}{HHV_{raw-syngas} \eta_{ORCcycle} \eta_{ORC,sb} \eta_{alt}} \tag{2.1.8}$$

$$V_{raw-syngas,EFGT} = \frac{3.6 P_{el} t_{work}}{HHV_{raw-syngas} \eta_{EFGTcycle} \eta_{EFGT,sb} \eta_{alt}} \tag{2.1.9}$$

$$V_{raw-syngas,Stirling} = \frac{3.6 P_{el} t_{work}}{HHV_{raw-syngas} \eta_{Stirlingcycle} \eta_{Stirling,sb} \eta_{alt}} \tag{2.1.10}$$

In the case of clean syngas combustion, the annual volume of syngas necessary is equal to:

$$V_{clean-syngas,ORC} = \frac{3.6 P_{el} t_{work}}{HHV_{clean-syngas} \eta_{ORCcycle} \eta_{ORC,sb} \eta_{alt}} \tag{2.1.11}$$

$$V_{clean-syngas,EFGT} = \frac{3.6 P_{el} t_{work}}{HHV_{clean-syngas} \eta_{EFGTcycle} \eta_{EFGT,sb} \eta_{alt}} \tag{2.1.12}$$

$$V_{clean-syngas,Stirling} = \frac{3.6 P_{el} t_{work}}{HHV_{clean-syngas} \eta_{Stirlingcycle} \eta_{Stirling,sb} \eta_{alt}} \tag{2.1.13}$$

In the above cases, the annual biomass consumption is estimated from the gasification model through equations 2.1.1 and 2.1.4 respectively. In case of direct combustion of biomass in a boiler coupled with one of the mentioned machines, the biomass consumption is calculated by:

$$m_{bio,ORC} = \frac{3.6 P_{el} t_{work}}{HHV_{bio} \eta_{ORCcycle} \eta_{ORC,bb} \eta_{alt}} \tag{2.1.14}$$

$$m_{bio,EFGT} = \frac{3.6 P_{el} t_{work}}{HHV_{bio} \eta_{EFGTcycle} \eta_{EFGT,bb} \eta_{alt}} \tag{2.1.15}$$

$$m_{bio,Stirling} = \frac{3.6 P_{el} t_{work}}{HHV_{bio} \eta_{Stirlingcycle} \eta_{Stirling,bb} \eta_{alt}} \tag{2.1.16}$$

IC engine and gas turbine modeling

The IC engines and the gas turbine operate with clean syngas only. Tars and particulate wear these engines hampering their operativity for long periods without maintenance. The annual volume of syngas has been calculated by Eq. 2.1.17 and 2.1.18 and the biomass annual consumption can be estimated from the "clean gas gasification model" (2.1.1).

$$V_{clean-syngas,IC} = \frac{3.6 P_{el} t_{work}}{HHV_{clean-syngas} \eta_{ICengine} \eta_{alt}} \tag{2.1.17}$$

$$V_{clean-syngas,GT} = \frac{3.6 P_{el} t_{work}}{HHV_{clean-syngas} \eta_{GTcycle} \eta_{alt}} \tag{2.1.18}$$

2.1.2 Results

Power plants scenarios comparison

Tab. 2.8 summarizes the biomass consumption, the char and tar productions and the electrical efficiency of the hypothetical energy plants over a year long of operating. The electrical efficiency has been evaluated as follows:

$$\eta_{el} = \frac{3.6 P_{el} t_{work}}{HHV_{bio} m_{bio}} \tag{2.1.19}$$

The IC engine plant working with clean syngas has the best calculated efficiency, as can be seen in fig 2.2. The annual biomass consumption is minimum due to the good efficiency of the engine compared with the other technologies. However, the disposal or reutilization in a different way of the yield tar and char is required. Moreover, this plant set-up needs more maintenance when compared with the other solutions proposed. The second best solution, in terms of electrical energy efficiency and back calculated biomass consumption, is the gas turbine plant working with clean syngas. In this case the maintenance operations are less than the IC engine solution but the disposal or reutilization of tar and char is needed as well.

Going through the ranking reported in Table 2.8, the next solution in terms of biomass consumption is the EFGT working with untreated syngas. This technology has a good efficiency, and the tar doesn't need to be disposed or reutilized because it is consumed with the syngas in the EFGT burner. This feature may leads to filter accurately the exhaust gas because tar combustion can lead to high particulate content in the exhaust gases, the cost of this process may increases the maintenance and the capital cost of the plant. All the solutions with the biomass burner instead of the syngas one have low efficiencies and the polluting emissions of these set-ups have to be reduced with an accurate and expensive filtering system. Stirling and ORC plants have a lower total efficiency if compared to the other set-ups, this is due to the low efficiencies of these engines. However, the maintenance costs of this technologies are lower than the IC engine when the clean syngas is used.

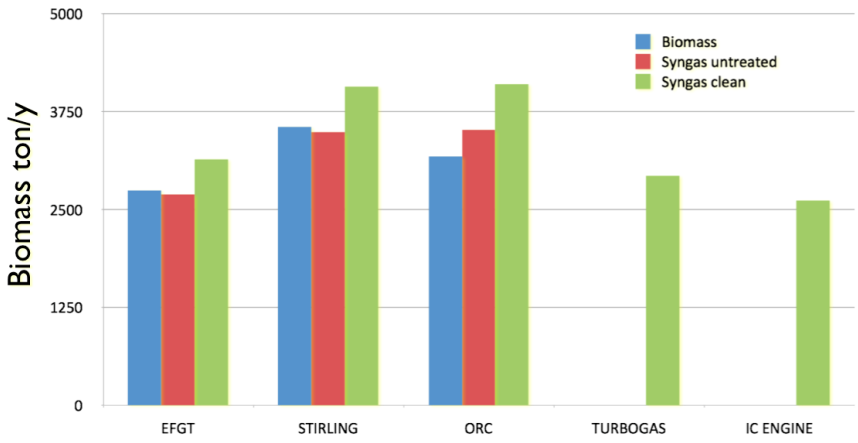

Figure 2.2: Annual biomass consumption differences between conversion technologies

Table 2.1: General Parameters

Electrical Power	P_{el}	250kW
Working hours	t_{work}	800 h/year
Alternator efficiency [10]	η_{alt}	0.96

Case study

A specific case analysis related to an experimental plant is described in this sub-section. The analyzed power plant experimental campaign is thoroughly discussed in Chapter 3 and consists of a stratified downdraft gasifier designed to produce $800kW_{th}$, which is fed with poplar wood chips; two diesel engines, able to produce up to $125kW_{el}$ each, connected to the gasifier and a cylindrical dryer, which dries the biomass using the exhaust and the cooling air of the engines. Before reaching the engines, the syngas is cleaned passing through a cyclone, a water scrubber and an electrostatic filter. The engines need 8 l/hours of diesel oil to ensure the ignition of the whole fuel mixture; this fuel fraction can be switched from diesel to vegetable oil after a start-up period. The gasifier is affected by an excessive production of tar and charcoal, that is hardly ever removed during the gas cleaning process. Even after a complex cleaning processes, like the one described above, a small part of the tar passes the filters and goes into the engines fouling the compressor, the valves, the combustion chambers and the turbines. This phenomenon decreases the durability of the engines and imposes frequent shutdowns of the plant to permit for the cleaning operations. The goal of the present analysis is to replace the IC engine with another technologies with good performance and less sensitivity to the tar amount suspended in the syngas. Table 2.9 resumes results related to hypothetical plant modifications. The EFGT system working with untreated gas is a good solution in terms of energy efficiency and maintenance costs. This solution permits to eliminate the water scrubber and the electrostatic filter, but a more efficient exhaust gas filtering is needed to reduce the environmental impact. Furthermore the disposal of the tar is not required, leading to economical advantages.

Table 2.2: Gasifier Parameters

Wet poplar wood chips HHV [11]	HHV_{bio}	17.7 MJ/kg
Clean gas HHV [3]	$HHV_{syngas,clean}$	5 MJ/Nm^3
Char to wood ratio [12]	x_{char}	0.10
Char HHV [11]	HHV_{char}	34.4 MJ/kg
Tar to wood ratio [12]	x_{tar}	0.01
Tar HHV [11]	HHV_{tar}	38.8 MJ/kg
Cold gas efficiency [5]	$\eta_{gas,clean}$	0.75

Table 2.3: ORC Parameters

ORC syngas burner efficiency [13]	$\eta_{ORC,sb}$	0.9
ORC biomass burner efficiency [10]	$\eta_{ORC,bb}$	0.85
ORC cycle efficiency with syngas [6,10]	$\eta_{ORCcycle,sb}$	0.198
ORC cycle efficiency with wood biomass [6,10]	$\eta_{ORCcycle,bb}$	0.178

2.2 Summary

This chapter discussed a simple energy-based model useful for the prediction of real consumption of a power plant. Different technologies were taken into account, in order to choose the most suitable one. The methods proposed here permited to calculate the annual biomass consumption, the tar and char annual productions and the electrical efficiency starting from the HHV of the biomass, the electrical nominal power output and the annual working hours. EFGT, ORC, Stirling, gas turbine and IC engine were considered. IC engine plant working with clean syngas produced by gasification has the best electrical efficiency, that reaches the 20%. Another system with good electrical energy efficiency is the gas turbine one (η_{el} =18%). Furthermore the solution with the EFGT working with untreated syngas has a interesting efficiency, especially in those power plant where the excessive production of tar prevents the possibility of installing more efficient solutions. Moreover the model has been applied to an experimental gasifier-IC engine system affected by an excessive production of tar and charcoal. The goal of the analysis is to find the best plant modification in terms of electrical efficiency and system maintenance. The results show a good advantage to replace the IC engine with an EFGT because the efficiency of the whole system is similar and there are no issues of tar disposal. The choice of the power plant set-up is driven by energetic, economic and environmental evaluations. This Chapter gives a simplified method focused on the energetic approach, a specific economical and environmental analysis are needed in order to find the most suitable solution. The next chapters will discuss in more detail, the experimental analysis of a gasifier power plant (Chapter 3) and more complex models for the gasification process (Chapter 4).

Table 2.4: Stirling Parameters

Stirling syngas burner efficiency [13]	$\eta_{ST,sb}$	0.9
Stirling biomass burner efficiency [14]	$\eta_{ST,bb}$	0.68
Stirling cycle efficiency [13]	$\eta_{STcycle}$	0.20

Table 2.5: EFGT Parameters

EFGT syngas burner efficiency [13]	$\eta_{EFGT,sb}$	0.9
EFGT biomass burner efficiency [14]	$\eta_{EFGT,bb}$	0.68
EFGT cycle efficiency [14]	$\eta_{EFGTcycle}$	0.259

Table 2.6: Gas Turbine Parameters

Gas turbine cycle efficiency [9]	$\eta_{GTcycle}$	0.25

Table 2.7: IC Engine Parameters

IC engine cycle efficiency [9]	$\eta_{ICcycle}$	0.28

Table 2.8: Comparison based on Design Values

Plant typology	Required biomass [10^3 kg/year]	Produced char [10^3 kg/year]	Produced tar [10^3 kg/year]	Total electrical efficiency %
ORC with biomass burner	2785	-	-	14.6
ORC with gasifier and clean syngas clean	3164	316.4	31.64	12.9
ORC with gasifier and untreated syngas	3074	307.4	-	13.2
STIRLING with biomass burner	3116	-	-	13
STIRLING with gasifier and clean syngas	3139	313.9	31.39	12.9
STIRLING with gasifier and untreated syngas	3050	305.0	-	13.3
EFGT with biomass burner	2406	-	-	16.9
EFGT with gasifier and clean syngas	2424	242.4	24.24	16.8
EFGT with gasifier and untreated syngas	2355	235.5	-	17.3
GAS TURBINE with gasifier and clean syngas	2260	226	22.6	18
IC ENGINE with gasifier and clean syngas	2018	201.8	20.18	20.2

Table 2.9: Comparison between model predictions and modified "design plants"

Plant typology	Required biomass [10^3 kg/year]	Produced char [10^3 kg/year]	Produced tar [10^3 kg/year]	Total electrical efficiency %
IC ENGINE* with gasifier* and clean syngas*	2018	201.8	20.18	20.2
IC ENGINE** with gasifier** and clean syngas**	2618[!]	390	155.4	17.7
ORC* with gasifier**and clean syngas**	4106	546.1	266.9	11.3
ORC* with gasifier** and untreated syngas*	3520	468.2	-	13.2
STIRLING* with gasifier** and clean syngas**	4073	541.7	264.7	11.4
STIRLING* with gasifier** and untreated syngas**	3492	464.4	-	13.3
EFGT* with gasifier** and clean syngas*	3145	418.3	204.4	14.8
EFGT* with gasifier** and untreated syngas*	2696	358.6	-	17.2
GAS TURBINE* with gasifier** and clean syngas**	2933	390.1	190.6	15.8
GAS TURBINE with gasifier and clean syngas	2260	226	22.6	18
IC ENGINE with gasifier and clean syngas	2018	201.8	20.18	20.2

Legend: * = model calculation; **=experimental data; $HHV^{**}biomass$= 15.5 MJ/kg; $HHV^{**}_{syngas,clean}$ = 3,5 MJ/Nm^3; x_{char} = 0.133; HHV_{char} = 17,7 MJ/kg; x_{tar} = 0.065; HHV_{tar} = 26,2 MJ/kg; $\eta_{gas,clean}$ = 0.66. Note: in the the [!] experimental plant about 8,67% of the thermal power of combustion in given by diesel oil (55.29 10^3kg/year) with HHV_{diesel}= 42 MJ/kg [163] to ensure a good combustion in the engine chambers. The biomass requirement in the Table is the sum of the biomass consumption (2392 10^3 kg/year) with the equivalent biomass consumption (2392 10^3kg/year) calculated by the following equation:

$$m_{bio,eq} = \frac{m_{diesel} HHV_{diesel}}{HHV^{**}_{bio} \eta^{**}_{gas,clean}} \tag{2.1.20}$$

Chapter 3

Gasification power plants experimental analysis

Chapter 2 introduced the advantages of gasification for power production, but also outlined how the decrease of gasifier efficiency, together with some issues related to the power plant can nullify the advantages previously discussed. For these reasons it is vital to monitor how the power plants run in order to keep efficiency, tar and char disposal under control. Some problems occurs when the power plant monitored has not been designed for a complete acquisition of the necessary thermochemical parameters. Especially for medium or large scale plants, every hour of plant stoppage is paid in terms of loss of earnings. For this reason the experimental campaign needs to be carried out when the plant is operational, without interfering with the routine operations if possible. Moreover, the larger the plant the higher the inertia of the whole system, this forces an adoption of investigation methods that take into account this peculiarity. In this chapter a possible approach for monitoring a $250kW_{el}$ power plant is discussed.

3.0.1 A 250 kW_{el} downdraft stratified gasifier experimental analysis

The plant here investigated consists of a stratified downdraft gasifier coupled with two diesel IC engines. As previously discussed in Chapter 2, these engines require a tar-free gas that avoids fouling problems in the compressor, valves, combustion chambers and turbine. For this purpose a downdraft gasifier is the best choice due to the low tar content in its syngas [6]. The stratified gasifier represents the simplest design for a downdraft reactor. It consists in a refractory cylinder with no nozzles and no reduction of diameters. Both air and wood fuel enter from the open top and pass through different zones of reaction as illustrated in Figure 3.1. Several researchers [7, 127, 125, 126, 120, 140, 164] suggest different approaches to the stratified downdraft gasifier modeling. A simple model of the process has been set up starting from energy balances as reported by [7]. The model implemented here is based on energy and mass balance equations and it is able to predict some of the thermochemical variables measured in situ. The analyzed power plant is depicted in Fig. 3.2 and consists of a stratified downdraft gasifier designed to produce up to 800 kW_{th}, which is fed with poplar woodchips. Two diesel engines connected to the gasifier produce up to 125 kW_{el} each. A cylindrical dryer is used to process the biomass using the exhaust and the cooling air of the engines. Before reaching the engines, the syngas is cleaned by passing through a cyclone, a water scrubber and an electrostatic

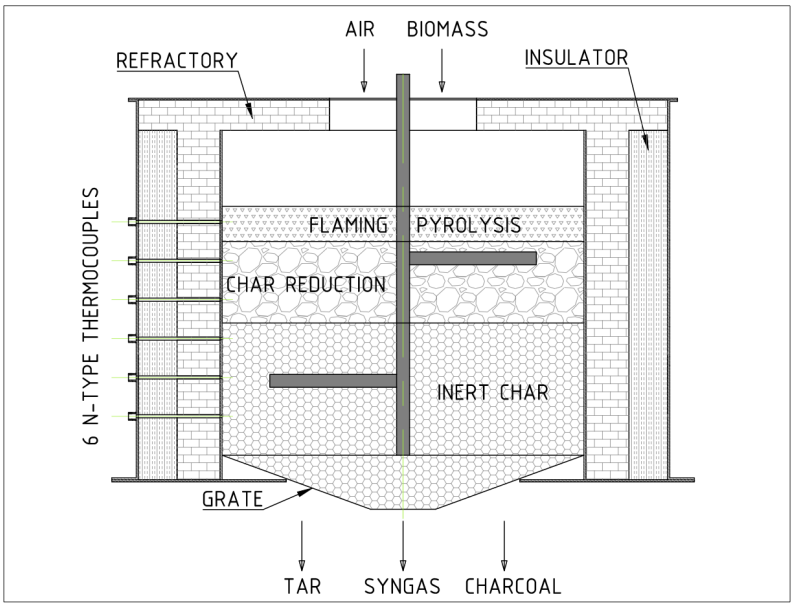

Figure 3.1: Throatless (stratified) downdraft reactor

filter. The engines need 4 to 8 l/h of diesel oil each to ensure the ignition of the whole fuel mixture. This fuel fraction can be switched from diesel to vegetable oil after a start-up period. The gasifier is affected by an excessive production of tar and charcoal; these are removed during the gas purifying process. Even after the cleaning phases described above, some tars pass through the filters and go into the engines. This phenomenon decreases the durability of the engines and causes the frequent shutdowns of the plant, this imposes the cleaning operations to take place. In order to investigate the overproduction of tar, the first step taken was to measure the thermochemical variables of the process. The efficiency of the gasifier was calculated via experimental analysis for an electrical power output set point of 200 kW_{el} and the experimental variables were compared with the output of the model. The obtained results were used to find better operating conditions related to low tar production and as the basis for future reactor design improvements. Some data (i.e. biomass consumption) was calculated in different ways, such as model prediction, experimental reading and mass balance equation. Differences between these values are being used for validating the effectiveness of the experimental procedures, outlining the parameters that need to be acquired in an alternative way.

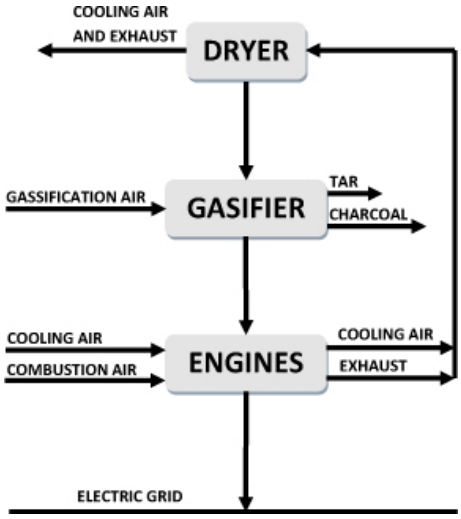

Figure 3.2: Power plant scheme

3.0.2 Energy and mass balance

Power generation unit model

This section describes the mathematics of the internal combustion engines connected to the alternators to produce electrical energy. The thermal power going into the engines is calculated by Eq. 3.0.1:

$$\dot{Q}_{eng} = \frac{P_{el}}{\eta_{eng}\eta_{alt}} \tag{3.0.1}$$

The engines are supplied by the syngas and by the diesel oil. The thermal power generated by the syngas combustion is given by Eq.3.0.2 and the thermal power generated by the diesel oil combustion is given by 3.0.3.

$$\dot{Q}_{syngas} = \dot{Q}_{eng} - \dot{Q}_{oil} \tag{3.0.2}$$

$$\dot{Q}_{oil} = \dot{m}_{oil} HHV_{oil} \tag{3.0.3}$$

The syngas volumetric flow rate and the diesel oil mass flow rate are calculated using their higher heat of combustion as follows:

$$\dot{V}_{syngas} = \frac{\dot{Q}_{syngas}}{HHV_{syngas}} \tag{3.0.4}$$

$$\dot{m}_{oil} = \rho_{oil}\dot{V}_{oil} \tag{3.0.5}$$

Moreover, the air and fuel mixture flow rate going into the engines is calculated as follows [7]:

$$\dot{V}_{engine} = \frac{NVn}{120} \tag{3.0.6}$$

The volumetric efficiency of the engines can be obtained combining Eq.3.0.4 and 3.0.7. The air flow rate to the engines are calculated by Eq.3.0.8.

$$\dot{V}_{syngas} = \frac{\dot{V}_{engine}\eta_v ol}{1+\phi_{eng}} - \dot{V}_{oil} \tag{3.0.7}$$

$$\dot{V}_{air,engine} = (\dot{V}_{oil} + \dot{V}_{syngas})\phi_{eng} \tag{3.0.8}$$

Table 3.1 reports the design parameters of the power generation unit.

Table 3.1: Power Plant Parameters

DESCRIPTION	SYMBOL	VALUE
Number of engines	N	2
Displacement	V_{eng}	0.0129 m^3
Nominal rpm	n	1 500 rpm
Air to fuel ratio	ϕ_{eng}	1.10
Nominal volumetric efficiency	η_{vol}	1.11
Maximum electrical power	P_{max}	320 kW
Nominal electrical power	P_{nom}	250 kW
Engines nominal efficiency	η_{eng}	29.4%
Alternator efficiency	η_{alt}	0.95
Diesel oil higher heat of combustion [163]	HHV_{oil}	42 MJ/Nm^3
Diesel oil density [163]	ρ_{oil}	830 kg/m3
Diesel oil volumetric flow rate	$\dot{V}_{oil}$	8 l/hour

3.0.3 Gasifier Model

The biomass rate of consumption is calculated as follows:

$$\dot{m}_{bio} = \frac{\dot{Q}_{syngas}}{\eta_{gas} HHV bio \phi_{eng}} \tag{3.0.9}$$

The higher heating value of biomass is calculated by the following equation, which takes the biomass moisture content into account [165]:

$$HHV_{bio} = HHV_{bio,dry}(1-\theta_{bio}) - r_{water}\theta_{bio} \tag{3.0.10}$$

An ultimate analysis of the biomass, reported in Table 3.2, was used to obtain the HHV_{bio}, dry by the following equation as reported in [166]:

$$HHV_{bio,dry} = 0.3491C + 1.1783H + 1.005S - 0.1034O - 0.0151N - 0.0211A \tag{3.0.11}$$

where C, H, S, O, N and A are the weight fraction of carbon, hydrogen, sulfur, oxygen, nitrogen and ash respectively.

The mass flow rate of the air entering the gasifier reactor is given by Eq. 3.0.12, as derived in [6] and [7]:

$$\dot{m}_{air,gas} = m_{st}\dot{m}_{bio}\phi_{bio} \tag{3.0.12}$$

Table 3.2: Biomass ultimate analysis

ELEMENT	C	H	S	O	N	A
Weight fraction%	47.7	6.07	0.00	42.48	0.60	2.75

For these kind of reactors, the mass of charcoal can be assumed to be equal to 10% of the entering biomass [6, 7] and the tar production in this kind of gasifier can be calculated assuming that 0.002 kg of tars are yielded for each Nm^3 of syngas generated [6, 7]. Poplar wood chips are used in this study. Table 3.3 summarizes the design parameters of the gasifier.

Table 3.3: Gasifier design parameters

DESCRIPTION	SYMBOL	VALUE
Gasifier nominal cold gad efficiency	η_{gas}	80%
Internal diameter	D	0.92 m
Gasifier bed height	H	0.6 m
Dry biomass high heating value	$HHV_{bio,dry}$	19.33 MJ/Nm^3
Biomass moisture rate	θ_{bio}	1% (very dry)
Water latent heat [167]	r_{water}	2.257 MJ/kg
Stoichiometric air-biomass ratio [6]	m_{st}	6.36 kg_{air}/kg_{bio}
Equivalence ratio [10, 6]	ϕ_{bio}	0.3

3.1 Materials and methods

At the beginning of the project, the thermochemical data were largely insufficient. For this reason the power plant was equipped with instruments measuring the air and gas flow rates, the biomass consumption, reactor temperatures, tar and charcoal production. All of these measurements permitted a more controllable gasification process Moreover they can also be used to compare model results to the system values.

3.1.1 Gas flow rate

The gas flow rate was measured by introducing a Pitot tube in the syngas intake pipe of each engine. The data logger, connected to the Pitot, was calibrated by syngas density and temperature. The Pitot acquires pressure values from the center of the gas pipe. More than 30 diameters of rectilinear pipe separate the acquiring section from the closer bent. For common spinning values of the fans moving the syngas, the average velocity in every pipe ranges from 3.6 m/s to 15.8 m/s, which corresponds to Reynolds values ranging from 2.1 10^4 to 7.6 10^4 ensuring a fully developed turbulent flow of syngas at 310 K.

3.1.2 Air flow rate

The air inlet is composed of different parts connected to a central pipe. This architecture creates plenty of secondary air entering from the chimney, the auger feeder and the hole for the laser meter. A proper assessment of the pressure drop from the outside to the inside of the reactor is not possible. The air inlet has a large diameter and is short in

length. Taking this into account, the choice of Venturi or diaphragms for the flow rate measurement are avoided. High temperature, dust and continuous biomass crossover can interfere with ultrasonic flowmeters. When the gasifier is running, the reactor produces syngas, and the mass flow changes passing through the reactor. Problems related to the inlet flow measurements can only be solved by correlating the inlet pressure drop to the analogous flow data, acquired by the Pitot, when the gasification process is turned down. Once the reactor had been turned off, it can be considered cold two days later. A differential manometer is plugged into the air inlet duct. Fans draw air from the outside through the gasifier and the filters, then air is sent to the engine compressors. Since the gasifier is cold, no gas is produced in the reactor, therefore the air drawn in and the air flow rate sent to the compressors are the same. The flow rate passing through the pipe on the way to the engines is detected by the Pitot, this procedure allows us to correlate every pressure drop to a flow rate value. Once the system is turned on, the correlation continues and indicates the actual flow rate entering the reactor. Fig. 3.3 shows the correlation between the pressure drop and the flow rate at the air inlet duct; the value related to the 200 kW_{el} is indicated.

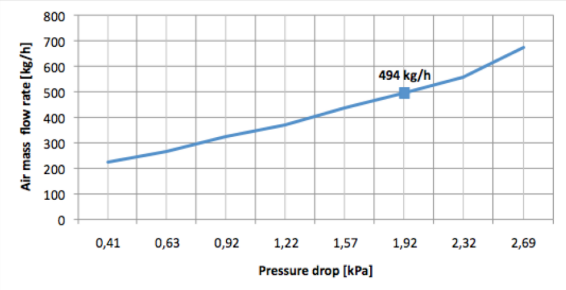

Figure 3.3: Pressure-flow

3.1.3 Biomass consumption and moisture content

When the steady-state is reached (about four hours after the plant start-up), the volume of biomass entering and exiting the dryer is the same assuming that the drying process reduce the water content of the fuel without reducing the particle size. The mass flow rate of the biomass is obtained calculating the time spent to consume a pre-weighted amount of wet biomass charged in the dryer under steady-state operating conditions.A sample of this fuel amount is analyzed using a PCE - MB 200 moisture meter for calculating the initial moisture content. Once the biomass starts exiting the dryer, another sample is tested, calculating the actual moisture content of the biomass entering the reactor. The real mass flow rate can be calculated as follows:

$$\dot{m}_{bio} = m_{fin}/t \tag{3.1.1}$$

$$m_{fin} = \frac{m_{dry}}{1 - \theta_{fin}} \tag{3.1.2}$$

$$m_{dry} = m_{in}(1 - \theta_{in}) = m_{fin}(1 - \theta_{fin}) \tag{3.1.3}$$

3.1.4 Temperatures

The reactor was implemented with six N type thermocouples with a diameter of 3 mm. An eight channel data logger was used in order to constantly record the six different temperatures plus the environmental temperature during the tests. The thick diameter of thermocouples guaranteed a good mechanical resistance, even in the high temperature zones. The thermal stratigraphy is used to control the process and to indicate the thickness and placement of the different zones in the reactor. The temperature data will be used in more detailed models to specify the different reactions taking place in the gasifier.

3.1.5 Tar and charcoal

For a complete understanding of the process, an assessment of all production waste is needed. Char is discharged from the bottom of the gasifier as well as from the cyclone. Tar is discharged by the filtering system. If the reactor starts to produce more tar, the excessive production will be read a few minutes after the tar is collected by the filters and sent to the discharge tank. All of these systems are electronically controlled, therefore they work in a discontinuous way. For this reason, a real time control of tar or charcoal production is not possible. The simplest solution consists in measuring the total amount of products generated during an entire test.

3.1.6 Syngas composition

For every power output, from 40 kW_{el} up to 220 kW_{el} a syngas sample has been analyzed. The gas samples were taken using vacuum cylinders connected to the gas pipe through a glass tank. The tank was pre-filled with syngas coming from the plant. This procedure avoids the possibility of air contamination in the syngas sample. Results of the 200 kW_{el} sample gas-chromatography are reported in Table 6. The HHV syngas can be obtained from the composition as follows:

$$HHV_{syngas} = HHV_{CO}X_{CO} + HHV_{H_2}X_{H_2} + HHV_{CH_4}X_{CH_4} \tag{3.1.4}$$

where X is the molar fraction of the different compounds. For ideal gases the molar fraction is equal to the volume fraction.

3.2 Results

The system was set at a 200 kW_{el} working point and the simulated results were compared to the experimental data. Two different tests were implemented:

- The model has been set on real values of HHV_{syngas} and η_{gas}. Results are reported in Table 3.4, related to experimental data.
- The model was set on design HHV_{syngas} and η_{gas} parameters. Table 3.5 shows the obtained results, related to model data.

For both tests, the comparison with the experimental case was indicated. The real gasifier cold efficiency was calculated by experimental data resulting 38.3 %. Δ [%] is the model percent error related to the experimental data. HHV_{syngas} was calculated

considering the syngas composition and the HHV values of every combustible component, as shown in Table 3.6.

Table 3.4: Energy balance modeling predictions vs experimental data

VARIABLE	MODEL	EXPERIMENTAL	Δ
η_{gas} [%]	38.3	38.3	0
HHV_{syngas} [MJ/Nm^3]	4.59	4.59	0
$\dot{m}_{bio}$ [kg/h]	311	261	+16%
$\dot{V}_{air}$ [kg/h]	555	468	+19%
$\dot{V}_{syngas}$ [kg/h]	496	417	+19%

Table 3.5: Design-based model vs experimental data

VARIABLE	MODEL	EXPERIMENTAL	Δ
η_{gas} [%]	80	38.3	-52%
HHV_{syngas} [MJ/Nm^3]	5	4.59	-8%
$\dot{m}_{bio}$ [kg/h]	149	261	+75%
$\dot{V}_{air}$ [kg/h]	237	468	+97%
$\dot{V}_{syngas}$ [kg/h]	455	417	-8%

Table 3.6: Syngas composition

GAS	%Vol.	HHV[MJ/Nm^3 [168]
CO	17.9	12.62
H_2	12.3	12.75
CH_4	2.80	39.72
N_2	55.6	/
CO_2	10.54	/
O_2	1	/

3.3 Summary

The proposed model is able to predict the behavior of a theoretical gasifier with a maximum error of 19%. This error cannot be reduced due to the initial hypothesis of low tar and charcoal production, as suggested by [6, 7, 8, 10]. The tar overproduction involves a discharge of un-reacted chemical energy. This phenomenum reduces the HHV of the syngas causing the cold gas efficiency to decrease. Comparing the results of the model run on the design inputs (HHV_{syngas} and η_{gas}) to the real experimental data, it can be noted that the system is far from its optimal conditions: The experimental HHV_{syngas} is lower than the design one (similar to the value reported in [6, 9, 8, 10]): this occurs because part of the chemical energy of the biomass is discharged in tar and charcoal as previously described, furthermore the air excess (97%) dilutes the syngas and increases the combustion reactions over the pyrolysis. The experimental η_{gas} is lower than the design one because the HHV_{syngas} decreases (8%), the biomass consumption increases (75%) and the decrease of

the syngas flow rate (8%). Both the sensitivity analysis and the model-real case comparison are significantly influenced by the reliability of the experimental data. The main errors in the air and gas flow rate analysis come from acquiring the single values of fluctuating variables instead of taking the average one. The main errors in the biomass flow rate are caused by the intermittent operation of the dryer. The dryer contains a volume of biomass several times greater than the amount used for the single tests. Moreover the rheology of wet and dry biomass is different. Due to the particular control method in the dryer, when a big quantity of wet biomass is charged into it, the biomass creates a compact pile interrupting the charging even if the rest of the dryer is not full. For these reasons the charging and discharging of the dryer are intermittent.This reduces the reliability of the method adopted for biomass consumption measurement. For a better control of the process, a new dryer has been designed. The plant can be easily switched from the main dryer to the new one. The new machine processes small amounts of biomass, about 1 m^3. The speed of the spinning plates and the hot air flow rate can be controlled to reach the desired moisture content. The mass flow rate of the biomass will be obtained calculating the time spent to consume all the cubic meters of biomass charged in the dryer. The major advantages of using this model include being able to monitor the system under different conditions (i.e by changing the power output of the engines). For every condition the model indicates how far the system is running from the theoretical results. If the optimum working point identified will not coincide with the nominal power output condition, the system will be forced to run with limited power. A possible solution for running the engines with full power, without demanding more syngas from the reactor, consists in installing an extra throttle between the reactor and the engine. The engine compressor draws both air and syngas, so the throttle could modify the air-gas ratio. Tar overproduction could be related to the air excess due to the biomass size. The system uses wood chips with a high content of very small pieces similar to sawdust. Air hardly penetrates the compact biomass bed. When it finds preferential passages the stoichiometric conditions may differ from zone to zone. The reactor dimensions, reported in Table 3, indicate very large and thin zones. Due to these dimensions, there is a risk that some of the biomass reagents will mix with another zone. Moreover the intermittent loading of the biomass in the reactor can temporarily extinguish the flaming pyrolysis every time the fresh fuel hits the reaction bed. These phenomena have inspired the "inception" code reported in Chapter 4. This mathematical model has been designed in order to predict the presence of channels in the biomass reacting bed. Moreover the study reported in Chapter 4 investigated the influence of duration of charging on the performance of the reactor.

Chapter 4

Modeling of channeling phenomenon in stratified reactors

This chapter investigates two important related phenomena in fixed bed reactors: the influence of biomass loading operations on the reactions that occur in the gasifier and the channels that modify the gasification conditions. Since the first employment of gasification technology for power production, most gasifiers have been designed to work with continuous loading, but the filling methods and controls actually discretize the charge in a series of small batches. The loading frequency of these batches, as well as other control variables in a gasification power plant, can deeply influence its performance, and in particular the syngas HHV and tar and water production. Downdraft stratified gasifiers seem to be the most influenced reactors by the loading conditions. This phenomenon is due to the limited thickness and superficial placement of the flaming pyrolysis layer in this kind of gasifier.

This work is aimed at investigating the influence of loading conditions on a 250 kW_e gasification power plant. Results have shown great variations in most of the plant outputs acquired during the experimental campaign; five days of tests for each loading condition (4-second-long and 15-second-long). The 15-second loading tests showed some scattered results that suggested the coexistence of pyrolysis and combustion zones in the reactor. These phenomena have been explained by the parallel running of two modified mathematical models that were obtained by coupling the Reed and Wang mathematical approaches. Models results confirmed the presence of "chimneys" in the reactor where the majority of the air passes.

4.1 Definition of channeling and loading frequency

It is proven that continuous loading of a gasifier reactor avoids strong fluctuations in the gasification performance [6]. These fluctuations are common in batch-working gasifiers due to the continuous changing of the reaction conditions [169]. Unfortunately, continuous feeding does not guarantee the complete absence of those oscillations: in concrete terms, most of the applications approximate the continuous feeding through a series of small batch loads. Every small load causes a pressure or temperature drop in the reactor, changing its internal conditions.

The gasifier design influences its sensitivity to operating conditions [7, 9]; the more distant the combustion zone is from the loading one, the less heavily the combustion reactions

are influenced by the loading operations. Stratified downdraft gasifiers are characterized by the proximity of the flaming pyrolysis zone to the top surface; moreover, the drier the biomass is entering the reactor, the thinner the drying zone is [6]. This presumes a higher sensitivity of stratified downdraft gasifiers performance to the variations of loading operations, if compared with other typologies.

This chapter is aimed at investigating the influence of the loading frequency on the performance of a stratified downdraft gasifier operating with dried biomass (worst case). The system analyzed here consists of a 800 kW_t power plant able to produce up to 250 kW_{el}e sending the filtered syngas to a couple of IC engines.

During the experimental campaign, the plant was run for five days, forcing the auger to load the reactor for 15 seconds every time the laser-meter gave the low-reactor signal. After three days of rest the test was repeated reducing the charging time to 4 seconds. The system was set up fixing the power output to 160 kWe in order to slow down the loading operations from the nominal power conditions. Running the plant at partial power output allows precise monitoring of the following parameters: biomass consumption; tar, water and charcoal production; superficial and inner temperatures; impellers spinning velocities and engine power output. Moreover, the HHVs of tar and charcoal were evaluated by experimental analysis for both the operating conditions. Results showed that the loading frequency is strongly correlated with many parameters, and reciprocal effects between operating parameters and loading frequency were observed. A possible explanation of the observed phenomena can be given after looking locally at the processes that occur on the reactor surface when the fresh biomass is loaded. A large amount of biomass can choke the flaming pyrolysis preventing the correct air flux to the zone. The air entering the reactor is diverted to preferential paths. The previous phenomenon, well known as channeling, has been reported in literature [170, 171] and it has been implemented in a model specifically set up for assuming the gasifier composed of two zones with different reaction conditions. The experimental data about water, tars and charcoal were compared with the model outputs in order to find out the reaction conditions of the two zones. Possible solutions capable of reducing the tar production through working on loading frequency influence are here suggested.

4.2 Materials and Methods

The experimental campaign was run on a full scale gasification power plant consisting of a 800 kW_t stratified downdraft reactor coupled with two IC engines with power output set to 100 kW_e. The system was fed with poplar wood chips that are dried with both exhaust and cooling air coming from the engines. In order to obtain enough clean gas to avoid frequent maintenance for the efficient operation of the engines, the syngas is forced to pass through a cyclone, a water scrubber and a battery of 24 electrostatic filters. The system is the same reported in Chapter 3.

4.2.1 Experimental campaign

The whole gasifier-filters-engines system is characterized by a high inertia: the gasifier takes hours to heat up properly, and the filtering system discharges tars produced hours earlier. For this reason the experimental campaign was designed dividing measurements

into two different categories: those obtained from the steady state plant (i.e. biomass consumption, syngas flow, temperatures and water production, impellers spinning velocities, power output) and those obtained from the whole experimental campaign (i.e. char and tar production). The campaign lasted five days for every loading condition. Every day, 4 hours after the plant start-up, the steady state measurements were taken.

4.2.2 Measurements

The gas flow rate was measured by a Pitot tube flowmeter inserted in the pipe connecting the filtering system to the engines. The measuring point was placed about the length of 30 diameters of rectilinear pipe away from the closest curve. In this case the average velocity in the pipe ensures a fully developed turbulent flow of syngas, this guarantees good reliability of the measurements.

For a precise measurement of the biomass consumption, the tests were started after 4 hours from plant start-up, while the plant is fed from the dryer. During the tests the dryer was stopped and the reactor was fed with a known quantity of biomass previously dried and weighed. The average mass of poplar wood chips used for every steady-state test was about 420 kg. In order to maintain the moisture level under control, three samples of biomass were tested for every plant run using a PCE - MB 200 moisture meter. All the tested biomasses resulted in a moisture content under 10 %. The water produced in the gasification process was collected from the water scrubber settling tank, then it was discharged to a 1 m^3 storage tank; after every test the water level was measured and the storage tank was weighed. The top readings from the reactor temperatures were obtained with three N type thermocouples 6 mm thick. The thermocouples were placed 10, 20 and 30 cm from the top reaction surface, the thermocouple tips were placed about 3 cm inside the reactor. The top surface temperature in the reactor was attained in continuous with a dual laser IR thermometer. Tar and char productions were collected at different points of the filtering system. The charcoal was discharged from the bottom of the reactor and the cyclone, while the tars were collected from the electrostatic filters or separated by floating or sinking in the water scrubber settling tank. These processes of separation and collection avoid an instantaneous monitoring of waste production. For this reason, the acquired data refer to five days of experimental campaign. The instantaneous power output as well as impellers spinning velocities were obtained from the plant management software.

4.3 Mathematical modeling

The mathematical model has been adapted from two different literature models with appropriate modifications and improvements. The first model was developed by Reed and Markson [126]; it predicts the flaming pyrolysis zone length l_p and the char reduction zone length l_c starting from biomass properties and gasifier dimensions with the following equations:

$$l_p = V_f t_p \tag{4.3.1}$$

$$l_c = V_f t_c \tag{4.3.2}$$

$$V_f = \frac{\dot{m}_{bio}(A_g F_d(1 - F_v))}{A_g} \tag{4.3.3}$$

where V_f is the fuel velocity, t_p is the pyrolysis time, t_c is the char reduction time, M is the input biomass flow, A_g is the area of the gasifier, F_d is the density of the biomass and F_v is the void fraction in the biomass.

The pyrolysis time t_p was obtained by the following equation [9]:

$$t_p = \frac{F_d V(h_p + F_m h_w)}{Aq} \tag{4.3.4}$$

where V is the volume of the biomass particle, A is the surface area of the biomass particle, h_p is the heat per unit mass released by the pyrolysis process at the temperature T_s, h_w is the water latent heat of vaporization and q is the heat transfer rate per unit area in the pyrolysis process by radiation. The values of h_p and h_w were tabulated by Reed and Markson [126] starting from Huff data [172]. The heat transfer rate q can be obtained with a weighted average calculation from the data reported in [126], where the weight of the calculation comes from the moisture of the biomass, the surface temperature and the surface area of the biomass particle. The char reduction time was calculated assuming a constant height H of the fixed bed from the following equation:

$$t_c = (H - l_p)/V_f \tag{4.3.5}$$

From the previous equations, it is possible to calculate the bed and zone heights, the time of the pyrolysis process, the char reduction process assuming a constant pyrolysis surface temperature and a constant biomass consumption.

An additional approach, presented by Wang and Kinoshita [124], was exploited to estimate the syngas composition, the air inlet flow, the syngas output flow and the charcoal and water production. This model does not consider the tar production, the temperature of the reduction zone and that the oxidant equivalence ratio are fixed parameters. It is based on the following general reaction of gasification [124]:

$$CH_\alpha O_\beta + yO_2 + zN_2 + wH_2O = \phi_1 C + \phi_2 H_2 + \phi_3 CO + \phi_4 H_2O + \phi_5 CO_2 + \phi_6 CH_4 + \phi_7 N_2$$

where the parameters α and β can be calculated from the ultimate analysis of the biomass normalizing with the specific weight of carbon, y and z are the molar number of the molecular hydrogen and nitrogen, that can be calculated from the reaction balance of the biomass oxidation considering the equivalence ratio ER. This one is defined as the ratio between the air flow and the stoichiometric air flow [6]; w is the water molar evaluated from the biomass moisture F_m, ϕ_i are the molar number of the products of the gasification. Eq. 4.3.6 can be written in mass flow mode and allows to calculate the syngas composition, the inlet and output flow rate assuming a constant biomass consumption. The variables ϕ_i are the unknowns of the problem. At the end of the flaming pyrolysis zone (subscript 0) these variables were calculated by solving the linear system below [124] assuming $\phi_{2,0} = 0$, $\phi_{3,0} = 0$ and $\phi_{7,0} = z$:

$$\phi_{1,0} + \phi_{5,0} + \phi_{6,0} = 1 \tag{4.3.6}$$

$$2\phi_{4,0} + 4\phi_{6,0} = \alpha + 2w \tag{4.3.7}$$

$$\phi_{4,0} + 2\phi_{5,0} = 2y + \beta + w \tag{4.3.8}$$

$$\phi_{4,0} = \lambda\phi_{5,0} + w \tag{4.3.9}$$

where $\lambda = 1$ is the ratio between water vapor and carbon dioxide formation [124]. In the reduction zone the temperature ranges from 1200 K to 1000 K. Here, char is consumed gradually due to char-gas reactions and gas-gas reactions as described by the following chemical reactions [124]:

1. Boudouard reaction: $C + CO_2 \rightleftarrows 2CO$
2. Water-gas reaction: $C + H_2O \rightleftarrows H_2 + CO$
3. Methanation reaction: $C + 2H_2 \rightleftarrows CH_4$
4. Steam reforming reaction: $CH_4 + H_2O \rightleftarrows CO + 3H_2$

Surface reactions 1 and 2 involve single gas molecules, while two molecules are involved in surface reactions 3 and 4. The Langmuir-Hinshelwood mechanism [173] is applied to calculate the net rate for reactions 1 and 2 given by Eq. 4.3.10 and Eq. 4.3.11, and the Langmuir-Rideal mechanism [173] was adopted to calculate the net rate for reactions 3 and 4 given by Eq. 4.3.12 and Eq. 4.3.13.

$$v_1 = -k_{a1}\frac{\phi_5 - \phi_3^2/(P_\phi K_{p1})}{\sum_{i=2}^{7}(K_i + 1/p)\phi_i}\left(\frac{\phi_{1,0}}{\phi_i}\right)^{1/3}\left(\frac{\phi_i}{\rho d_p}\right) \tag{4.3.10}$$

$$v_2 = -k_{a2}\frac{\phi_4 - \phi_2\phi_3/(P_\phi K_{p2})}{\sum_{i=2}^{7}(K_i + 1/p)\phi_i}\left(\frac{\phi_{1,0}}{\phi_i}\right)^{1/3}\left(\frac{\phi_i}{\rho d_p}\right) \tag{4.3.11}$$

$$v_3 = -k_{a3}\frac{\phi_2^2 - \phi_6 P_\phi/K_{p3}}{P_\phi K_{p1}\sum_{i=2}^{7}(K_i + 1/p)\phi_i}\left(\frac{\phi_{1,0}}{\phi_i}\right)^{1/3}\left(\frac{\phi_i}{\rho d_p}\right) \tag{4.3.12}$$

$$v_4 = -k_{a4}\frac{\phi_4\phi_6 - \phi_3\phi_2^2/(P_\phi^2 K_{p4})}{\sum_{i=2}^{7}(K_i + 1/p)\phi_i}\left(\frac{\phi_{1,0}}{\phi_i}\right)^{1/3}\left(\frac{\phi_i}{\rho d_p}\right) \tag{4.3.13}$$

$$P_\phi = \frac{1}{p}\sum_{i=2}^{7}\phi_i \tag{4.3.14}$$

where v_i is the net reaction, k_{ai} is the apparent rate constant, K_{pi} is the equilibrium constant and K_i is the adsorption constant for the reaction i, p is the pressure in the gasifier, P_ϕ is the pressure constant, $\phi_{1,0}$ is the initial molar number of atomic carbon at the beginning of the reduction zone, ρ is the density of the atomic carbon, d_p is the initial equivalent diameter of the char particle. The equilibrium constants K_{pi} were calculated by the JANAF thermochemical tables [140] and the adsorption constants K_i were both taken from [174] at a fixed reduction temperature T. The apparent rate constants were calculated by the following Arrhenius equation [171]:

$$k_{ai} = A_i \exp\left(\frac{-E_{ai}}{RT}\right) \tag{4.3.15}$$

where A_i is the pre-exponential factor, E_{ai} is the activation energy for reaction i, T is the reduction temperature and R is the universal gas constant. A_i and E_{ai} of each reaction were taken from the regression reported in [124]. The molar number of the products at the end of the reduction zone was obtained integrating the following differential equations system from zero to t_c:

$$\begin{cases} \frac{d\phi_1}{dt} = v_1 + v_2 + v_3 \\ \frac{d\phi_2}{dt} = -v_2 + 2v_3 - 3v_3 \\ \frac{d\phi_3}{dt} = -2v_1 - v_2 - v_4 \\ \frac{d\phi_4}{dt} = v_2 + v_4 \\ \frac{d\phi_5}{dt} = v_1 \\ \frac{d\phi_6}{dt} = -v_3 + v_4 \end{cases} \tag{4.3.16}$$

The molar flow rate of syngas, char, and water at the end of the reduction zone were evaluated using the molar mass of each product and assuming steady state conditions. The syngas was considered an ideal gas and its HHV_{syngas} was calculated using the method illustrated by Waldheim and Nilsson [168]. The tar mass flow rate was evaluated using an energy balance:

$$\dot{m}_{tar} = \frac{HHV_{syngas}\dot{m}_{syngas}/\rho_{syngas} - \dot{V}_{syngas,exp}HHV_{syngas,exp}}{HHV_{tar,exp}} \tag{4.3.17}$$

where HHV_{syngas} is the calculated higher heating value of the syngas, $\dot{m}_{syngas}$ is the syngas mass flow, ρ_{syngas} is the density of the syngas at normal conditions calculated considering the gas composition and the density of each component, $\dot{V}_{syngas,exp}$ is the experimental volumetric flow rate, $HHV_{syngas,exp}$ is the experimental syngas higher heating value and $HHV_{tar,exp}$ is the experimental tar heating value.

A Matlab^{TM}software was used to implement the mathematical model discussed below. The biomass adopted in this work was poplar wood-chip and Table 4.1 collects the chemical, physical and geometrical proprieties of the biomass. Table 4.2 shows the model input parameters adopted in the simulation. Table 4.3 and Table 4.4 show the comparison between experimental data and model output that was reported. A heuristic upgrading of the present model was employed to consider the presence of channels in the 15-second-long loading operation mode. The channels were modeled considering them as a part of the reactor with a total area A_1, while the rest of the reactor bed was assumed to have a section with total area $A_2 = A - A_1$. Biomass consumption in each sub-reactor was considered proportional to its area. Each part was simulated with different boundary conditions: ER_1, $\dot{m}_1 = \dot{m}A_1/A$ for the first part; ER_2, $\dot{m}_2 = \dot{m}A_2/A$ for the second part. A method that randomly changed the boundary conditions was applied to verify if the channelling theory could explain both the high water and tar production. Table 4.4 collects the boundary conditions that better fit with the experimental output.

Table 4.1: Biomass proprieties

Poplar wood chip	Proximate analysis (%wt)			Ultimate analysis (%wt)		
	Volatile matter	Fixed carbon	Ash content	C	H	O
	79.1	18.15	2.75	47.7	6.07	rest
Chip equivalent diameter	d_p	0.0156	m			
Biomass density	F_d	0.4	kg/m^3			
Biomass void fraction	F_v	0.63	-			
Biomass moisture	F_m	0.03	-			

Table 4.2: Model parameters

Parameter		Value	Unit
Gasifier area	A_g	0.668	m^2
Flaming pyrolysis temperature	T_s	1173.5	K
Fixed bed height	H	0.6	m
Biomass coefficient	α	1.52	-
Biomass coefficient	β	0.67	-
Equivalence ratio	ER	0.3	-
Reduction temperature	T	1073.5	K
Pressure in the gasifier	p	1	atm

4.4 Results and Discussion

4.4.1 Temperatures

The thermal stratigraphy of the top part of the gasifier is reported in Fig. 4.1. The temperatures are lower than what literature suggests in both the loading conditions. The temperature in the center of the reactor should be higher than what was attained by the thermocouples because the reactor diameter is big and the biomass cannot properly reach the peripheral part of the gasifier. Here the biomass creates a small ash annulus that protects the thermocouples from the higher temperature of the gasifier. During the plant maintenance operations, the ash layer was measured and it proved to be 4 cm thick. The small thickness signifies that this phenomenon is neglected in the model.

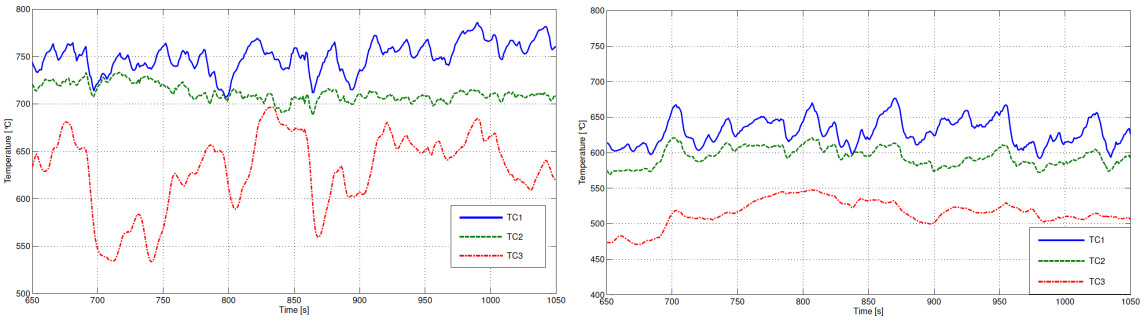

Figure 4.1: Thermal stratigraphy in the 4-second-long loading test (left) and in the 15-second-long loading test (right)

Fig. 4.1 shows the different temperature trends of the top of the reactor for the two load-

Table 4.3: Comparison between the model output and the 4-second-long loading experimental data

Variable		Model output	Experimental data	Unit
Biomass consumption	$\dot{m}_{bio}$	519	519	g/s
Syngas higher heating value	HHV_{syngas}	4.99	5.25	MJ/Nm^3
Syngas volumetric flow rate	$\dot{V}_{syngas}$	112	103	l/s
Air volumetric flow rate	$\dot{V}_{air}$	80.6	91.2	l/s
Char flow rate	$\dot{m}_{char}$	5.00	6.90	g/s
Tar+water flow rate	$\dot{m}_{tar+water}$	11.9	12.7	g/s
Cold gas efficiency	η_{gas}	66.5	66.6	%

Table 4.4: Comparison between the model output and the 15-second-long loading experimental data

Parameter		Value	Unit	
Chimney area	A_1	0.318	m^2	
ER of the chimney area	ER_1	0.667	-	
Pyrolysis area	A_2	0.350	m^2	
ER of the pyrolysis area	ER_2	0.048	-	
Variable		Model output	Experimental data	Unit
Biomass consumption	$\dot{m}_{bio}$	531	531	g/s
Syngas higher heating value	HHV_{syngas}	4.22	3.97	MJ/Nm^3
Syngas volumetric flow rate	$\dot{V}_{syngas}$	122	103	l/s
Air volumetric rate	$\dot{V}_{air}$	87.9	91.2	l/s
Char flow rate	$\dot{m}_{char}$	6.80	7.77	g/s
Tar+water flow rate	$\dot{m}_{tar+water}$	17.3	21.8	g/s
Cold gas efficiency	η_{gas}	62.1	66.6	%

ing conditions. In the 15 second load feed, the large amount of biomass for every "batch" decreases the reactor temperature due to the sensitive heat adsorbed by the biomass and chokes the flaming combustion reactions on the top surface of the reactor bed. The 15-second-long loading test shows lower temperatures and small fluctuations, especially for the thermocouple placed under the flaming pyrolysis zone (TC-3). In fact, the reactor is not able to recover the high temperature suggested by literature for these zones. The 4-second-long loading condition creates high temperatures, greatly fluctuating even for the deeper thermocouple. These variations are related to an irregular gasification zone: the peaks width is about 60 seconds, this is the stand-by period for every 5 second run of the mixer. In the 15-second test, the thermal substratum has a low temperature and is quite homogeneous; for this reason the mixer does not create significant variations, but during the 4-second test this substratum is characterized by higher temperatures raging form 500 to 700^o C, which are the extremes of gasification reactions temperatures as reported by Reed and Das [6].

Such a non-homogeneous zone is greatly modified by the passage of the mixer, thus justifying the large measured variations. Fig. 4.2 shows two trends obtained acquiring the superficial temperature of the reacting bed with the IR thermometer. The thermometer is a dual laser infrared thermometer with focus 50:1 inches fixed on the air inlet chimney.

Table 4.5: Superficial temperature of the reacting bed comparison

Variable		4 sec load	15 sec load	Unit
Fraction time over 250^o C	t_{hot}	67.89	38.6	%
Minimum average temperature	T_{min}	42.6	31.8	^{o} C
Maximum average temperature	T_{max}	896	739	^{o} C
Average temperature	T_{mean}	422	259	^{o} C

Table 4.6: Propellers frequencies comparison

Variable		4 sec load	15 sec load	Unit
Minimum average propellers frequencies	f_{min}	21.4	21.3	Hz
Maximum average propellers frequencies	f_{max}	37.8	38.9	Hz
Average propellers frequencies	f_{mean}	29.9	30.78	Hz
Standard deviation of the propellers frequencies	std, f_{mean}	2.71	3.08	Hz

The thermometer placement was chosen pointing at the reacting surface and focusing the lasers on the top surface of the reactor for a bed height of incipient loading signal from the laser meter.

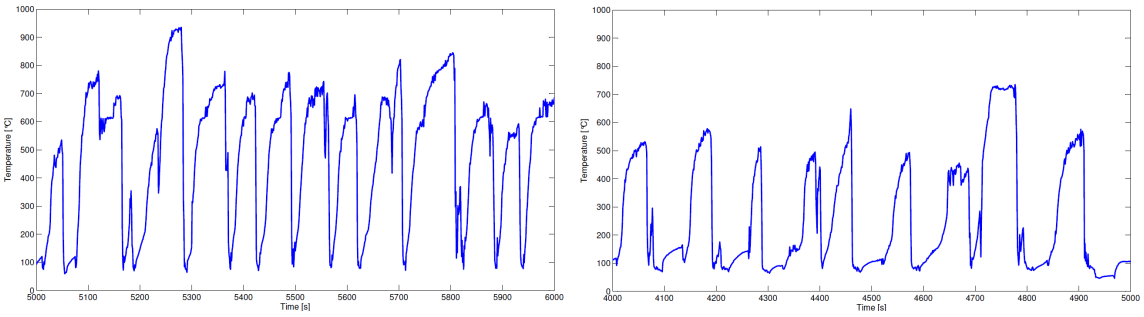

Figure 4.2: Superficial temperature in the 4-second-long loading test (left) and in the 15-second-long loading test (right)

The differences between Fig. 4.2 (left) and Fig. 4.2 (right) consist in the maximum temperature reached by the surfaces; moreover the high value recovery is slower in the 15 second loading. The 15 second loading shows 9 big peaks during the 1000 seconds of the screenshot, it results in a 15 seconds long loading every 111 seconds. For the 4-seconds test this value decreases to 77 seconds on average. In order to estimate the amount of time in which the combustion reactions are locally choked due to the sudden loading, the temperature trends have been divided in two zones: above and below 250^o C. This value is the average autoignition temperature for wood [175]; for this reason, during the periods with a reactor surface temperature above 250^o C, a wood parcel on the top surface can start its flaming pyrolysis if it is able to reach the right amount of oxidant. Results of this analysis are reported in Table 4.5. The 4-second loading condition results in a surface reactor temperature above the autoignition one for the 67% of the duration of the test. During the 15 second loading campaign this value was lower (39% of the duration of the test). A lower value can be related to a higher tar production because temperatures under 250^o C, associated with the choking effect of long loading, generate a reaction more similar

to the torrefaction than the flaming pyrolysis [176].

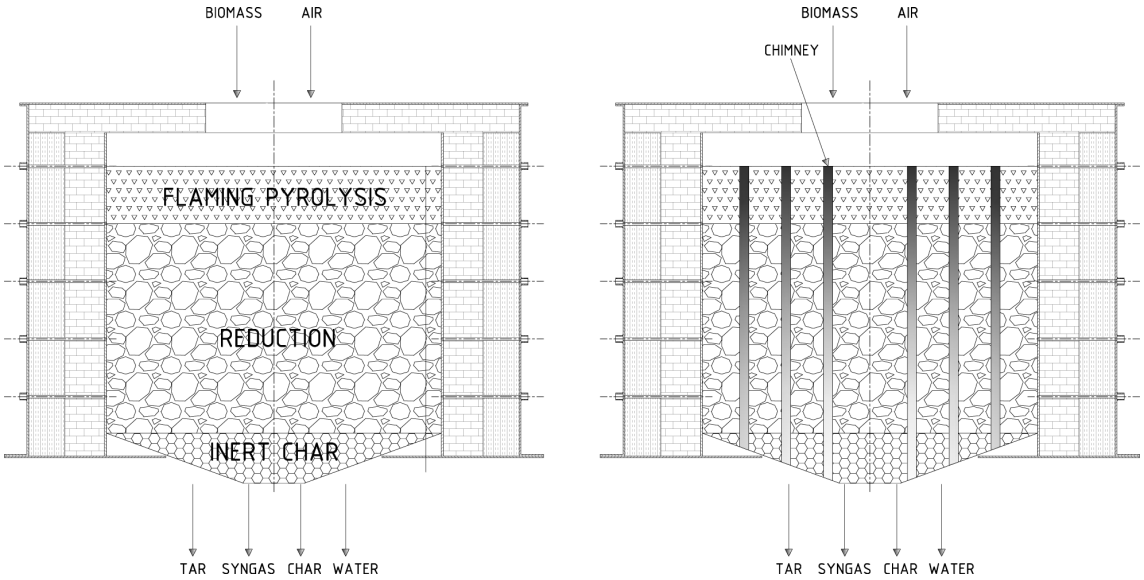

Figure 4.3: Reaction bed scheme in the 4-second-long loading test (left) and in the 15-second-long loading test (right)

4.4.2 Power output and propellers frequencies

The power plant studied here is controlled on a power output basis. Once the power output is set, the controller changes the impellers frequencies, increasing or decreasing the amount of syngas drawn from the reactor and sent to the engines, in order to maintain the fixed power generation. Changing the syngas flow, constantly modifies the reaction conditions. This phenomenon creates oscillations in the propellers frequency and in the instantaneous power output registered from the controller data logger.

In order to quantify differences in the instability of the whole system under the two loading conditions, the instantaneous values of the impellers spinning frequencies and power output were acquired. The mean value and the standard deviation were calculated and reported in Table 4.6. For the 15-second loading the impellers spin faster on average. This can be related to a poorer quality of syngas because a grater amount of gas is necessary for the same power output. Moreover, the standard deviation of the spinning frequency is higher in this case too and this suggests that the great thermal and physical oscillations on the top of the reactor, influence the behavior of the propellers too. The result obtained for the power output is different and Table 4.7 shows a lower standard deviation of this parameter in the 15-second loading. This phenomenon can be explained looking at the temperature trends in Fig. 4.2: during this loading condition the temperatures rise slowly after every reactor fill. For this reason, even if the impellers are forced to greatly change their spinning velocities due to the large changes in the reacting conditions, these changes occur slowly, so the impellers can properly "follow" the changes maintaining a more constant power output.

4.4.3 Model and Experimental output

Table 4.3 and Table 4.4 collect the main outputs for the two different loading conditions compared with the analogous simulated system. The amount of biomass consumed per hour seems to not be influenced by the loading conditions and it depends only on the set power output of the whole system. The second important set of data acquired is the charcoal production, which is similar in the two conditions. This is somehow an unexpected result, because a higher amount of energy was presumed to be discharged by the char in the 15 second loading case. For this reason, the different charcoals had been tested in a bomb calorimeter in order to estimate their high heating value. The charcoal produced during the 15-second-loading test has a HHV of 24.87 MJ/kg, higher than the 17.89 MJ/kg obtained testing the charcoal produced during the 4-second-loading test. This phenomenon is caused by the char discharging system, which works maintaining a fixed pressure drop at the bottom of the reactor, ignoring the fact that the char had or had not finished to react. The water production data can be considered in contrast to the tar data, because a higher equivalence ratio brings to low tar and high water production due to the preponderance of the combustion reactions. The opposite condition is related to a low equivalence ratio that produces oils and tars instead of water. The 15-second loading campaign resulted in a high production of both water and tar. The scientific explanation resulted from the 'inception' model of the reactor, which simulated a reactor characterized by the coexistence of combustion paths in the reactor in channels and the rest of the reactor in low equivalence ratio condition.

4.5 Chapter summary

The experimental campaign showed a deep relation between loading parameters and performance of a downdraft gasifier. Subdividing the loading in small amounts reduced the tar formation and the water production in the reactor. The results obtained from a 15 second-long loading founded a theoretical structure thanks to the "inception" mathematical model. This model, based on the coupled Reed-Wang models, explains the effect of large loads that choke the superficial reactions, forcing the air to run through few paths in the reacting bed. This phenomenon creates channels with a high equivalence ratio where most of the water is produced, while the rest of the reactor runs with a low equivalence ratio, producing a great amount of tar. These observations outline the importance of working on control parameters and modeling before designing structural modifications to the plant or the reactor. Future work will be aimed at both modeling the heat exchange between the channel and the reactor and creating a 'buffer' layer of drying biomass on the top of the reactor in order to evaluate if it can reduce the influence of loading condition on the performance of the power plant.

Table 4.7: Engines power output comparison

Variable		4 sec load	15 sec load	Unit
Minimum average electrical power	P_{min}	119.5	116.6	kW
Maximum average electrical power	P_{max}	207.7	204.6	kW
Average electrical power	P_{mean}	158.2	158.5	kW
Standard deviation of the electrical power	std, P_{mean}	4.79	4.17	kW

Chapter 5

Design guidelines for an innovative calorimetric-based method for cold gas efficiency evaluation and tar production monitoring

Every gasifier reactor can be characterized by efficiency values: cold gas efficiency or hot gas efficiency represent the amount of chemical and sensible energy content in the syngas referred to the chemical energy content in the biomass used as fuel [8, 6, 10]. These efficiencies determine the capability of the reactor to convert the solid fuel into a gaseous product, maintaining its energy content. These definitions consider that the gas can lose part of its sensible heat and chemical energy during the cleaning process, reducing the reactor efficiency [7]. This chapter is aimed at establishing a simple method for the assessment of the cold gas efficiency and tar content of a gasifier through a sampling train able to evaluate the clean and raw gas heating values. The system has been developed working on the gas drawn from a pilot scale 20 kW_{el} Imbert gasifier coupled with a Junker calorimeter modified in order to process high temperature raw gases [177]. The first results obtained have been used in Chapter 2 for the assessment of the overall efficiency of systems run with raw syngas. The results obtained are encouraging, they show the effectiveness of this approach and its capability to be used for continuous monitoring of a gasifier performance. For a better comprehension, these results need to be compared with standard methods such as the tar sampling protocol and gas chromatography [155].

5.1 Analytical redefinition of η_g

The effectiveness of the thermochemical conversion in a gasifier can be expressed as the comparison between the energy content of its exploitable products and the energy content of the starting fuel. During direct gasification the solid fuel is not simply converted into a gaseous vector, the process also produces heat (necessary for reactions sustainability), char and tar. For these reasons different definitions of efficiency can be found in literature: First hot and cold gas efficiencies can be defined:

$$\eta_{g,hot} = \frac{\text{chemical and sensible energy of gas}}{\text{chemical energy content in the biomass}} = \frac{\dot{V}_g HHV_g + \dot{Q}_g}{\dot{m}_{bio} HHV_{bio}} \tag{5.1.1}$$

$$\eta_{g,cold} = \frac{\text{chemical energy of gas}}{\text{chemical energy content in the biomass}} = \frac{\dot{V}_g HHV_g}{\dot{m}_{bio} HHV_{bio}} \tag{5.1.2}$$

The first one considers the sensible heat content in the gas. Both equations 5.1.1 and 5.1.2 are referred to the clean gas, but it can also be possible to distinguish a clean and a dirty gas efficiency:

$$\eta_{g,clean} = \frac{\text{chemical energy of filtered gas}}{\text{chemical energy content in the biomass}} = \frac{\dot{V}_g HHV_g}{\dot{m}_{bio} HHV_{bio}} \tag{5.1.3}$$

$$\eta_{g,raw} = \frac{\text{chemical energy of gas and tar}}{\text{chemical energy content in the biomass}} = \frac{\dot{V}_g HHV_g + \dot{m}_{tar} HHV_{tar}}{\dot{m}_{bio} HHV_{bio}} \tag{5.1.4}$$

Equations 5.1.3 and 5.1.4 are both cold gas efficiency but in 5.1.4 the heating value of the syngas is increased due to its tar content. In this case equations 5.1.2 and 5.1.3 lead to the same result. A univocal definition of efficiency is not conceivable and its choice depends on the purpose of the gasification system. When the syngas is burned in a furnace the hot-untreated gas efficiency can be applied, because in direct combustion there are no limitations in tar content, moreover the sensible heat of the gas can also be exploited in the furnace. On the other hand, fuel cells and gas turbines work well with a hot and clean gas, [25] in these cases a hot-clean gas efficiency can be used. For IC engines coupled with gasifiers the cleaned cold gas efficiency is used. The internal combustion engines do not tolerate high tar content in the gas, and even if the cleaning process usually reduces the gas temperature, a gas cooling is always necessary in order to increase the volumetric efficiency of the engine. Milne et al. suggest a maximum amount of tar of 50-100 g/Nm^3 for engines [9].

The HHV of the tar depends on the gasifier design, fuel composition and running parameters, but usually these range up to 40 MJ/kg [168]. This means that 50-100 g/Nm^3 of tars can increase the heating value of the gas up to 4 MJ/Nm^3 (80% of its heating value). The aim of this chapter is to define a sampling train able to determine the cold gas efficiency and the tar content, starting from the differences in heating values of the clean and raw gases evaluated through a modified Junker calorimeter. The core issue can be summed up as: the more tars are yielded by the gasifier, the more energy is discharged with them. In this case less energy is transferred to the clean gas, decreasing the efficiency of the reactor if based on clean gas heating value. Some analytical passages, based on the assumption of big differences between the volume of gas and the volume of tars transported in it, are proposed here and an innovative formulation of the cold gas efficiency has been formulated. The sampling train was developed working on a 20 kW$_{el}$ downdraft gasifier using a Junker calorimeter. Future work can be focused on design and testing a specific gas probe able to give the same results requiring a smaller amount of gas.

5.2 Material and method

5.2.1 The calorimetric approach

The first assumption for the proposed method of efficiency analysis, considering the raw gas and the clean gas volumetric flows equal, even if the raw gas has a higher high heating value. This means that the condensables occupy little volume if compared with the volume of the gas in which they are diluted. For this reason the raw gas heating value can be defined as follow:

$$HHV_{g+t} = HHV_g + \frac{\dot{m}_{bio} x_t}{\dot{V}_g} = [MJ/Nm3] + [(kg/sMJ/kg)/(Nm3/s)] = [MJ/Nm3] \tag{5.2.1}$$

Where HHV_{g+t} is the high heating value of the raw gas (gas + tars), HHVg is the heating value of the clean gas, x_t is the mass fraction of tars, $\dot{m}_{bio}$ the mass flow rate of biomass, $HHV_t$the high heating value of the tars, $\dot{V}_g$ the gas volumetric flow rate.

Expressing $\dot{m}_{bio}$ explicit from the previous function:

$$\dot{m}_{bio} = \frac{\dot{V}_g(HHV_{g+t} - HHV_g)}{HHV_t x_t} \tag{5.2.2}$$

Substituting the new definition of $\dot{m}_{bio}$ in eq.5.1.2:

$$\eta_g = \frac{\dot{V}_g HHV_g HHV_t x_t}{HHV_{bio}\dot{V}_g(HHV_{g+t} - HHV_g)} \tag{5.2.3}$$

Where $\dot{V}_g$ can be simplified obtaining:

$$\eta_g = \frac{HHV_g HHV_t x_t}{HHV_{bio}(HHV_{g+t} - HHV_g)} \tag{5.2.4}$$

This is a new equation for the evaluation of the cold gas efficiency. It is $\dot{V}_g$ and $\dot{m}_{bio}$ independent and can be calculated measuring the heating value of the different products of the process.

Moreover, eq. 5.2.1 can be written starting from $x_{t,v}$, defined as the mass of tar in every cubic meter of gas.

$$HHV_{g+t} = HHV_g + \frac{\dot{V}_g x_{t,v} HHV_t}{\dot{V}_g} = [MJ/Nm3] \tag{5.2.5}$$

This can be rearranged as follows:

$$HHV_{g+t} - HHV_g = x_{t,v} HHV_t \tag{5.2.6}$$

$HHV_{g+t} - HHV_g$ is the heating value per cubic meter of tar when diluted in an inert gas stream with the exact flow rate $\dot{V}_g$.

So, eq.5.2.4 can be written as follow:

$$\eta_g = \frac{HHV_g HHV_t x_t}{HHV_{bio} HHVt x_{t,v}} \tag{5.2.7}$$

Where HHV_t can be simplified:

$$\eta_g = \frac{HHV_g x_t}{HHV_{bio} x_{t,v}} \tag{5.2.8}$$

defining ρ_{gas} the density of the clean syngas [m^3/kg], the cold gas efficiency can be expressed as the multiplication of three variables:

$$\eta_g = \rho_g \eta_g \Gamma \tag{5.2.9}$$

where η_e represents the energetic conversion efficiency, it is the ratio of energy content in defined mass of gas to the amount of energy contents in the same amount of biomass. Γ coefficient of gasification, is the ratio between x_t and $x_{t,v}$. It represents the amount of syngas produced by every kg of biomass. It can be ascribed to its starting formulation ($\frac{\dot{V}_g}{\dot{m}_{bio}}$) or ($\frac{V_g}{m_{bio}}$) through the following passages:

$$\Gamma = \frac{x_t}{x_{t,v}} = \frac{\text{Mass of tars}}{\text{Mass of biomass}} \frac{\text{Volume of gas}}{\text{Mass of tar}} = \frac{V_g'}{m_{bio}'} = \frac{V_g}{m_{bio}} \tag{5.2.10}$$

Where V_g' and m_{bio}' are the volume of gas and the mass of biomass necessary for producing the same amount of tar. More generally, Γ defines, through the tar production, how much gas is the biomass converted in. The same results would be achieved subtracting eq. 5.2.5 to eq.5.2.1.

5.3 Examples

5.3.1 Evaluation of tar content

The tar content in the gas stream can be easily obtained from eq.5.2.6, once the heating value of the clean and raw gas stream have been evaluated, $x_{t,v}$ can be calculated as follow:

$$x_{t,v} = \frac{HHV_{g+t} - HHV_g}{HHV_t} \tag{5.3.1}$$

5.3.2 Analysis of energy losses in the gasification process

The generic energy balance of the gasification system can be described as follows (masses and volume are used to intend flows in order to balance energies and not powers):

$$m_{bio} HHV_{bio} = V_g HHV_g + x_t m_{bio} HHV_t + L \tag{5.3.2}$$

where L represents the generic losses of the system. L is composed of thermal losses, irreversible processes and energy discharged in the char.

$$L = m_{bio} HHV_{bio} - V_g HHV_g - x_t m_{bio} HHV_t \tag{5.3.3}$$

Substituting $V_g HHV_g$ obtained from eq. 5.1.2 and $x_m HHV_t$ obtained from eq. 5.2.4.

$$L = m_{bio} HHV_{bio} - m_{bio} HHV_{bio} \eta_g \frac{HHV_{g+t} - HHV_g}{HHV_g} - m_{bio} HHV_{bio} \eta_g \tag{5.3.4}$$

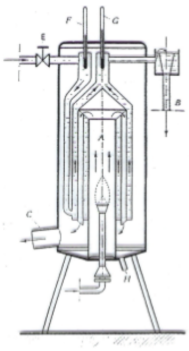

Figure 5.1: Junkers Gas Calorimeter [177]

Collecting $m_{bio}HHV_{bio}$,

$$L = m_{bio}HHV_{bio}(1 - \eta_g(\frac{HHV_{g+t} - HHV_g}{HHV_g} + 1)) \tag{5.3.5}$$

$$L = m_{bio}HHV_{bio}(1 - \eta_g(\frac{HHV_{g+t}}{HHV_g})) \tag{5.3.6}$$

Using the gas sampling train able to estimate the differences in the two gas streams (raw and clean), and acquiring some data from literature, such as the heating value of the biomass, the gasification efficiency can be estimated using eq. 5.2.4 and the losses can be calculated using eq.5.3.4.

5.4 Experimental apparatus

The previous equations will be in an experimental facility composed of three major components: a downdraft Imbert gasifier, a filtering system and a modified Junker calorimeter. The calorimeter will be fed with both raw gas coming from the cyclone or a cleaned gas. A schematic of the system is illustrated in Fig.5.1.

5.4.1 Gasifier

Two solutions can be set for the experimental part of this work:

- The first gasification reactor suitable for this study is the G.E.K. downdraft Imbert gasifier, produced by All Power Labs inc. This gasifier is part of the bio-energy efficiency laboratory at the department of Engineering of the University of Modena, it has been implemented with an experimental kit in order to control the thermal stratification in the reactor, the pressure drops in the system and the air and gas flows. For all the tests the gasifier will be fed with poplar wood chips. For every test a start-up period of 40 minutes has been considered as reported by [33]; inner gasifier temperatures can be monitored assuring the reaching of the steady state condition. This particular gasifier uses a compressed-air powered Venturi ejector for drawing the syngas from the reactor and, at the same time, diluting it for a better combustion in the torch. The methods proposed here cannot be applied with diluted gas. For this

reason it is necessary to modify the gasifier using a blower able to process the hot raw gas from the reactor instead of the Venturi ejector. Every component involved in the raw gas transport to the calorimeter needs to be wrapped in heating tapes and insulation. This procedure avoids tar condensation and deposition before entering the Junker. Moreover the length of all the pipes carrying the raw syngas needs to be designed to be as short as possible, using the minimum required number of bends and valves. Different solutions wll be adopted for the clean gas flow; instead of sampling after the cyclone, the gas will be forced through a bio-filter before reaching the blower. This will allow a consistent tar content reduction and a significant temperature drop. Then the gas will pass through a glass wool filter for solid separation, a chiller and a silica adsorber for tar removal, finally the gas can be heated up again and sent to the calorimeter.

- The GEK reactor is designed for research, but despite its design, this work here discussed needs a gasifier where all the parameters could be taken under control, increasing the repeatability of the tests. For this reason a stratified gasifier was designed and tested. Preliminary tests are reported in Chapter 8. This reactor has all the components and features necessary for this analysis. The schematic is reported in Figure 8.4.

5.4.2 Tar and gas sampling and analysis

For a complete resolution of the proposed equations, a preliminary analysis of the process products is required. During the preliminary tests the Junker needed to be substituted with a tar sampling train, following the tar sampling protocol [178] for tar production estimation. Then,in a future test the heat exchanger for gas cooling could be used instead of the tar sampling train. The tar collected in the heat exchanger will be tested in a Mahler bomb calorimeter calculating its heating value. Moreover, in these preliminary tests, is will be necessary to send part of the clean gas to cylinders for gas sampling. The gas sampled in future will be analyzed through gas chromatography calculating its composition. The average gas components molar fractions (x) will be used for the HHV_g evaluation through the following formula and for a precise evaluation of gas properties used in the Junker correlations:

$$HHV_g = x_{CO} HHV_{CO} + x_{CH_4} HHV_{CH_4} + x_{H_2} HHV_{H_2} \tag{5.4.1}$$

A schematic of the preliminary test set up is reported in Figure 8.4.

5.4.3 The Junker calorimeter

These kinds of calorimeters are commonly used for continuous measurement of the enthalpy of combustion of gaseous fuel [179, 177]. The unknown heating value of a gas is evaluated through temperature rise of a steady flow of water that passes two times in the external jacket of the combustion chamber. The energy balance of the system results in:

$$\dot{m}_{H_2O} h_0 + \dot{m}_a h_a + \epsilon \dot{m}_f HHV_f = \dot{m}_{H_2O} h_1 + \dot{m}_{ex} h_{ex} + Q_d \tag{5.4.2}$$

Where $\dot{m}_{H_2O}$,$\dot{m}_a$,$\dot{m}_f$,$\dot{m}_{ex}$ are the water, air and fuel flow rates entering the calorimeter and exhaust fumes flow rate exiting the combustion chamber respectively. The generic

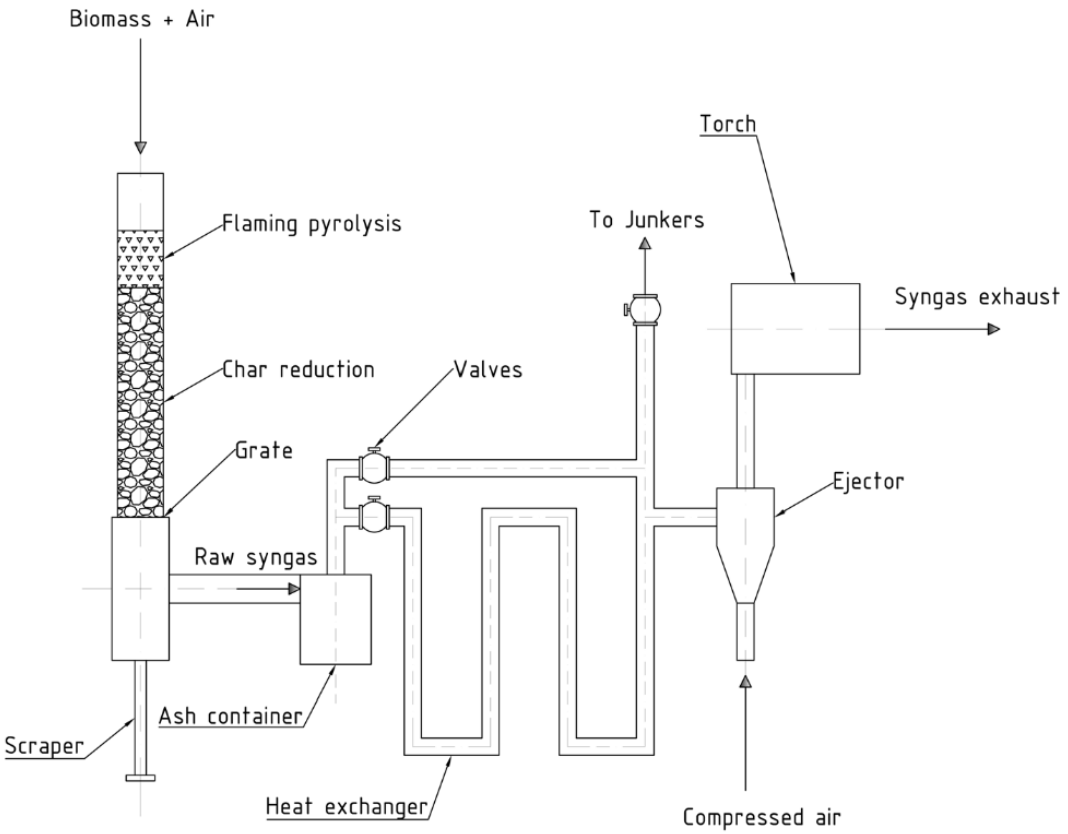

Figure 5.2: Micro scale downdraft stratified reactor

h_i is the enthalpy of the i component. ϵ is the combustion efficiency; it depends on the presence of unburned fuel due to the low permanence time in the combustion chamber. Q_d represents the thermal losses of the calorimeter.

With an experimental approach it is difficult to distinguish the effect of combustion efficiency from the thermal losses. For this reason Junker calorimeters instructions suggest to use the following approach: A parameter θ is defined as follows, it represents the efficiency of thermal transfer of the calorimeter is the function of ϵ and Q_d.

$$\theta = \frac{\dot{m}_{H_2O}\Delta T_{H_2O}c_{p,H_2O}}{\dot{V}_a HHV_f} \tag{5.4.3}$$

It is assumed to be independent of the fuel choice, and is characteristic of a calorimeter. It is necessary to calculate θ burning a known amount of fuel with renown HHV. Once θ has been calculated the HHV of a generic fuel (f) is obtained as follows:

$$HHV_f = \frac{\dot{m}_{H_2O}\Delta T_{H_2O}c_{p,H_2O}}{\dot{V}_a\theta}[MJ/m^3] \tag{5.4.4}$$

This approach is effective with standard working conditions and is based on different approximations:

- $\dot{m}_{ex} = \dot{m}_f + \dot{m}_a \approx \dot{m}_a$

- $\dot{V}_{ex} = \dot{V}_f + \dot{V}_a \approx \dot{V}_a$
- $c_{p,a} \approx c_{p,f} \approx c_{p,ex} \approx c'_p$
- $c_{p,water}$ constant despite the temperature variations
- θ constant for every gaseous fuel
- the fuel and the air enter the calorimeter at standard temperature

In this study some of the working conditions may move far from these approximations. In particular, the necessity to keep all the tubes and pipes at high temperatures in order to avoid tar condensation makes the last approximation untrue.

The problem related to the high temperature analysis can be bypassed as follows: The high temperature measurements are necessary for the raw gas only, the clean gas can be analyzed indifferently heated or not. Moreover equations 5.2.4 and 5.3.1 used in this experimental campaign always required the difference between the raw and clean gas heating values, the raw gas heating value never appears by itself.

The calorimeter efficiency factor θ is the ratio between the energy entering the calorimeter through the fuel and the energy released to the water. When the calorimeter is working with hot fuel the HHV_f calculated from eq. 5.4.4 is not the real heating value and here it is indicated as $\underline{HHV}_f$ underlining that this value is the sum of the real HHV_f and the sensible heat released by the fuel. Equation 5.4.4 is not able to distinguish the two contributions but, if the other approximation can be assumed true, it is easy to run the calorimeter with heated gases when it works with clean and raw gases and see that the differences between the heating values are the same under different temperature conditions:

$$HHV'_{g+t} - HHV'_g = HHV_{g+t} - HHV_g + \Delta T_{g+t} c_{p,g+t} - \Delta T_g c_{p,g} = HHV_{g+t} - HHV_g \quad (5.4.5)$$

This is true if the previous approximations are true and moreover if the clean and the raw gas are heated at the same temperature. Lastly the heat capacities of the clean and raw need to be similar. This condition is far from being true due the high number of carbons in the tar molecules. It is necessary to estimate the error related to these approximation as function of the tar composition, the temperature and the air-fuel ratio.

FInally, for the resolution of the proposed equations, it is necessary to evaluate the heating value of the clean gas. In this case the gas can be cooled (or not re-heated) and the Junker can be operated in standard conditions. Moreover θ is a function of combustion efficiency and thermal losses. Both these two variables are temperature-dependent, therefore it is necessary to repeat the calibration of the calorimeter and calculate θ heating up the fuel used for calibration at the same temperature of the raw gas.

5.5 Calorimetric approach to syngas composition analysis

Basically the Junkers calorimeter uses a number of inputs to calculate the unknown HHV of the fuel, but from an analytical point of view, a Junker calorimeter can give more information if it is assumed that a fixed number of chemical species can compose the gas. In fact when air is the oxidant, the syngas is always composed of a mixture of H_2, N_2, CO, CO_2 and CH_4. Once the gas species (but not the proportions between them) are

defined, it is possible to use the output of the calorimeter in order to calculate the exact gas composition.

5.5.1 basic approach

The first step to discuss the gas composition analysis is carried on calculating the H_2,CO, CH_4 contents only. The equations set is based on the following approximations:

- Dry syngas
- Dry air
- The air that enters the calorimeter is exactly the stoichiometric amount required for complete combustion of the species
- All the moisture in the exhaust gases is discharged from the bottom valve of the Junkers (dry exhaust gases).
- No tar content in the gases
- All gases are considered ideal

Under these conditions, it is possible to calculate the gas composition following a few assumptions:

1. As previously explained the Junkers calorimeter cools down the gases and evaluates the HHV of the gaseous fuel through the temperature increase in the water jacket. The temperature drop of the gases causes the condensation and discharge of part of the moisture produced during the fuel combustion in the calorimeter. The water discharged can originate from:

   (a) Moisture content in the air entering the calorimeter (not present in this basic approach)

   (b) Combustion of methane $CH_4 + 2O_2 \rightarrow CO_2 + 2H_2O$

   (c) Combustion of hydrogen $2H_2 + O_2 \rightarrow 2H_2O$

   There is also a fraction of water that leaves the calorimeter in the exhaust gases. This is taken into account in the next section only (complete syngas analysis).

   In this basic approach, the combustion of hydrogen and methane only creates a moisture of the content in the hot exhaust gases stream, the moisture is completely condensed and discharged from the Junkers before the gases exit the calorimeter.

2. The equation 5.4.1 explains how the three species contribute to the main output of the calorimeter, HHV_g.

   $HHV_g = x_{CO}HHV_{CO} + x_{CH_4}HHV_{CH_4} + x_{H_2}HHV_{H_2}$

3. The air entering the gasifier contains the stoichiometric amount of oxidant, necessary for:

   (a) Combustion of methane $CH_4 + 2O_2 \rightarrow CO_2 + 2H_2O$

(b) Combustion of hydrogen $H_2 + 1/2O_2 \rightarrow H_2O$

(c) Combustion of carbon monoxide $CO + 1/2O_2 \rightarrow CO_2$

Because the amount of oxygen in the air can be considered constant, the air necessary for complete combustion of the fuel can be related to the amount of hydrogen, methane and carbon monoxide in the syngas.

These equations can be organized in a system able to predict the percentages of the three different combustible composing the syngas:

$$\begin{cases} HHV_g = x_{CO}HHV_{CO} + x_{CH_4}HHV_{CH_4} + x_{H_2}HHV_{H_2} \\ x_{H_2,syngas}\dot{n}_{syngas}t + 0.5x_{CH_4,syngas}\dot{n}_{syngas}t = \frac{m_{H_2O}}{m_{mol,H_2O}} \\ 0.5x_{H_2,syngas} + 0.5x_{CO,syngas} + 2x_{CH_4,syngas} = x_{O_2,air}\frac{\dot{n}_{syngas}}{\dot{n}_{air}} \end{cases} \tag{5.5.1}$$

All the terms are explained in the next section. This simple system of 3 equations in 3 unknowns can be solved and the outputs are the molar fractions of the gases. In order to guarantee a stoichiometric combustion, the air entering the calorimeter needs to be adjusted and measured. This solution can be achieved implementing the air inlet line with a throttle valve and a flowmeter. The signal coming from an oxygen sensor (lambda sensor), placed after the combustion zone, is used to control the throttle valve.

5.5.2 Complete gas analysis

Once the basic approach is clear, it is possible to create a full equation set to complete the gas analysis with calorimetric approach, but for the prediction of nitrogen and moisture content two new equations are necessary. New equations can contain new unknowns, for this reason the final system proposed here is composed of 9 equations in 9 unknowns. The unknowns are:

1. Molar fraction of hydrogen x_{H_2} in the syngas
2. Molar fraction of carbon monoxide x_{CO} in the syngas
3. Molar fraction of methane x_{CH_4} in the syngas
4. Molar fraction of nitrogen x_{N_2} in the syngas
5. Molar fraction of carbon dioxide x_{CO_2} in the syngas
6. Molar fraction of carbon dioxide x_{CO_2} in the exhaust gases
7. Molar fraction of nitrogen x_{N_2} in the exhaust gases
8. Molar fraction of water x_{H_2O} in the exhaust gases
9. $\dot{n}_{exhaust}$, molar flow rate of exhaust gases

The input of the system are:

- Syngas flow rate $\dot{V}_g$
- Air flow rate $\dot{V}_{air}$

- Duration of the test t
- Mass of water condensed m_{H_2O}
- HHV syngas
- Relative humidity of air entering the calorimeter ω_{air} used to evaluate the molar fraction of water x_{H_2O} in it
- Temperature of syngas at the calorimeter inlet T_g
- Air temperature T_{air}
- Exhaust temperature at the calorimeter outlet $T_{exhaust}$

This new approach allows to set the equations necessary for system resolution using less assumptions if compared with the previous method. The only assumptions that remain from the basic approach are:

- Dry gas
- The air that enters the calorimeter is exactly the stoichiometric amount required for complete combustion of the species
- All the moisture in the exhaust gases is discharged from the bottom valve of the Junkers (dry exhaust gases).
- Exhaust with similar properties of air.
- All gases are considered ideal

The ten equations necessary for gas analysis are:

1. The first equation is the syngas species balance, it assumes that the gas is composed of five gaseous species only, with variable molar fractions:

$$x_{N_2} + x_{H_2O} + x_{CH_4} + x_{CO_2} + x_{CO} = 1 \tag{5.5.2}$$

2. The same equation can be written for the exhaust gases:

$$x_{CO_2} + x_{N_2} + x_{H_2O} = 1 \tag{5.5.3}$$

3. As described in the previous section, the heating value of the syngas is the composition of the heat of combustion of the three combustible species:

$$HHV_g = x_{CO} HHV_{CO} + x_{CH_4} HHV_{CH_4} + x_{H_2} HHV_{H_2} \tag{5.5.4}$$

4. The first atomic balance that can be set is the carbon one, any kind of carbon entering the gasifier is converted in carbon dioxide, $\dot{n}$ is the molar rate (mol/s), it can be related to the input data through eq. 5.5.11:

$$\dot{n}_{syngas} x_{CO,syngas} + \dot{n}_{syngas} x_{CH_4,syngas} + \dot{n}_{syngas} x_{CO_2,syngas} = \dot{n}_{exhaust} x_{CO_2,exhaust} \tag{5.5.5}$$

5. The following equation is the same of the previous section, it describes the stoichiometric combustion of one mole of oxygen with a specific amount of syngas. In this approach it is not possible to set the oxygen content in the air. In fact the humidity of air "dilutes" the nitrogen and the oxygen contents:

$$0.5x_{H_2,syngas} + 0.5x_{CO,syngas} + 2x_{CH_4,syngas} = x_{O_2,air}\frac{\dot{n}_{syngas}}{\dot{n}_{air}} \tag{5.5.6}$$

Where $x_{O_2,air}$ is 0.2095*$(1 - x_{H_2O,air})$, and $x_{H_2O,air}$ is the molar fraction of vapor in the air. The molar flow rates can be related to volumetric flows thanks to the approach reported for air in equation 5.5.11.

6. The nitrogen content in the exhaust gases can derive from the air or the syngas, but, because nitrogen doesn't take place in the combustion reactions, the equilibrium can be written as follow:

$$\dot{n}_{syngas}x_{N_2,syngas} + x_{N_2,air}\dot{n}_{air} = \dot{n}_{exhaust}x_{N_2,exhaust} \tag{5.5.7}$$

Where $x_{N_2,air}$ is 0.7808*$(1 - x_{H_2O,air})$, and $x_{H_2O,air}$ is the molar fraction of vapor in the air. As explained above, the molar flow rates can be related to volumetric flows thanks to the approach reported for air in equation 5.5.11

7. The following equation is the H_2 balance, it can be discharged in the form of condensed water or can leave the gasifier as vapor in the exhaust:

$$\begin{aligned} x_{H_2,syngas}\dot{n}_{syngas}t + 0.5x_{CH_4,syngas}\dot{n}_{syngas}t + x_{H_2O,air}\dot{n}_{air}t = \\ = \frac{m_{H_2O}}{m_{mol,H_2O}} + x_{H_2O,exhaust}\dot{n}_{exhaust} \end{aligned} \tag{5.5.8}$$

8. The following equation is the mass balance of the whole system:

$$\begin{aligned} \dot{n}_{syngas}t(m_{mol,H_2}x_{H_2,syngas} + m_{mol,CO}x_{CO,syngas} + m_{mol,CH_4}x_{CH_4,syngas} \\ +m_{mol,N_2}x_{N_2,syngas} + m_{mol,CO_2}x_{CO_2,syngas}) + \dot{n}_{air}t(m_{mol,O_2}x_{O_2,air} \\ +m_{mol,N_2}x_{N_2,air} + m_{mol,H_2O}x_{H_2O,air}) = \dot{n}_{exhaust}t(m_{mol,CO_2}x_{CO_2,exhaust} \\ +m_{mol,N_2}x_{N_2,exhaust} + m_{mol,H_2O}x_{H_2O,exhaust}) + m_{H2O} \end{aligned} \tag{5.5.9}$$

9. The last equation assumes that the exhaust gases are saturated with vapor, following the psychometric approach reported in [167]:

$$x_{H_2O,exhaust} = \frac{p_{vap,exhaust}}{p_{atm}} \tag{5.5.10}$$

Some of the equations previously written are based on molar rate, the molar flow of air and syngas are calculated with the following equation (here reported for air only):

$$\dot{n}_{air} = \frac{\dot{V}_{air}273.15}{0.0224T_{air}3600} \tag{5.5.11}$$

This equation gives a molar flow rate in mol/s.

5.6 Summary

The analytical methods proposed here were developed during the experimental campaign reported in Chapters 2,3,4. This chapter tries to explain the basic equations that make it possible to determine the behavior of a gasifier thanks to the calorimetric analysis of its gases. A modified Junkers calorimeter can be connected to the reactor, then the clean and the raw gases are burnt in it. With this simple procedure it is possible to determine the efficiency of the gasifier, or its tar production rate and, with some expedients, even the gas composition can be calculated.

Chapter 6

Use of light scattering for online detection of tar and particulate matter from biomass gasification

The overall objective of this work was to investigate possible solutions for tar and particulate sampling through light-scattering measurements. The major subgoals of the proposed apparatus were:

- To measure the amounts of tars produced during gasification of biomass.
- To measure the amount of fine particulate matter associated with the gasification gas product.
- To obtain quality information about the particle size distribution of particulates or tar droplets.
- To obtain quality information on the fraction of char and sand particulate in the gas stream.

6.1 Project Scope: gasifier, instruments and tools

The designed apparatus needed to satisfy some design and applicability limits. First, the use of perforated tube is strongly recommended, This kind of tube has the major advantage that the gas used for the dilution is injected through the wall, protecting the tube from tar deposition and, at the same time, this increases the chance of condensing the tar in the stream. The perforated tubes used for this work have an OD of 12.7 mm (1/2") and a length of 151 mm (6"). The inner diameter is 9.6 mm (3/8").

The second group of conditions that needed to be considered during the design were the flow rate and the maximum particulate mass flow rate imposed by the sampling instrument. For this work, a DRX dust-track was used. This instrument always processes 3 l/min of gas and is able to read aerosol concentration range from 0.001 to 150 mg/m^3. This flow rate and the tube diameter impose the maximum gas velocity in the perforated tube.

The apparatus was installed to capture particles entrained from the bubbling bed gasifier in the UBC Pulp & Paper Centre during a run in which woody biomass was being

gasified during this work. In order to ensure no interaction between the tar sampling test and the gasifier run, the apparatus was placed in one of the catch basins for condensation downstream of the last cyclone of the plant.

6.2 Preliminary tests

The facility chosen for the preliminary tests had no previous data related to the particulate content in the product syngas. The gas exiting from the gasifier was forced to pass through an internal cyclone for bed recirculation, and then through two cyclones in series in order to reduce the dust content of the gas stream. Due to the age of the facility and numerous modifications over the years, it was not possible to find accurate information about the geometry of the cyclones, so it was not possible to deduce their cutoff dimensions.

For this reason, during two preliminary runs, it was decided to try and calculate back to the solid content in the stream, analyzing the weight difference of the glass wool used for solid separation before the tar condensation branch. However, the small flow rate and the presence of cold spots in the sampling line (where local tar condensation occurs) nullified the effectiveness of this approach. The results of this test are reported in Table 6.1.

Table 6.1: Experimental masses during gasification run

Biosolids+biomass Run	Glass wool mass difference for 250 liters of gas processed
Initial mass	3.723 g
Final mass	3.88 g
Difference	0.157 g

The glass wool was also analyzed by electron scanning microscopy (SEM). The SEM analysis of the glass wool revealed why the mass difference was so small. The first image (Fig. 6.1) reproduced here shows that the glass wool did not retain large particles. In fact, it was necessary to observe the surface of the fibers with high magnification to show the deposits (Fig. 6.2). This suggests that most of the particles were separated from the gas stream when they passed through the cyclones.

The contents of the material separated by the two cyclones were analyzed. In Figures 6.3 and 6.4, it is possible to identify the three major components of the solid matter in the gas stream: a. char, b. ash, c. soot.

6.3 Apparatus design

The first series of tests were done without any pre-filtering. In this case, the instrument measured the particulate content in the stream without distinction between tar droplets, char ash or soot. For this reason, the dilution rate of the gas stream was chosen to be maintained over 1:100.

1:100 dilution

The perforated tubes in this work have no specification about the maximum dilution obtainable or the optimal pressure difference across the tube surface. Therefore, the total 1:100 dilution was obtained in a two stage process, using two different perforated pipes as shown in Fig. 6.5.

Design 1.0

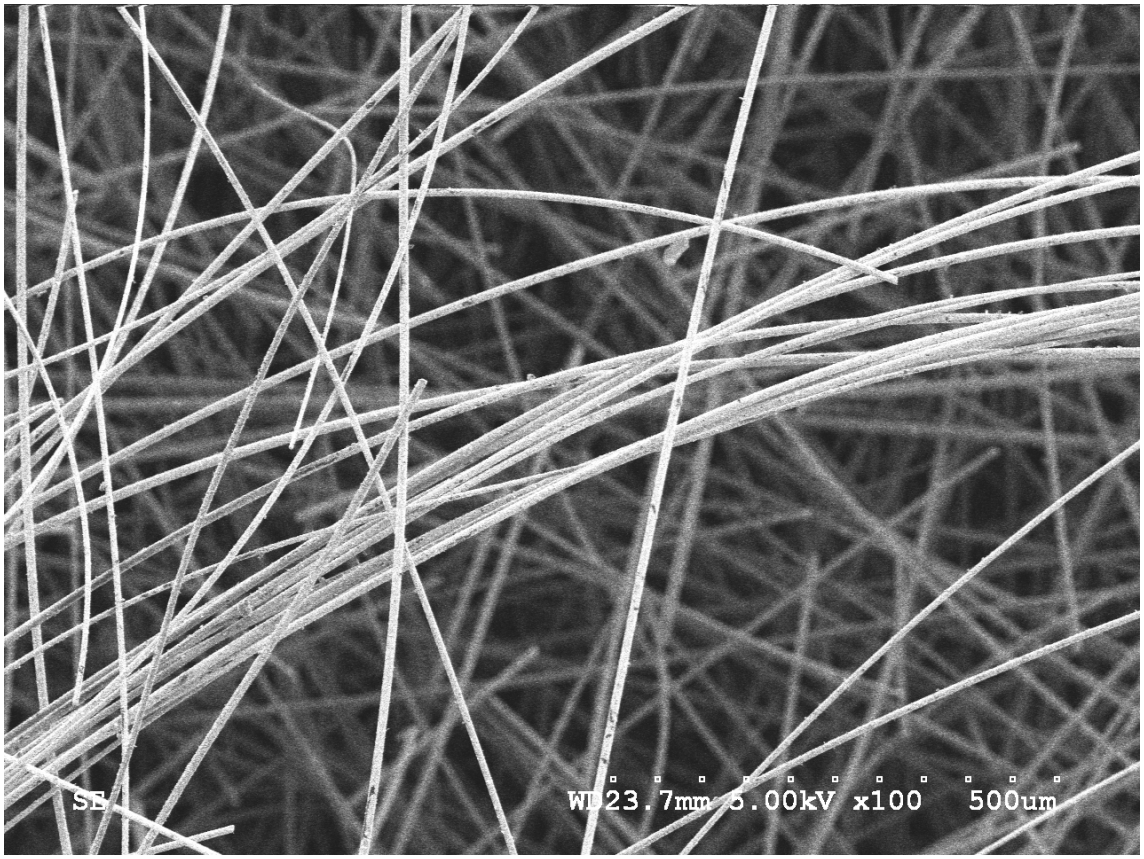

Figure 6.1: SEM picture of glasswool used for solid separation in tar sampling line of the gasifier

The first design attempted resulted in a conceptual design of the apparatus, as shown in Fig. 6.6 and 6.7.

The perforated tubes are held in the two 1" pipes that compose the two diluting sectors of the apparatus. In both cases the external pipe and the inner tube are held in place by machined metal plates. The grooves in the plates were equipped with silicon or graphite gaskets. Three threaded rods held the apparatus tight, ensuring sealing and mechanical stability of the system.

The last unknown required for a complete determination of the system was the diameter of the small tube used for 1/10 separation of the stream. Figure 7 shows a needle cut tube, cut from the axis of the 1" pipe to the wall. Once the tube diameter is fixed, it is possible to correlate the flow drawn from the pump to the area of the cut tube projection on a plane orthogonal to the pipe axis for isokinetic sampling.

Two solutions were considered as shown in Fig. 6.10. The second one featured a bent tube with no cut. In this solution the tube faces the gas stream with a smaller area, imposing a higher velocity in the 1" pipe and a higher flow draw from the pump. The higher velocity in the 1" pipe has the main advantage of a shorter permanence time that reduces tar deposition in this part of the apparatus.

For this configuration the flows are reported in Figure 6.8.

The distance between the end of the first perforated tube and the small tube for stream

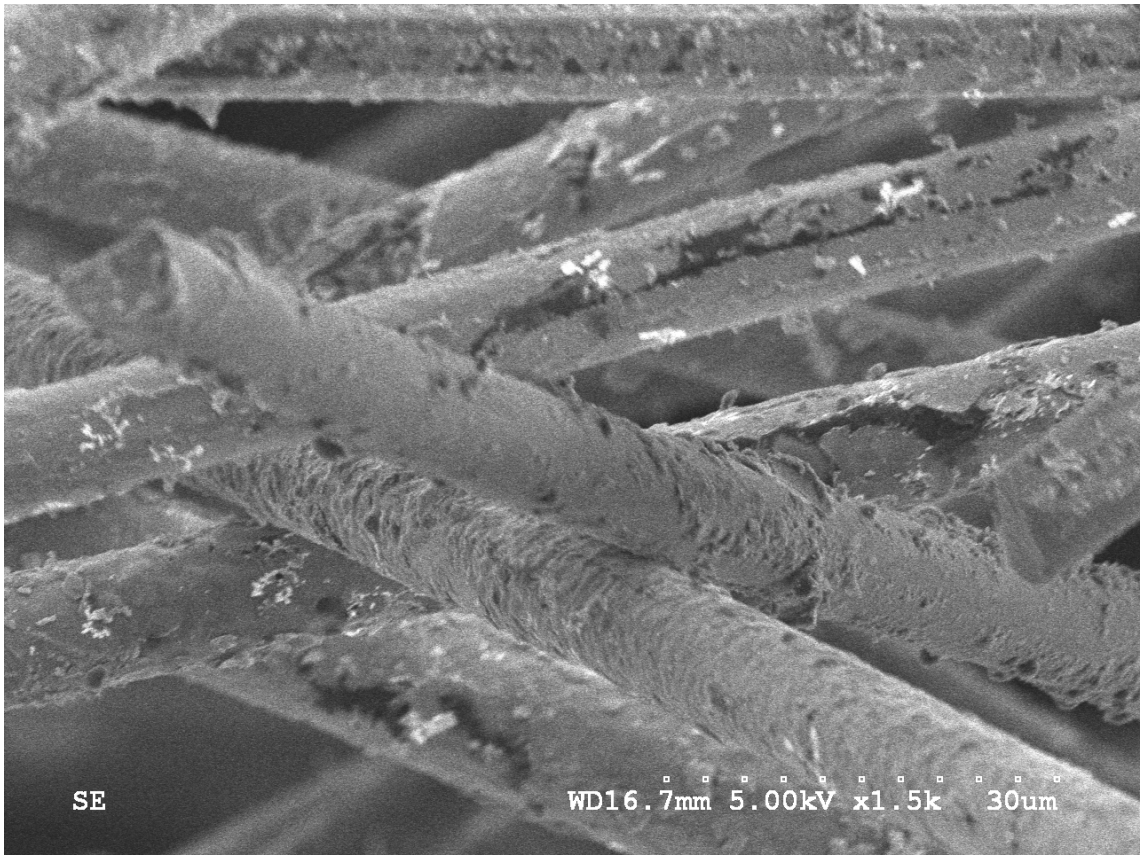

Figure 6.2: High magnification SEM picture of glasswool used for solid separation in tar sampling line of the gasifier

separation needs to be long enough to ensure flow development. With these proposed flows, the resulting length was about 18 cm or 7 ".

Table 6.2: Diameters, velocities and Reynolds numbers

	Perforated Tube	External Pipe
Inner diameter [m]	0.00953	0.0253
Inlet velocity [m/s]	0.01446	0.226
Outlet velocity [m/s]	1.59	0.205
Re_{in}	2.98	123
Re_{out}	328	112
0.06ReD [m]	/	0.187

Note that the small velocities increased the influence of the weight of the particles on the fluid dynamics force equilibrium. For this reason the apparatus was designed to hang vertically.

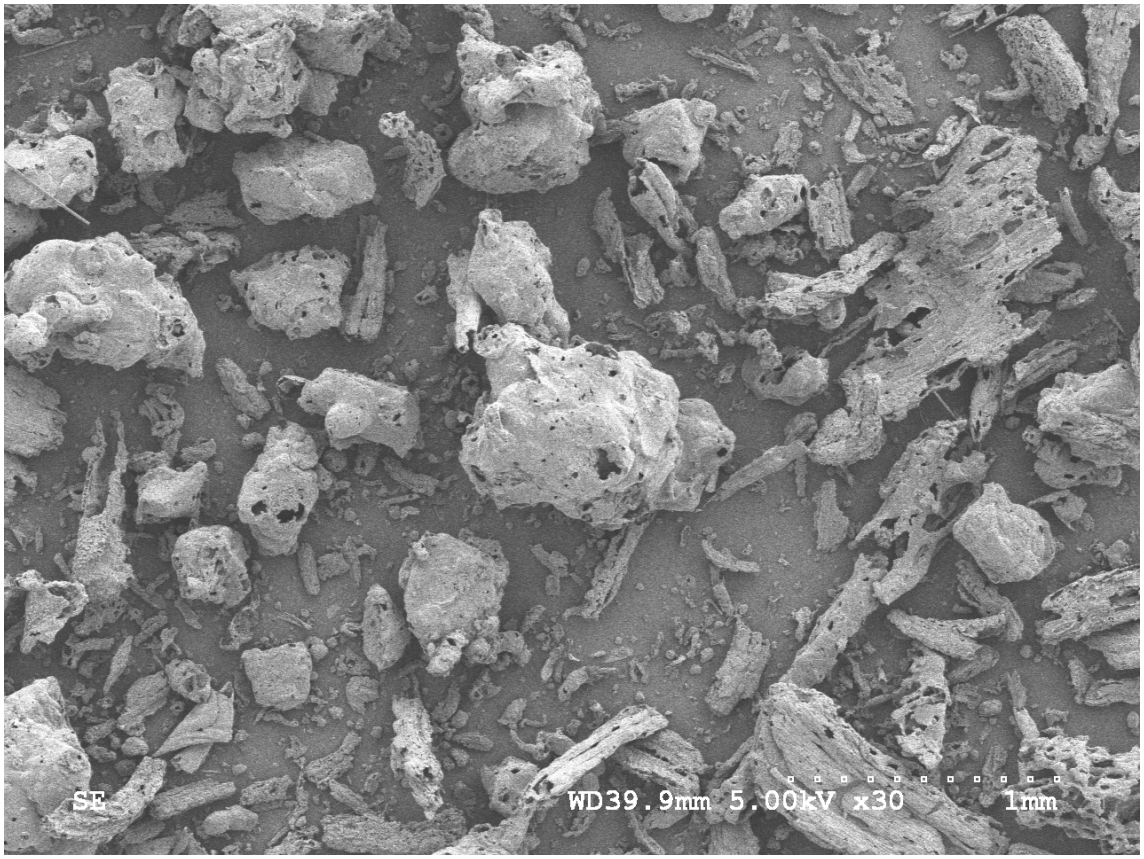

Figure 6.3: 1st Cyclone content after woody biomass gasification run

6.3.1 Limits and problems

This design is just a concept solution of a possible large scale product gas diluter. It includes all the parts necessary to accomplish this goal. The major problems related to this configuration are its cost and the time necessary to fabricate all the special parts. After the design, the short time left to finish the preliminary tests required the adoption of commercial components. Hence, it was not possible to reach the optimum solution, but these components ensures low costs, wide availability and high reliability (with all components guaranteed for temperature and pressure stresses).

6.3.2 Design 2.0

Commercial components, bill of materials (See also Figures 6.9 and 6.10) External pipes:

- 4 Standardwall Blk Steel Threaded Pipe Nipples 1" pipe size x 7" length
- 2 Low Pressure Galv. Iron Threaded Pipe Fittings 1" X 1" X 1/2" Pipe Size, Right Angle Reducing Tee
- 4 High Pressure Forged Blk STL Threaded Pipe Fittings 1" X 1/2" Pipe Size, Female
- 1 Low pressure Blk Malleable Iron Threaded Fitting 1" pipe size, Wye (1"x1"x1")

Figure 6.4: 2nd Cyclone content after woody biomass gasification run

Inner Tubes:

- 2 x 6" perforated tubes
- 1 x Type 304 Smoothbore seamless SS Tubing 1/4" OD, .0.21" ID, 0.02" thick wall
- 3 x 1/2" OD steel tubes used for connections

Fittings:

- 6 x Standard Brass Compression Tube Fitting Adapters for 1/2" Tube OD X 1/2" NPTF Male Pipe
- 3 x Standard Brass Compression Tube Fitting Adapters for 1/4" Tube OD X 1/4" NPTF Male Pipe
- 1x Brass YorLok Tube Fitting Reducing Couplings for 1/2" X 1/4" Tube OD

6.3.3 Modifications

1/2" ID collars were used to hold the perforated tubes in place. This method was used in order to ensure that the apparatus could be completely disassembled. The perforated

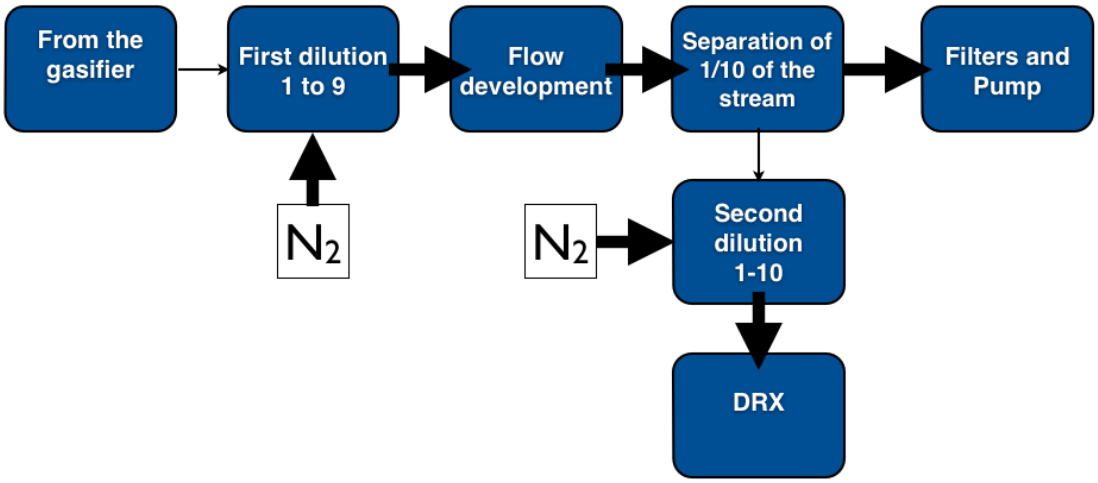

Figure 6.5: Schematic of 1:100 dilution method

tubes were not welded as the sintered material cannot maintain its mechanical and physical properties (including porosity) when welded.

As reported above, the apparatus was inserted into the hot gas line after the main gasification tests on the facility. This was necessary to ensure no influence of the dilution test on the gasification conditions during the main biomass gasification test. Moreover, in this way, it was possible to use the same GC for syngas analysis during the first test and dilution rate back-calculation during the apparatus testing. For this purpose the apparatus was equipped with an intake tube long enough to slide into the gas line and reach the middle of the gas stream.

The gas line in the bubbling bed facility was equipped with a stainless steel compression fitting with a teflon ferrule (to facilitate tube sliding). The two nitrogen lines and the tube from the apparatus to the pump were equipped with rotameters and valves for flow monitoring and adjustment.

6.4 Test and results

The apparatus was tested during a full biomass gasification run in the bubbling bed facility of the UBC Pulp and Paper Center. The gasifer hopper was filled with extra biomass in order to ensure enough fuel to complete the gasification test and the additional time of about an hour when the apparatus was connected to the facility to test the gas with the DRX.

6.4.1 DRX output

Once the DRX dust-trak had been plugged in the diluted line, it started to record concentration data mg of particulate in every Nm^3 of gas. Fig. 6.12 is the full output for the entire test.

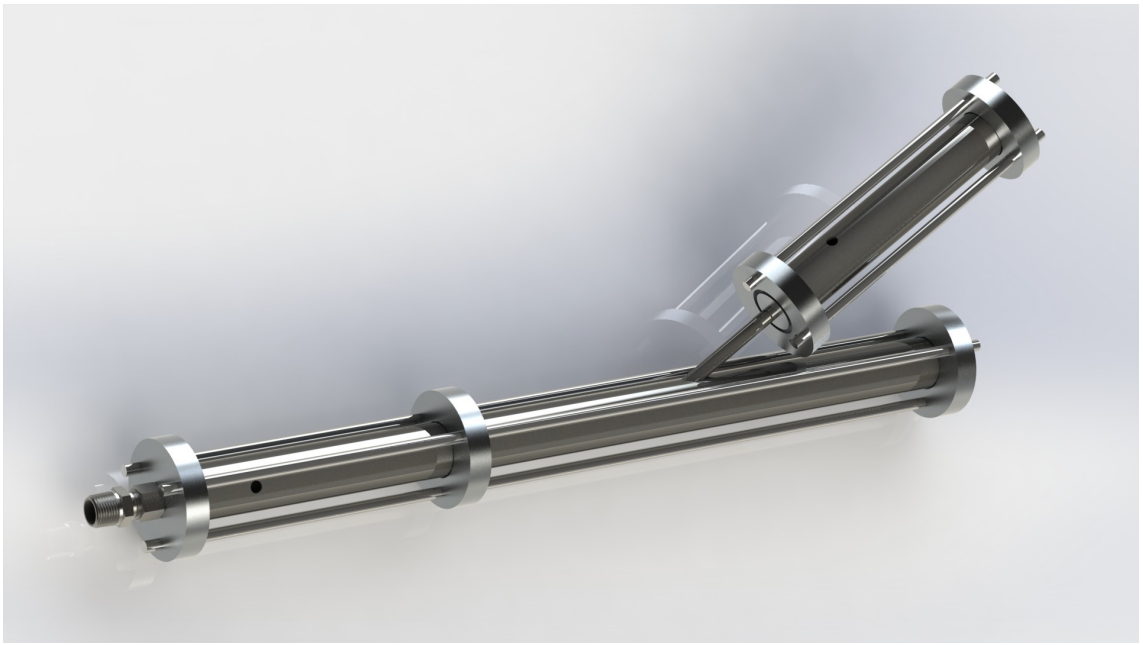

Figure 6.6: Conceptual design of the apparatus

Looking at the trend in 6.12, it is possible to divide it into three different parts reported in 6.13.

it is important to highlight that this test is the very first attempt to use this apparatus. For this reason during the first part of the test (here called transient state) it was necessary to set the valves properly to stabilize the flows trying to keep the flow values close to the design ones.

After about 15-20 minutes of big fluctuations, the flows were stabilized and minor adjustments were necessary from that moment. For this reason, this part of the test was called 'almost' steady state. The steady state condition lasted for about 50 minutes.

After 54 minutes something changed in the operating conditions because, for no apparent reason, the flows started to be really unstable, and after a few attempts to stabilize the flows (terminal part) the test had to be terminated. Probably these instabilities in the last part of the test were caused by the fouling of the inlet tube of the apparatus, Fig.6.14. In fact this component was placed in the hot, not diluted syngas steam creating an obstacle for the flow, expediting the dust and tar deposited on its surfaces.

6.4.2 Design flows vs real flows

In order to stabilize the flows, the experimental setup in the steady state part differs from the design one. The nitrogen flow in the primary dilution (through the first perforate tube) had been decreased from 6.8 to 6.7 l/min, on the other hand, the pump flow had been risen from 6.5 to 7.55 l/min, reducing the primary dilution rate and increasing the speed of flow in the tube inserted in the gasifier.

This solution drastically decreased the dilution rate from 1:100 to 1:58.

It is important to outline again that the first part of the test was used for flow stabilization changing the dilution rate. There was an attempt to reach the 1:100 dilution but,

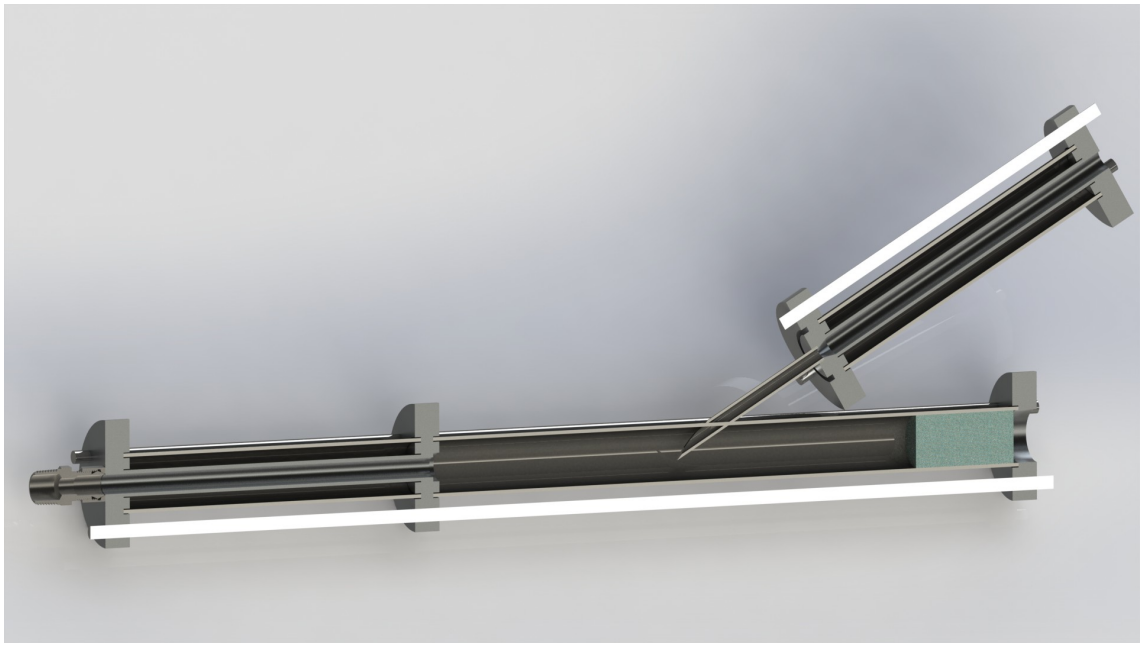

Figure 6.7: Conceptual design of the apparatus, Sectioned view

every time the dilution was increased, the amplitude of the fluctuations of concentration brought the value under the sensitivity of the DRX. On the other hand, small decreases from 1:58 dilutions were experienced to bring the concentration values over the maximum acceptable value for the DRX. These instabilities made the tuning operations particularly difficult.

Figure 6.15 is the cropping of the almost steady state part of the diagram shown in figure 6.13. It is possible to distinguish two different fluctuations, high frequency fluctuations with apparent frequency of 1 Hz (it is also the time step of the DRX) and slow fluctuations that seem to have no particular repeatability.

In this part of the test the average particle concentration in the diluted gas stream is 34.4 mg/m^3.

6.4.3 Dilution rate check with micro GC

The dilution value was calculated starting from the flows shown by the rotameters. This value was checked with a micro GC. During the test different gas samples were taken with 'Tedlar' bags. Then the bags content was analyzed in a microGC looking at the nitrogen concentration. The value of nitrogen concentration obtained from the diluted gas analysis needed to be compared with the starting nitrogen concentration in the not diluted syngas of the gasifier.

The starting gas had a nitrogen content of 51.59%.

The bags test gave an N_2 content of 99.371, 99.032 and 99.435%. These three values refer to the three GC analyses made during the steady state condition. The dilution rate based on GC analysis calculated starting from these valued ranges from 1:48 to 1:73 with an average value of: 1:67.

Because of the high nitrogen content, the GC error is close to the value of non nitrogen

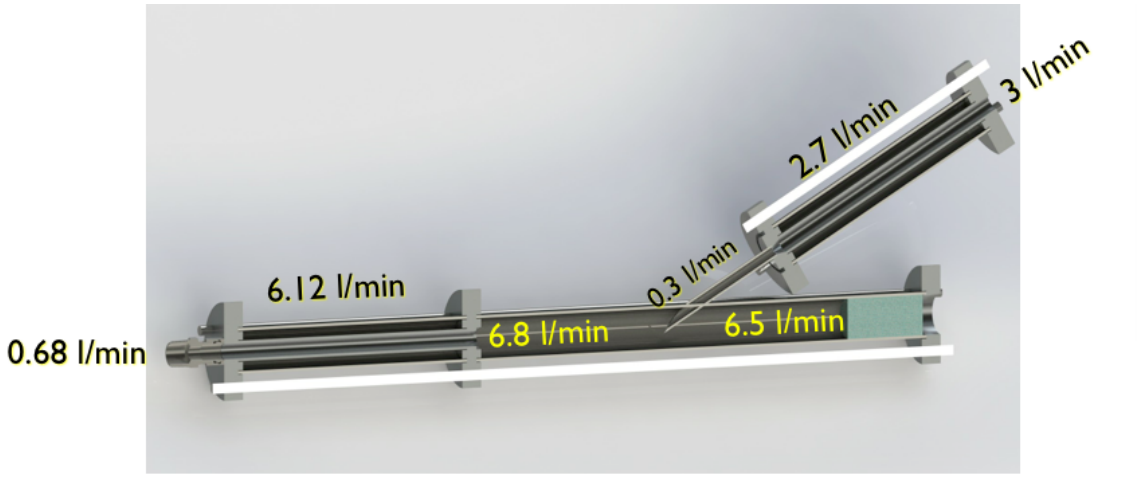

Figure 6.8: Design flow rates

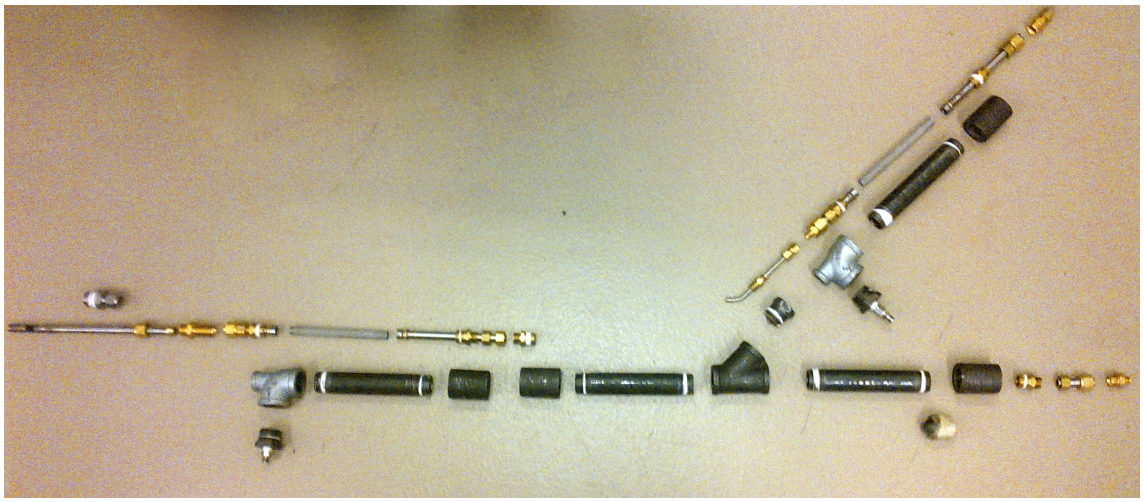

Figure 6.9: Bill of materials

gases. For this reason, both the flow rate based and the GC based dilution rates are considered correct and two different concentration of particulate in the undiluted gas are calculated.

The particulate concentrations in the syngas calculated starting from rotameters based dilution rate and GC-based dilution rate are: 1993.46 and 2308.36 mg/m^3.

6.5 Discussion and future work

This work is here discussed looking at its main goal: analyzing the tar and particulate contents in a hot gas stream through dilution with perforated tubes and analysis in a DRX dust-tracker.

The results have shown the capability of the proposed method to reach its goal, but the system has different points of optimization.

A fundamental step that needs to be taken consists in introducing the possibility of

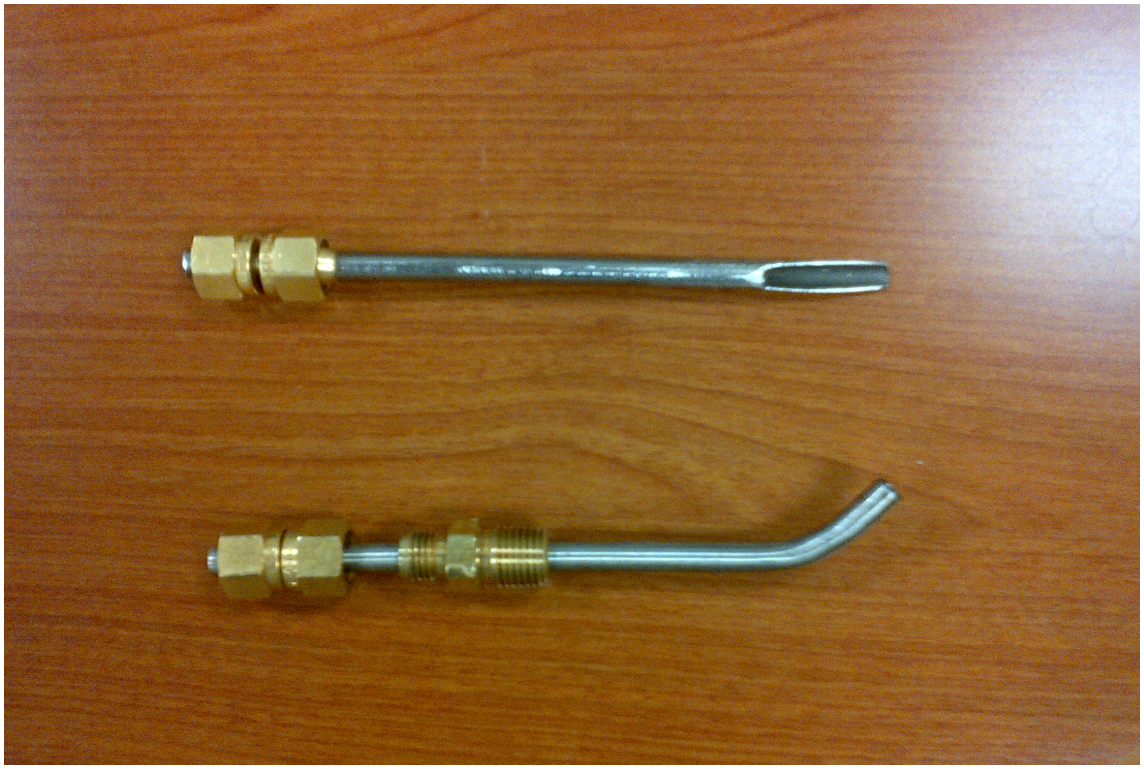

Figure 6.10: Two solutions designed for separation of 1/10 of the gas stream

solid separation (e.g. with glasswool or a ceramic filter) before the dilutor.

If the solids (char, ashes and soot) are separated before the dilutor and the DRX, it is possible to study the capability of the system to process tars.

Then the separator can be removed and the test can be run again, processing tars and particulates together.

In this way the differences between the results from the filtered and unfiltered streams allow to completely understand the influence of tar droplets and solid particulates on the DRX output, distinguishing the causes of the total output value obtained during this work.

Moreover sampling from different points in the facility (i.e. before and after the gas heat exchanger) can give different results:

- A sort of effectiveness of the facility filtering and condensation system can be evaluated.
- It is possible to investigate the origin of the fluctuations recorded in the DRX output. Maybe a different sampling point brings a less fluctuating output.

From a technical point of view, it should be possible to improve the system reducing the part of it where tar deposits can still occur (i.e. using shorter tubes and less fittings).

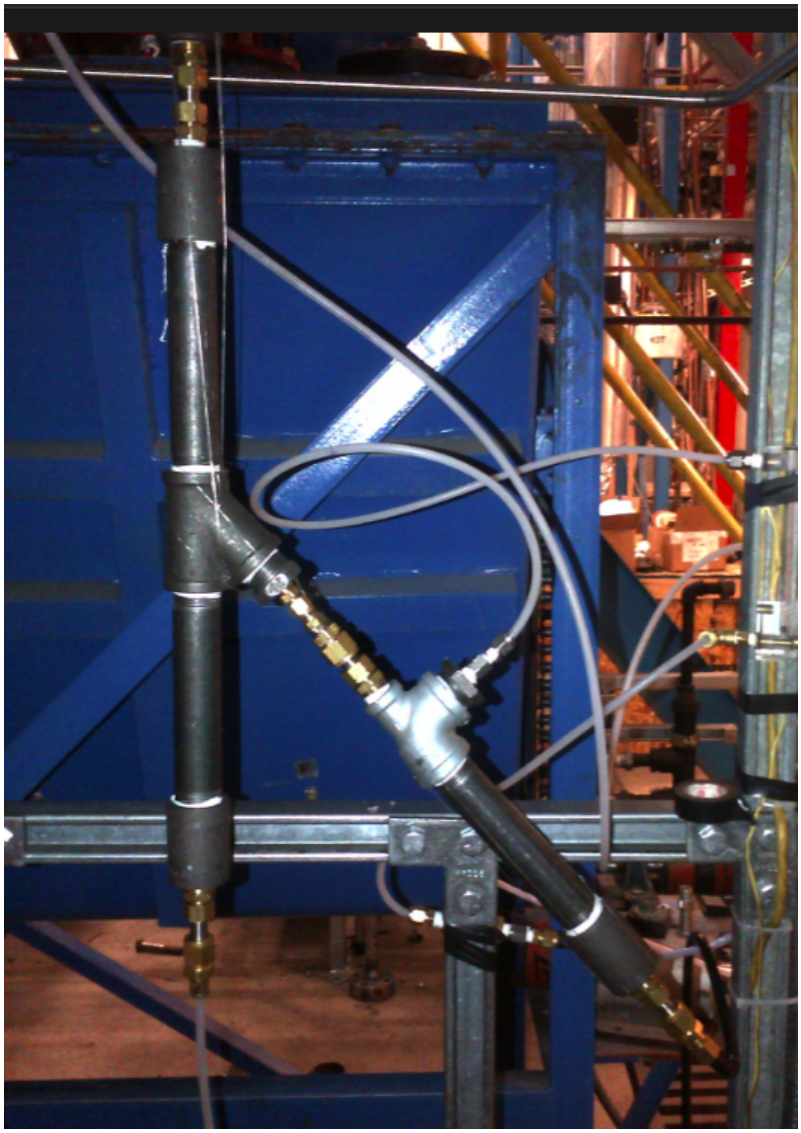

Figure 6.11: Apparatus inserted in gas line between the cyclones and heat exchanger

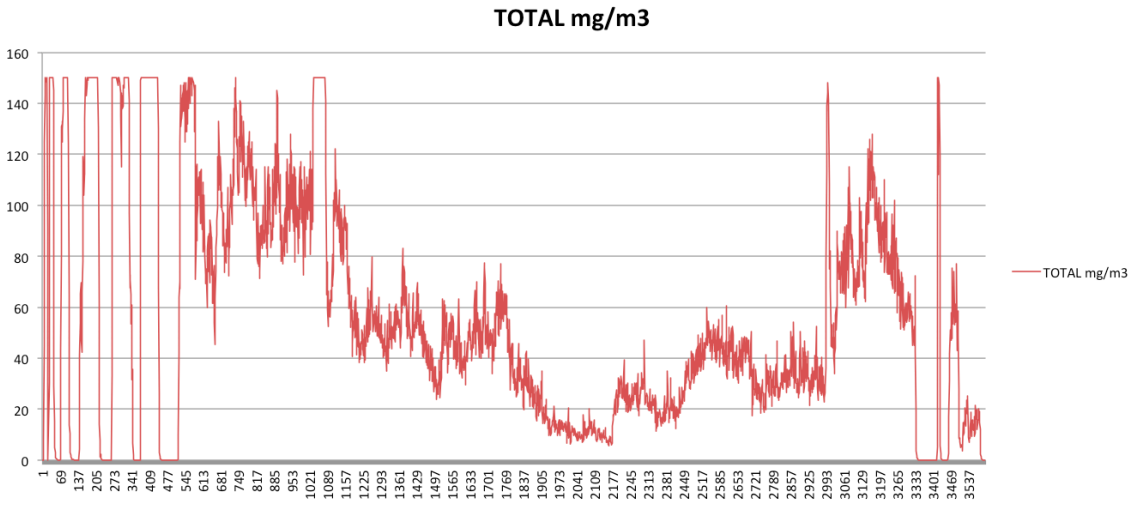

Figure 6.12: Particulate concentration trend, mg/Nm^3

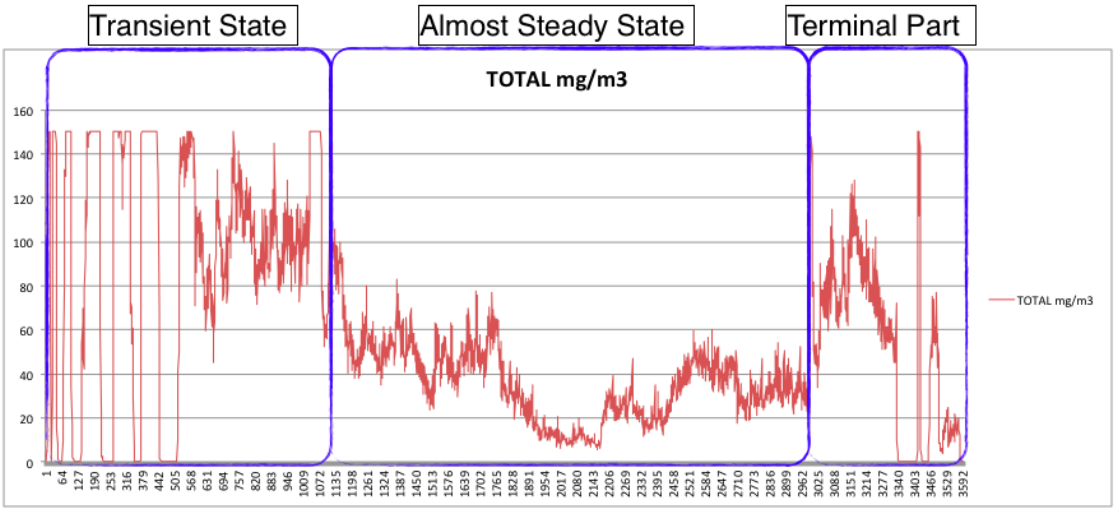

Figure 6.13: Test subdivision in three parts: Transient state, almost steady state, terminal part

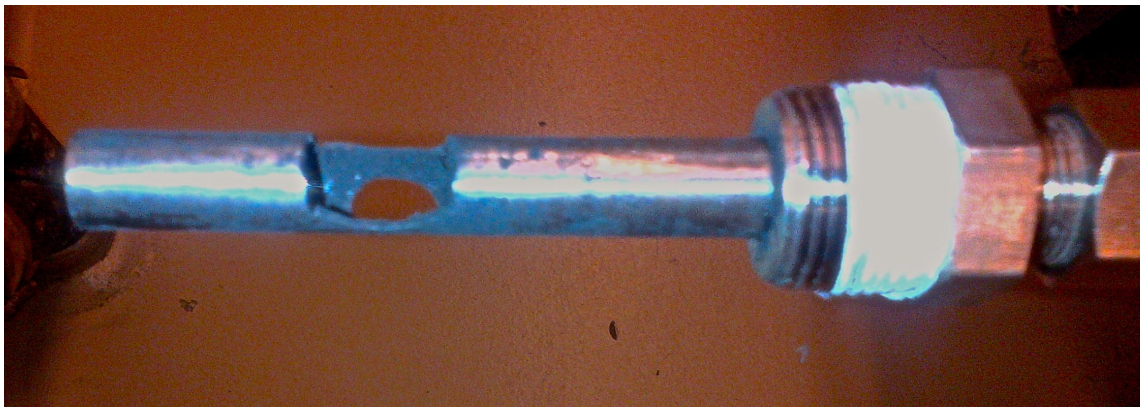

Figure 6.14: fouling of the inlet tube

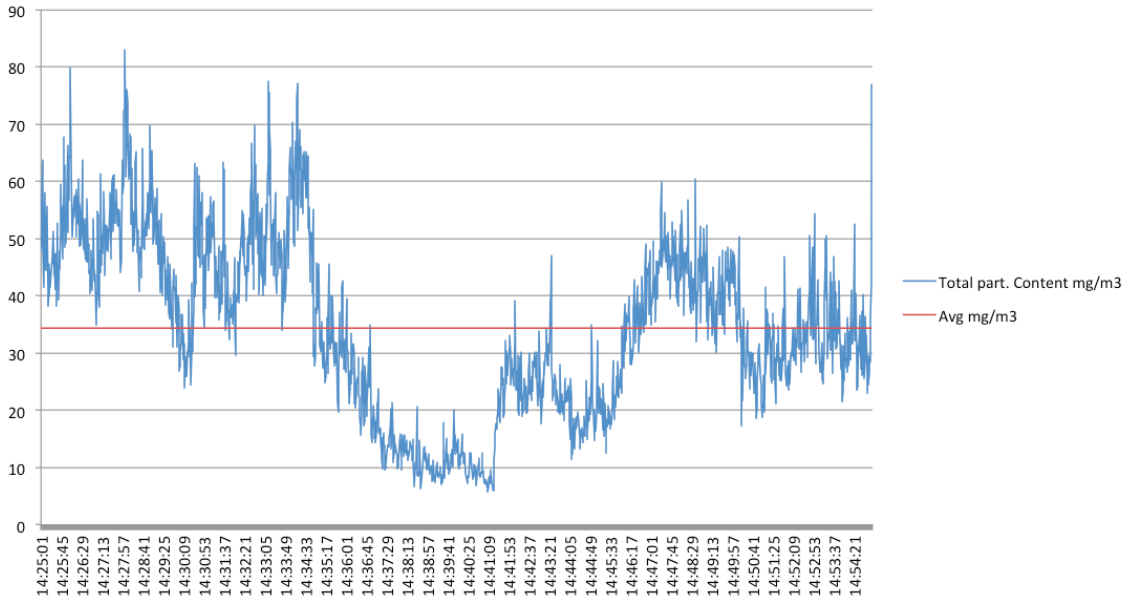

Figure 6.15: Particulate concentration trend in the almost steady state part of the test

Chapter 7

An innovative approach to integrated exploitation of energy cultures for on-field biodiesel production

This chapter is aimed at demonstrating the advantages of on-field oil extraction and protein cake exploitation from biomasses produced by a three-year crop rotation. The rotation that was taken into account was rapeseed-sunflower-flax, suitable for most Mediterranean climatic zones. The process was divided into different phases: extraction of PVO (pure vegetable oil) from seeds, gasification of the protein cake remaining from oil extraction and transesterification of the PVO using the methanol obtained by conversion of part of the syngas from gasification. In this way, instead of selling the seeds to the market, it was possible to sell the biodiesel and the electrical energy obtained from an IC engine operating with the syngas in excess. The effectiveness evaluation of this approach was obtained through energetic and economical modeling of the whole system. The system was simulated using $ASPEN\ PLUS^{TM}$ and $MATLAB^{TM}$ codes. The results show the advantages related to the installation of micro power plants of 10 kWel, involving little surfaces tilled. The minimum surface necessary for system self-sustainability was estimated as a function of field productivity and fuels characteristics. Moreover, the outputs of the economical analysis show the effectiveness of this innovative approach.

7.1 Basis of the innovative approach

Energy crops are raising interest in the world agricultural market from energetic, ecological and economical points of view. They have been used for dietary integration in crops rotation avoiding diseases and improving field profit [180]. In the last decades, with the increasing demand and price of crop derived fuels, some rotations have been suggested aiming at total utilization of products and by products for energy production [181]. In this work, a crop rotation adequate to Mediterranean zones was considered: rapeseed, sunflower and flax. The simulations were based on data obtained from literature about average oil production for these cultures in the Emilia Romagna region of Italy. Here rapeseed crops can easily produce 4.0-4.5 ton/ha of seeds with 9% of moisture, with peak production up to 4.9-5.7 ton/ha [182]. About 46-47% of rapeseed seeds can be converted into PVO by mechanical processes [182], whereas the selling price of the seeds on the European market

increased to 487 €/ton in October 2012 [183]. Sunflower crops can produce more than 2.8 ton/ha of seeds [184]. About 45% of sunflower seeds can be converted into PVO by mechanical processes [185], whereas the market price of the seeds in the Emilia Romagna region of Italy increased to 425 €/ton in November 2012 [186]. Oleaginous flax crop yields 1.1-1.7 ton/ha of seeds with 9% of moisture, with peak production up to of 2.1 ton/ha [187, 188]. About 35-45% of flax seeds can be converted into oil (with about 5-6% converted to mucilage) by mechanical processes [188]. The system layout proposed here is represented in Fig. 7.1. The approach of single culture cultivation is as follows: every year a different crop is cultivated on the whole surface and the seeds are converted into PVO by a mechanical process. The protein cake obtained as a by product of the oil extraction is gasified to syngas in a downdraft stratified reactor connected to an electrical generator of 10 kW peak power. A small part of the syngas is converted to methanol in a chemical reactor. The methanol is then used in the transesterification of the PVO to produce biodiesel. Only the flax oil is not converted to biodiesel because its production is lower than other cultures and the oil value is much higher than rapeseed and sunflower oils. The gasifier model is based on the following parameters: ultimate analysis of the protein cake, dimensions and physical properties of the cake pellets, and geometrical parameters of the gasifier. The biodiesel production is simulated considering two different reactors one for syngas to methanol reaction and another for PVO+methanol to biodiesel reaction. The methanol production conversion reactions are simulated with an equilibrium-based approach whereas the biodiesel production is modeled by a stoichiometric approach with a known conversion typical of the catalytic reactions. The whole model allows to calculate the mass of biodiesel oil or flax oil obtained every year and the electrical energy produced by the generator connected to the gasifier. An economical analysis is made to evaluate the return of the investment and the economical difference between simple seed selling and this innovative approach.

7.2 Gasifier mathematical model

The mathematical model of the downdraft stratified gasifier was adopted from the model reported in Chapter 4. Table 7.1 represents the chemical, physical and geometrical properties of the protein cakes used as model input in this work. Table 7.2 shows the geometrical and physical parameters of the gasifier and the generator. Furthermore, Table 7.3 resumes the syngas compositions, the HHV_{syngas} and the gasifier cold gas efficiency η_{cold} for each protein cake gasification.

7.3 Biodiesel production model

The biodiesel production model was developed in ASPEN^{TM} Plus software. The model uses two different kinds of input: the PVO flow rate input is based on the data coming from a literature review on seeds and oil production of rapeseed and sunflower in Emilia Romagna . The oil produced from flax cultivation is sold to the market and its cake is used in the gasifier. The model uses the data obtained from the kinetic model of the gasification process of the three different protein cakes resulting as byproducts of oil extraction [189]. The process is subdivided into two steps:

- Syngas to methanol conversion

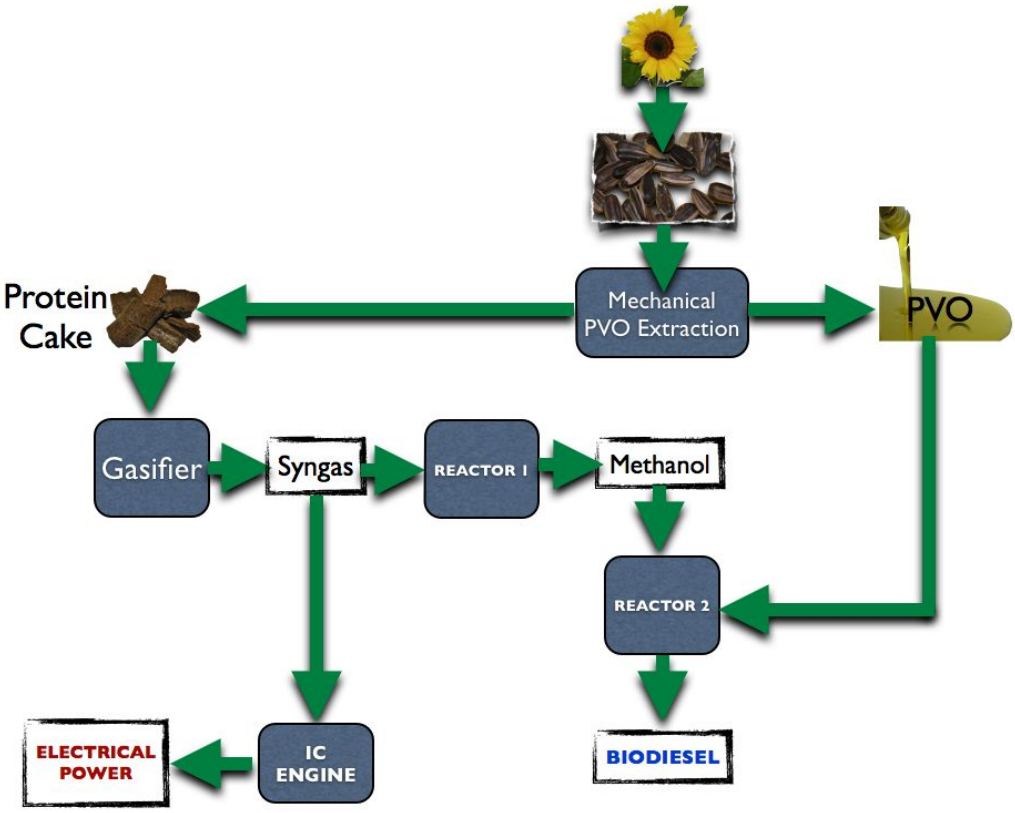

Figure 7.1: System layout

- Biodiesel production from the reaction of PVO with the produced methanol

The amount of oil produced every year from one hectare of crop rotation is known. The amount of methanol (therefore syngas) for total conversion of PVO in biodiesel is initially unknown. For this reason, the algorithm of the process needs to be followed from the bottom up: Biodiesel production is modeled in ASPEN Plus. The biodiesel production model is used for back-calculating the required methanol amount for the reaction of the known amount of PVO produced. Methanol production is modeled in the ASPEN plus model as the previous stage before the biodiesel reaction starting from the syngas composition obtained as output in the gasifier model running with different protein cakes.

The output of the ASPEN simulation of Biodiesel production combined with Methanol production is the amount of syngas necessary for the reaction of the known amount of PVO produced by one hectare of culture. This is done by the function 'Design Specification' available in ASPEN Plus. The gasifier model gives the syngas volume produced by the gasification of known amount of protein cake. The difference between the syngas produced from cake gasification and the syngas required for methanol production represents the gas excess that can be sent to the IC engine for electrical power production. Biodiesel production from methanol and PVO The biodiesel production model from PVO and methanol is based on the reaction of Transesterification of Triolein [190]:

$$TRIOLEIN + 3CH_3OH \rightarrow^{KOH} 3METHYLOLEATE + GLYCEROL$$

Table 7.1: Protein cakes parameters

Parameter	Rapeseed protein cake	Sunflower protein cake	Flax protein cake
Equivalent pellet diameter d_p	0.01 m	0.01 m	0.01 m
Density F_d	0.4 kg/m^3	0.4 kg/m^3	0.4 kg/m^3
Void fraction F_v	0.63	0.63	0.63
Moisture	0 [17]	8,6 % [17]	0 [17]
C (wt%)	43.2%[17]	42.9%[17]	46.6%[17]
H (wt%)	6%[17]	6.1%[17]	5%[17]
O (wt%)	37,07%[17]	38,46%[17]	43,24%[17]
N (wt%)	5.6%[17]	5.47%[17]	0.6%[17]
S (wt%)	0.93%[17]	0.27%[17]	0.16%[17]
Ash (wt%)	7.2%[17]	6.8%[17]	4.4%[17]
Higher heating value	17.507 MJ/kg[17]	18.343 MJ/kg[17]	17.225 MJ/kg[17]

Table 7.2: Parameters of the downdraft stratified gasifier and the generator

Parameter	Value
Gasifier diameter D_g	0.28 m
Gasifier area A_g	0.0616 m2
Fixed bed height H	0.4 m
Flaming pyrolysis temperature T_s	1173 K
Char reduction temperature T	1073 K
Equivalence ratio ER [18]	0.35
Pressure in the gasifier p	1 bar
Generator electrical efficiency η_{gen} [19]	25%

In this part of the model the inputs are: mass of PVO produced by one hectare of soil during the rotations, typology of reactor and its operating conditions as reported in Table 7.4.

A reactor configuration of RSOITC based on Stoichiometric approach with a defined conversion was used for simulating the biodiesel production process. Due to the presence of highly polar components, universal quasi-chemical (UNIQUAC) thermodynamic activity model was used. The outputs are the amount of biodiesel and glycerol produced by the process and the amount of methanol required for 95% of PVO conversion. Fig. 7.2 schematizes the process as reported in ASPEN^{TM} plus. Results, reported in Tab. 7.5, are used for the second part of the model.

Syngas to Methanol conversion. The methanol formation is based on the following reactions[191]:

$CO + 2H_2 \rightarrow CH_3OH$(19)

$CO_2 + 3H_2 \rightarrow CH_3OH + H_2O$(20)

$CO_2 + H_2O \rightarrow CO_2 + H_2$(21)

The conversion from syngas to methanol based on previous reactions has been described analytically and modeled with ASPEN^{TM} plus. The employed reactor configuration for this part of the simulation was REQUIL which employs an equilibrium approach. The syngas obtained from biomass gasification is not composed of carbon monoxide and hydrogen only as it contains also different gases like carbon dioxide, nitrogen and methane. The

Table 7.3: Results of the gasification model

Variable	Rapeseed protein cake	Sunflower protein cake	Flax protein cake
H_2 [%vol]	10.1 %	10.75 %	14.96 %
CO [%vol]	11.93 %	12.22 %	19.43 %
CH_4 [%vol]	6.6 %	6.73 %	3.11 %
CO_2 [%vol]	16.81 %	17.02 %	14.76 %
N_2 [%vol]	54.55 %	53.28 %	47.73 %
Syngas production	6140 kg	4334 kg	2012 kg
HHV_{syngas}	5.36 MJ/Nm^3	5.32 MJ/Nm^3	5.18 MJ/Nm^3
η_{cold}	94.6 %	89.36 %	90.34%

Table 7.4: Parameters of the biodiesel production model

Parameter	Value
Methanol reactor pressure	76 bar
Methanol reactor temperature	523.15 K
Recycle ratio	8
Biodiesel reactor pressure	1 bar
Biodiesel reactor temperature	343.15 K

CO and CO_2 are in stoichiometric excess compared to Hydrogen, therefore the molar flow rate of Methanol produced in the reactor is limited by the conversion of H_2. For the operating conditions of the reactor given in Table 7.4 the hydrogen conversion is about 15%. The syngas composition is in function of the solid fuel used (biomass chemical equivalent molecule $CH_\alpha O_\beta$, moisture and dimensions), the thermal stratigraphy and the equivalence ratio of a specific gasifier. An average syngas composition has been used in this part of the model. The inputs are the methanol amount required by the first part of the model, the syngas composition from the gasifier model, temperature and pressure of the methanol reactor (available in Tab.7.4). The whole system has been resolved using 'Design Specification' function of Aspen Plus in order to obtain the flow-rate of syngas necessary for producing the methanol required for PVO conversion. The results are reported in Tab. 7.5: the amount of syngas required for the process, the amount and the composition of the syngas purged due to the presence of inert N_2.

7.4 Results and discussion

7.4.1 Chemical balance

The first step that needs to be discussed is the chemical balance of the whole system. Tables 7.5 and 7.6 show the differences between the syngas deliverable from one hectare of a specific culture and the syngas required for a complete conversion of the PVO deliverable from the same hectare of the very same culture. The three cultures chosen for this work produce more syngas than required. The system is then self-sustainable from a chemical point of view. The decision of not converting the PVO obtained from flax seeds is based only on economical reasons: flax oil is a valuable product that would be wasted if used for fuel production. The fact remains that flax is necessary to complete the rotation, moreover

Table 7.5: Results of the biodiesel production model for 1 hectare of soil

Variable	Rapeseed	Sunflower	Flax
Seeds	4000 kg	2800 kg	1100 kg
PVO	1840 kg	1260 kg	385 kg
Biodiesel	1466 kg	992 kg	/
Glycerine	440 kg	299 kg	/
Methanol required	205 kg	136 kg	/
Syngas required	5513 kg	3353 kg	/
Syngas purged	5308 kg	3217 kg	/
H2 purged	4.1 %	4.2 %	/
CO purged	9.8 %	9.9 %	/
CH4 purged	7.3 %	7.5 %	/
CO2 purged	18.5 %	18.9 %	/
N2 purged	60.2 %	59.4 %	/
HHV_{purged}	4.28 MJ/Nm^3	4.39 MJ/Nm^3	/

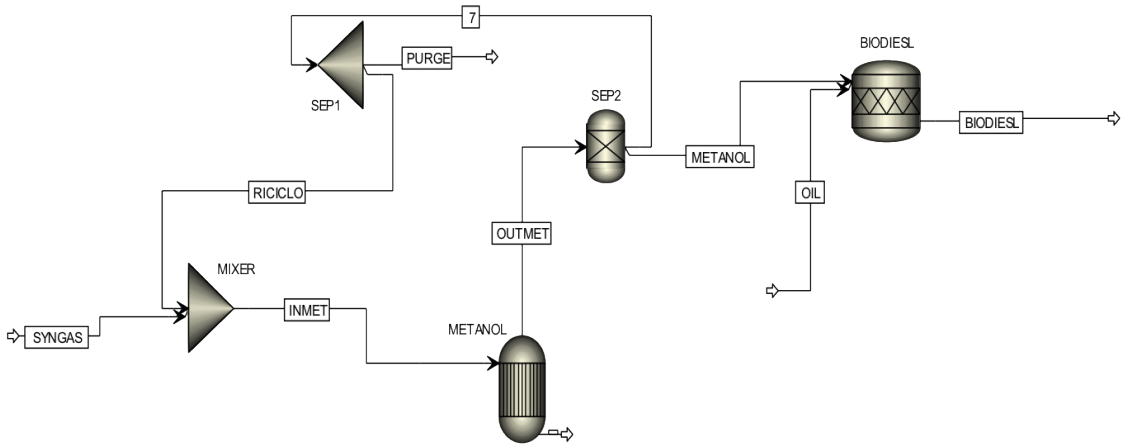

Figure 7.2: Biodiesel production model in $ASPEN^{TM}$ plus software

its protein cake can be gasified in order to increase the syngas amount used for IC engine feeding. Once the system proves to be self-sustainable, it is possible to design the plant on the basis of the engine peak power value. This value determines the total surface that needs to be tilled because it is related to the syngas excess previously discussed. One of the major advantages of the approach proposed here is the energy recovery during the process: Even if the methanol reactor has a low conversion rate, the unreacted gas chemical energy is not wasted because the purge line is connected with the engine. The results obtained here show that every hectare of culture allows the engine to run from 111 to 314 hours depending on the kind of culture (see Tab.7.6). The engine has been designed to run at 7 kW of average power, allowing small fluctuations in the gas production rate or in the gas composition without exceeding the maximum power productable [6, 8]. The waste heat coming from the methanol reactor and the engine can be used for the biodiesel production and cake drying. The first result discussed here is the productivity differences between the

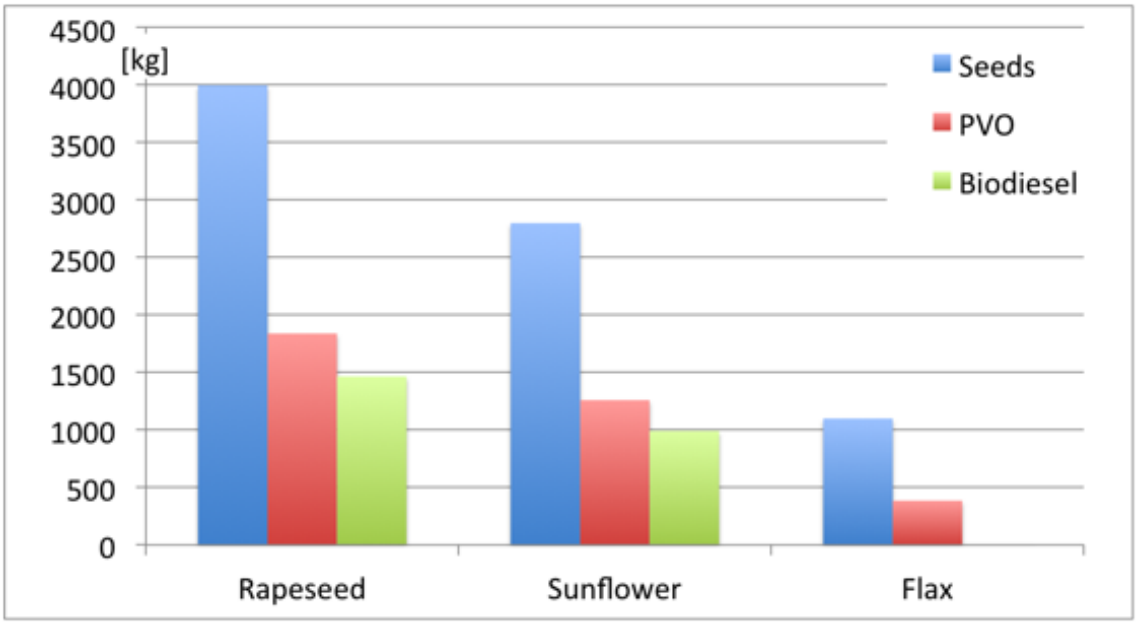

Figure 7.3: Productivity differences

energy crops, Fig.7.3 shows the trend of seeds, oil and biodiesel production.

Once the mass conversion has been shown, it is possible to focus on the gasifier engine system. Table 7.6 shows the number of hours and the energy produced by one hectare of different crops.

Table 7.6: IC engine output for 1 hectare

	Rapeseed	Sunflower	Flax
Gasified protein cake kg/ha	2160	1540	715
Operating hours at 7 kWel	314	230	111
Energy produced kWh/ha	2198	1610	777

The data discussed here allows the calculation of the number of hectares necessary to guarantee the running of the plant for 8 hours a day every year. Because the cost of cultivation decreases as the surface tilled is increased, the system considers only one crop a year. If the protein cake is properly dried, there is no reason to consume all the cake in one year. Under these conditions it is possible to balance the whole system after 3 years of running, when the rotation is ended. Figure 7.4 shows the different increases in hours of operation of the IC engine for the three different crops as a function of the surface tilled. Horizontal dashed lines are placed at 8760 and 13140 total hours in a 3-year time interval, that is 2920 and 4380 hours per year, respectively. The higher the number of hours to run the plant per year, the higher the surface required to ensure the feeding of the gasifier. The line with the higher slope is the cumulative line. It crosses the first horizontal one for a surface of 13.37 hectares, which can be approximated to 14 for losses compensation. The rapeseed seeds can generally be collected once a year, but they allow the plant operations for 8 hours a day for more than 17 months, sunflower seeds allow the plant operations for more than 12 months, and flax seeds for 7 months only. At the end of the third year all

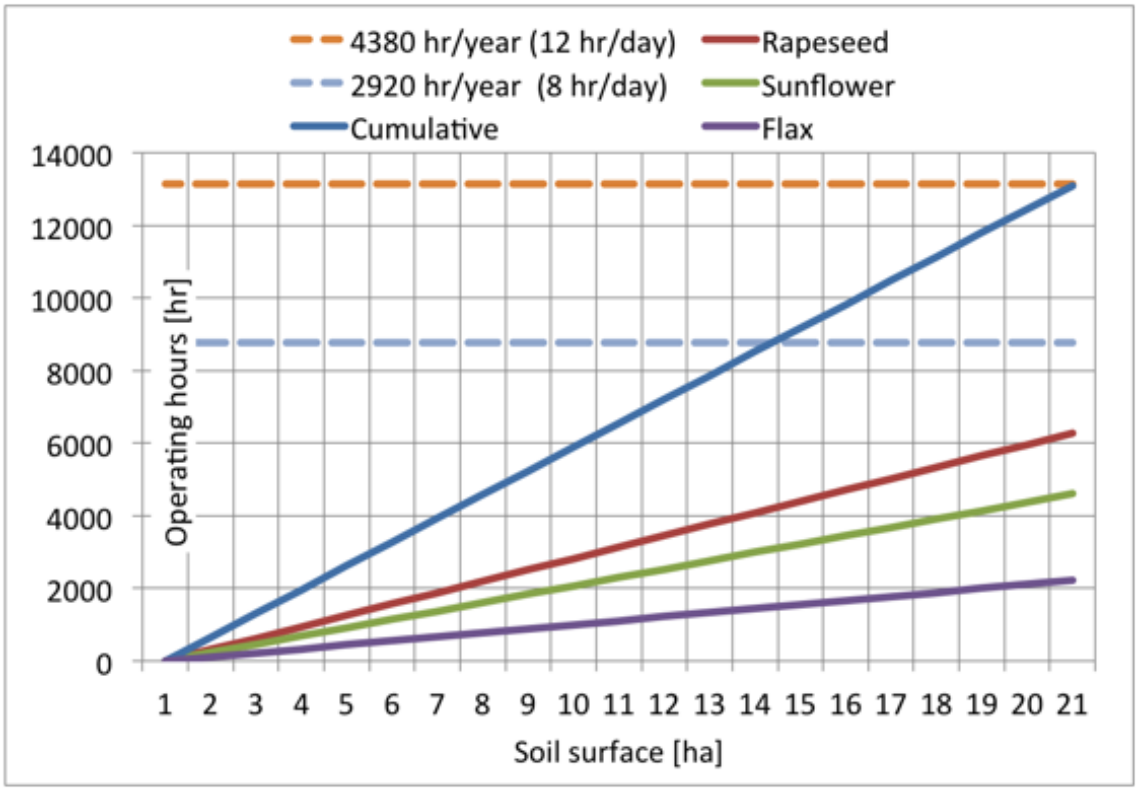

Figure 7.4: Hours of plant running per hectare of tilled surface

the biomass is consumed and all the oil is converted to biodiesel.

7.4.2 Economical analysis

The analysis was based on a few conservative assumptions:

- Seed cultivation is profitable, therefore the return of the investment for the considered system is the difference between total income from sale of biodiesel, electrical energy and flax oil ($I_{bd+ee+fo}$) and total income from sale of rapeseed, flax and sunflower seeds ($I_{seeds,rs+sf+fl}$). In this simplified approach, the income from sale of flaxseed oil is assumed to be at least equal to that from sale of flax seeds, therefore it does not affect the economical balance (flax cultivation is mainly needed for crop rotation, nonetheless flaxseed oil extraction also leaves the flax protein cakes available for gasification and electrical energy production). For this reason the return of the investment has been evaluated as the difference between I_{bd+ee} and $I_{seeds,rs+sf}$ only.
- The cost for oil extraction is generally compensated by the minor cost for external transportation of biodiesel and flaxseed oil with respect to the much larger masses and volumes of seeds that need to be brought to the collection point.
- This analysis does not take into account the electrical energy surplus obtainable through gasification of stalks and other vegetable by products of seed crops. This surplus of energy might be necessary for the seed press and other auxiliary equipment that were not taken into account for this study.

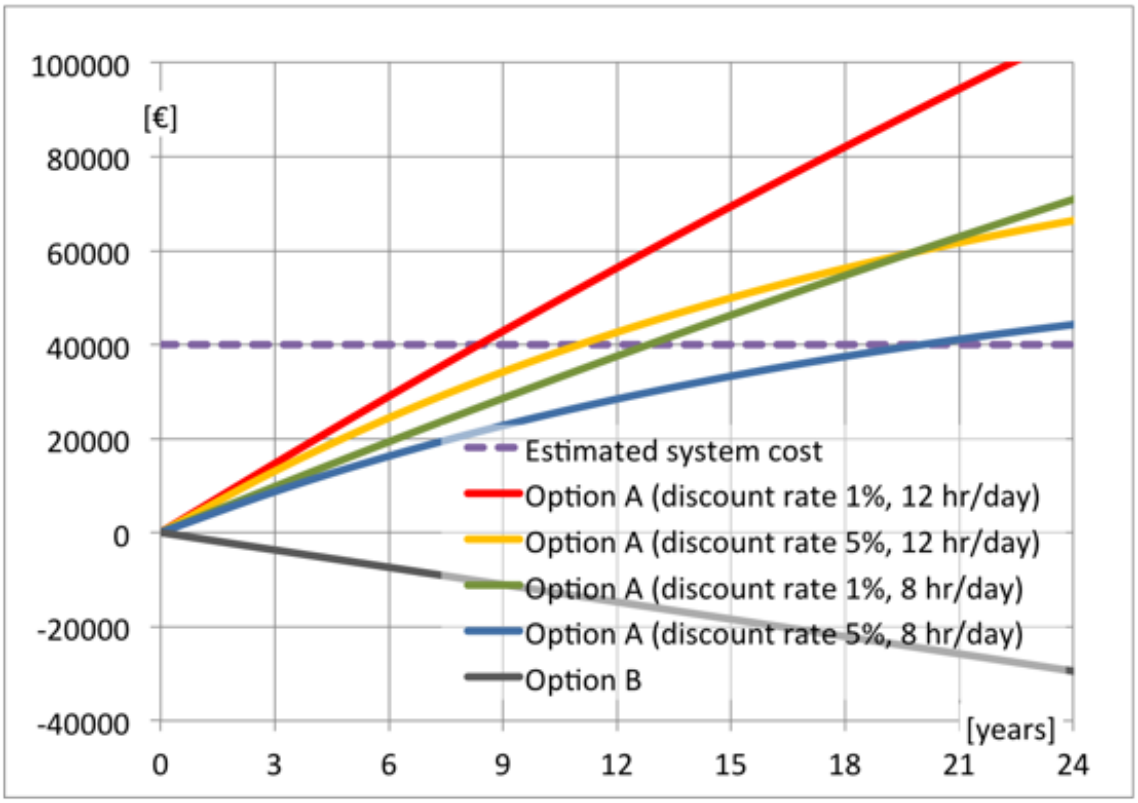

Figure 7.5: Net present value analysis

- The income from sale of glycerine resulting from biodiesels production is neglected

With regard to the sale of biodiesel and electrical energy, two different options are considered, both referred to 8 and 12 hours of plant running a day.

A Biodiesel sale price set at 0.982 €/L (with biodiesel density <0.90 kg/L), that is the current value on the Italian industrial market [192], and a feed-in tariff of electrical energy set at 0.257 €/kWh$_{el}$ for production from biomasses by means of small size plants thanks to a recent incentivation program in force in Italy (Ministerial Decree 06/07/2012 for the incentivation of electrical energy production from renewable sources different from photovoltaic systems [193])

B Self consumption of all the biodiesel, which is accounted for at the net industrial price of fuel for agricultural uses (about 0.790 €/L in 2012 [192]), and self consumption of all the electrical energy as allowed by current Italian legislation (on-site metering scheme), thus accounting the electricity at the current grid price for industrial uses (up to 0.1565 €/kWh$_{el}$ in November 2012 [194]).

Generally speaking, future biodiesel prices are expected to rise in the EU above the value considered in Option A due to obligation of 10% mixing in fossil fuels for vehicles. On the other hand, the net industrial price of fossil fuel for agricultural uses is considered in Option B as it is not clear if self consumption of biodiesel instead of fossil fuels requires or not the payment of VAT and other taxes (which would however be about 0.20 €/L for

agricultural uses). Option B was found to yield a negative cash flow of about 1230 €/year, that is a net loss with respect to selling seeds. On the other hand, Option A yields a positive cash flow of about €3370 a year with 8 hours of plant running a day, and 5055 €/year with 12 hours of plant running a day. A conventional net present value analysis is showed in Figure 7.5. It is based on an investment of about 40000 €for the whole system and the capital cost is recovered within about 8 years with the 1% discount rate (i) typical of alternative investments in government bonds (adjusted for inflation), whereas 11 years are needed if the discount rate is that typical of mortgage, al least 5% in Italy. The choice of the more suitable gasifier for this application, is determined by the characteristics of the protein cakes processed. For this non-conventional fuel an open core or an Imbert gasifier are good choices due to the capability of these reactors to process different kind of biomasses. The market offers different reactors for the power output required [112, 33, 113]. For cost estimations the All Power Labs device has been used as an example. The cost of the whole system has been estimated on the following assumptions:

- A 10 kW gasifier equipped with internal combustion engine can be found on the market for about 22000 €comprehensive of shipping extra costs [33].
- The costs of the methanol and biodiesel production reactors and the seed-press have been approximated to be 18000 €[195].

The following formula was used to calculate the net present value (NPV) at the N-th year as the sum of the discounted cash inflow in the years from 0 to N:

$$NPV = \sum_{n=0}^{N} \frac{(I_{bd+ee} - I_{seeds,rs+sf})}{(1+i)^n} \tag{7.4.1}$$

It is interesting to find that 69% of all income of Option A come from biodiesel, thus about 31% comes from electricity. Increasing the production of syngas and electrical energy through exploitation of stalks and other by products of seeds crop can thus improve significantly the cash flow. Further improvements can come from substituting flax with some other cultivation adequate for crop rotation, but also for production of PVO and biodiesel.

7.5 Future Work

For a complete comprehension of the complex phenomena and interactions that occur in this system, an experimental analysis is vital. There are many points that need to be investigated, such as capability to avoid ashes slagging in the gasifier or the effect of syngas composition fluctuations on methanol conversion rates. Once the system model is validated, different rotations can be simulated in order to maximize the profit.

Chapter 8

Influence of diameter on stratified downdraft reactors

Chapters 2, 3, 4 introduced, analyzed and modeled stratified reactors from different points of view. Chapter 2 introduced the advantages of gasification on other thermal conversion technologies, with a particular focus on the real case analysis of a 250 kW_{el} downdraft stratified gasifier. This power plant was described in Chapter 3, where experimental methods for a complete investigation of the system are proposed and discussed. Finally, Chapter 4 uses a kinetic modeling for a better prediction of the bridging phenomena that occurred in the studied power plant. this chapter is based on the ostensible contradiction of two different assumptions:

On the one hand the models discussed in this thesis [125, 126, 120, 124] use a few equations to describe the behavior of stratified reactors, these models, despite the basic approach employed, are able to analyze the differences between the zones in terms of reactions and temperatures. On the other, all these models do not take into account the diameter of the gasifier as a parameter that can influence its performance. In other words with these models two gasifiers of the same height but different diameters produce a perfectly proportional power output obtained, burning a gas with exactly the same composition. On the other hand experimental campaigns carried out during this study showed how, once the height is fixed (60 cm for the reactors here discussed), reactors with large diameters (80 cm) as well as small ones (7.62 cm) are characterized by running issues and accentuated differences in the main thermo-chemical outputs. This chapter tries to discuss the analytical basis of this contradiction and gives hints for an experimental analysis that can be used for separation of the thermal and rheological/fluid-dynamical differences between reactors. Moreover, the basic literature about stratified reactors indicates these gasifiers for avoiding bridging problems [8, 12]. This work has pointed out how this is only partially true and it is related to the biomass loading method.

8.1 Model Analysis

For a brief discussion of diameter influence consideration in the models proposed in this thesis, the Reed model is here reported with annotations about its use of diameter data. The same approach can be repeated for the Wang, model whose equations are reported in Chapter 4.

The model proposed by Reed and Markson [126] predicts the flaming pyrolysis zone length l_p and the char reduction zone length l_c starting from biomass properties and gasifier geometry:

$$l_p = V_f t_p \tag{8.1.1}$$

$$l_c = V_f t_c \tag{8.1.2}$$

$$V_f = \frac{\dot{m}_{bio}(A_g F_d(1 - F_v))}{A_g} \tag{8.1.3}$$

where V_f is the fuel velocity, t_p is the pyrolysis time, t_c is the char reduction time, M is the input biomass flow, A_g is the area of the gasifier, F_d is the density of the biomass and F_v is the void fraction in the biomass. The pyrolysis time t_p is obtained by the following equation [9]:

$$t_p = \frac{F_d V(h_p + F_m h_w)}{Aq} \tag{8.1.4}$$

where V is the volume of the biomass particle, A is the surface area of the biomass particle, h_p is the heat per unit mass released by the pyrolysis process at the temperature T_s, h_w is the water latent heat of vaporization and q is the heat transfer rate per unit area in the pyrolysis process by radiation. The values of h_p and h_w were tabulated by Reed and Markson [126] starting from Huff data [172]. The heat transfer rate q can be obtained with a weighted average calculation from the data reported in [126], where the weight of the calculation comes from the moisture of the biomass, the surface temperature and the surface area of the biomass particle. The char reduction time is calculated assuming a constant height H of the fixed bed from the following equation:

$$t_c = (H - l_p)/V_f \tag{8.1.5}$$

From the previous equations, it is possible to calculate the different heights of the reaction zones, the time of the pyrolysis process, the char reduction process assuming a constant pyrolysis surface temperature and a constant biomass consumption.

In this model the diameter of the reactor appears only in eq: 8.1.3, because A_g is proportional to it. The presence of A_g in the model can, at first, lead to suppose that this model considers the diameter as an influent parameter for gasifier modeling.

The following theoretical discussion allows us to understand how the diameter influence is nullified by the reset of the equations employed in the model:

Imagine if we have a large stratified reactor, biomass and air entering from the top and ideally distributing on the top surface of the gasification bed. Because of this perfect distribution of fuel and oxidant, the gasifier is perfectly stratified. All the particles at the same height are at the same temperature and equal reaction are occurring.

Now, imagine plunging a large tube in the gasifier, as sketched in Fig. 8.1, nothing changes from the previous situation, the tube is open at both ends allowing air and biomass to enter from the top and char and gas to exit from the bottom. The tube wall is thin and does not disturb the thermal behavior of the gasifier. But from a topological perspective, the tube wall defines a gasifier in the gasifier, something similar to the 'inception' model

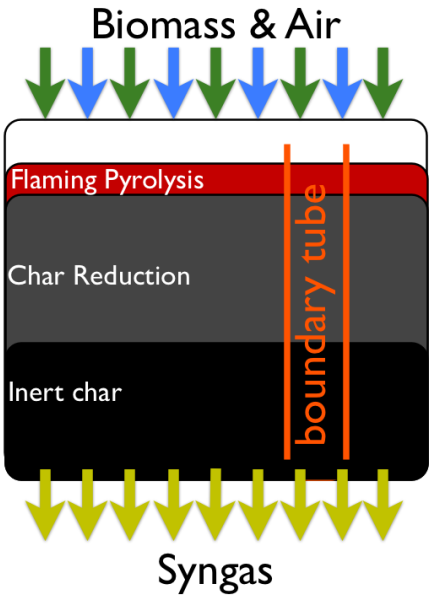

Figure 8.1: Theory of the gasifier in the gasifier

described in Chapter 4; but now the first gasifier and the small one have the very same boundary conditions.

The air and the biomass entering the reactor are uniformly distributed, for this reason the biomass or the air that enters in the tube are going to be proportionally less than the fuel and air consumption of the whole system. Moreover this proportion is the same as one on the surface.

The less biomass entering the tube, the less air balancing each other maintaining the fuel velocity constant inside and outside the tube. Because the tube does not disturb the gasifier, it is easy to visualize that the biomass particles move down all at the same velocity, inside or outside the boundary created by the tube.

For this reason, when in model, the A_g value is changed, other parameters such as velocity or fuel consumption need to be tuned, this nullifies the influence of the diameter on the model that is not able to evaluate differences related to diameter variations on the performance of a downdraft gasifier. Even in a more complex model, such as the Wang-Kinoshita model proposed in Chapter 4, the only geometrical parameter that influences the output (for a fixed fuel velocity), is the height of the bed. The next section is going to analyze the issues related to different size reactors. For a better comprehension of the problem a G.E.K. reactor has been completely modified in order to create a stratified downdraft gasifier, see fig. 8.9.

8.2 Different reactors analyses

8.2.1 250 kW reactor

The downdraft stratified reactor studied in Chapters 3, 4 has the distinctive trait of a diameter larger than the bed height (60 cm x 80 cm). This feature makes this reactor perfect for rewiring the issues related to large diameter reactors:

1. The syngas needs to be drawn uniformly from the bottom of the reactor, if the suction area doesn't coincide to the bottom area, the layer distribution is deformed and the stratification is compromised.

2. The air needs enough space to distribute on the top surface of the reactor. On a fluid-dynamic point of view a completely open top reactor is the best solution, but, is not applicable for a large scale power plants for safety reasons. If the engines stop running, there is always a moment before the gas is sent to the torch when the gasifiers produce an amount of gas that is not drawn. This gas exits from the top of the reactor. If the gasifier top is not partially closed, the gas finds the flamed surface and enough air to blow up. Moreover, from a thermodynamical perspective, an open top, represents a critical point of heat dispersion. The stratified gasifier, especially if operated with dry biomasses, presents the flaming pyrolysis zone on the very top of the reactor. This flaming surface can disperse a high amount of heat. For this reason the top part of the reactor needs a proper design, the height of the walls and the dimension of the air and biomass entering deeply influence the thermal dispersion of the reactor. Otherwise, a small air inlet is characterized by higher air speeds, for this reason in large reactors is fundamental to leave enough space between the flaming bed and the top lid of the reactor. The reactor analyzed here has a characteristic air inlet sketched in Fig.8.2. In this way, the air has enough speed to 'push' the flaming pyrolysis zone deeper into one side of the reactor. This phenomenon was discovered analyzing the stressed zones in the steel jacket Fig. 8.2, 8.3.

3. Similar to the air distribution, the biomass spreading in the reactor is equally important. When the biomass cannot be introduced in a proper way, a mixer can be used for biomass bed levelling. The critical situation that can occur is that, if the FP zone rises, the mixer can disturb the reactions that occur there, moreover the high temperature developed in this zone forces the use of highly resistant materials and layouts that reduce the thermal creep effect.

4. As discussed in Chapter 4, large reactors, in contrast with some reviews [8, 12] are susceptible to bridging problems. This problem is partially related and caused by air and biomass imperfect distribution, but biomass rheology, local slagging or char packing can causes or increase this problem as well. In this case a second mixer in the char reduction zone can solve part of the problems presented here in Fig. 8.2, but the fragility of char increases the risk of pulverization during the mixing process, changing the gasification conditions and increasing the complexity of the gas cleaning process.

8.2.2 Lab scale gasifiers

The opposite design for a gasifier is the lab scale reactor. For comparison purposes a 3 inches diameter downdraft gasifier was designed and built. The height of the gasifier was fixed at 80 cm (60 cm for bed reactions and 20 for air and biomass spread). The reactor is illustrated in Fig. 8.4, it is composed of all the basic elements of a gasifer and is able to work continuously. This facility was used for this preliminary test on small diameter reactors and is going to be the basis for the calorimetric approach for performance monitoring as reported in Chapter 5. Reactors with such a small diameter have different

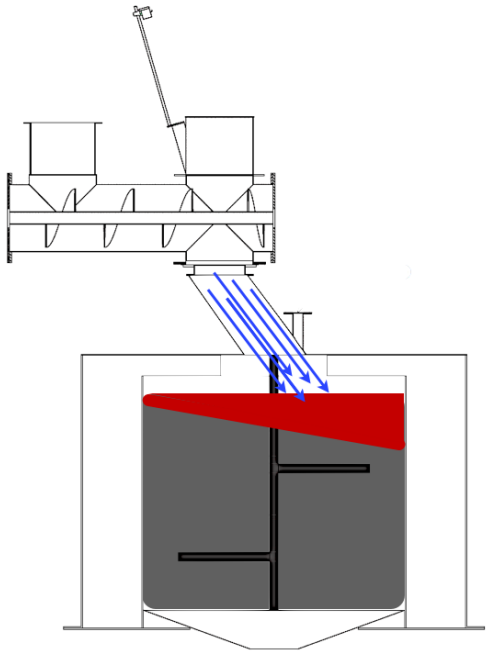

Figure 8.2: Flaming pyrolysis shift for asymmetric air inlet

problems if compared with the large scale. They require a continuous monitoring of the inner temperature in order to promptly discover biomass packing in some part of the reactor, creating a dome that avoids the descent of the biomass in the reactor. Moreover, differently from the large scale gasifier, in this case the wall of the reactor is the primary source of heat dispersion. A preliminary test on this facility gave results on temperature distribution similar to large scale gasifiers, but the reactor showed high fluctuation in gas quality with numerous self extinguishings of the torch flame. Preliminary results are reported in Table 8.1

Table 8.1: Lab-scale gasifier preliminary test

Diameter	3" (7.62 cm)
Bed height	60 cm
Flaming pyrolysis wall temperature	710 ^{o}C
Char reduction top temperature	630 ^{o}C
Biomass consumption	4.3 kg/h
Syngas flow rate	9 m^3/h
Char production	4.5 %

This test shows that the gasification reaction are shifted a little to combustion with a smaller char production and higher gas flow if compared with literature of the stratified reactor [6, 10]. In fact, the higher thermal dispersion needed to be compensated with a higher equivalence ratio in order to increase the heat produced in the reactor.

This reactor will be upgraded in order to continue this study on the influence of down-draft reactors following the guidelines discussed in the next section.

Figure 8.3: Steel jacket collapsing

8.3 Design of a heated reactor with feedback control

In the previous section the differences between large and micro scale gasifiers are reported and discussed. These differences can be attributed to many causes, included the thermal losses of the reactor from the walls or the gasifier lid or different air and fuel distribution. Actually, during the tests with different diameters it is extremely hard to distinguish the causes of the different behaviors of the reactors. For this reason, an approach similar to the guarded ring of the hot plates used for thermal conductivity measurements was adopted:

Six high temperatures, heavy insulated heating tapes were wrapped around the reactor as reported in Fig. 8.5, moreover an 80 cm crystal tube was plugged in the reactor. The tube was filled with 6 k-type thermocouples placed at different heights in the gasifier. An Arduino-based CPU was used to 'read' the temperatures of the thermocouples and impose the same temperature to the heating tapes. In this way an average value of the temperature in every layer of the reactor is set at its walls. This permits the nullification of the thermal losses. In Section 8.2 the differences between reactors are explained using the concept of the small tube in a large gasifier. Here, after a transient time, the heating tapes controlled by the inner thermocouples allow to simulate the lab-scale gasifier to be placed in a bigger reactor. In this way an experimental campaign can be repeated, the difference between the heated and not heated micro gasifier outputs can be ascribe to thermal losses. Moreover the differences between large diameter reactors and the heated lab-scale one can be now ascribed to other causes different from the thermal one.

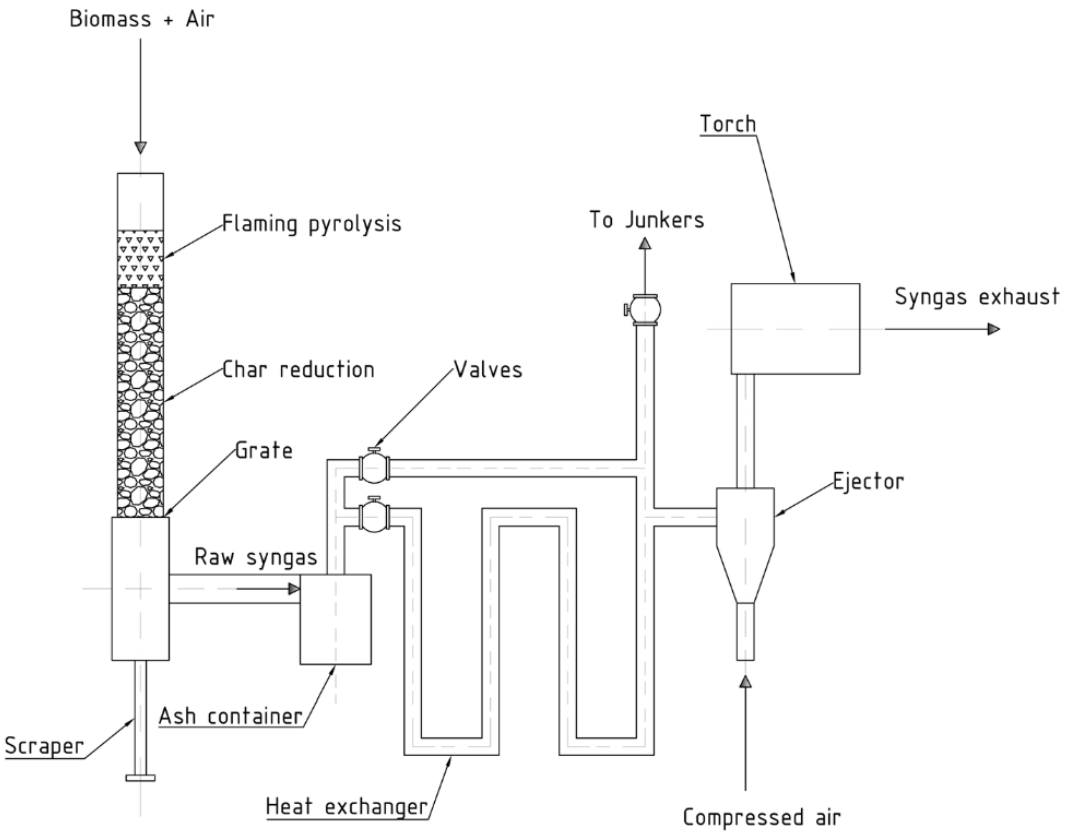

Figure 8.4: Lab-scale (stratified) downdraft reactor

8.4 Micro-scale gasifiers

Because of the limits of the large and lab scale gasifiers, the best solution seems to be between the proposed diameters. For this reason a modified G.E.K. was used as a basis for the design and creation of a stratified reactor. The internal part of the reactor was substituted with a stainless steel tube with ID of 26 cm. The bed height is 55 cm. The original path for the syngas drawing was maintained, in this way the gas passes in the annulus between the external jacket and the reactor tube as reported in Figures 8.8 and 8.9. Contrary to the original design, the stratified reactor does not use the sensible heat of syngas for air pre-heating. This reduces the efficiency of the gasifier, but on the other hand, this design has different advantages:

- The stratified reactor is able to process biomasses with non homogeneous size or wood type
- There are no nozzles or throats that need to be designed properly for a specific fuel
- The open top does not require a sealed reactor because there is no issue about the combustion zone rising.

In order to investigate the capability of this reactor to process low quality biomasses, two tests were carried out on two different fuels: Both were obtained by bio-shredding the

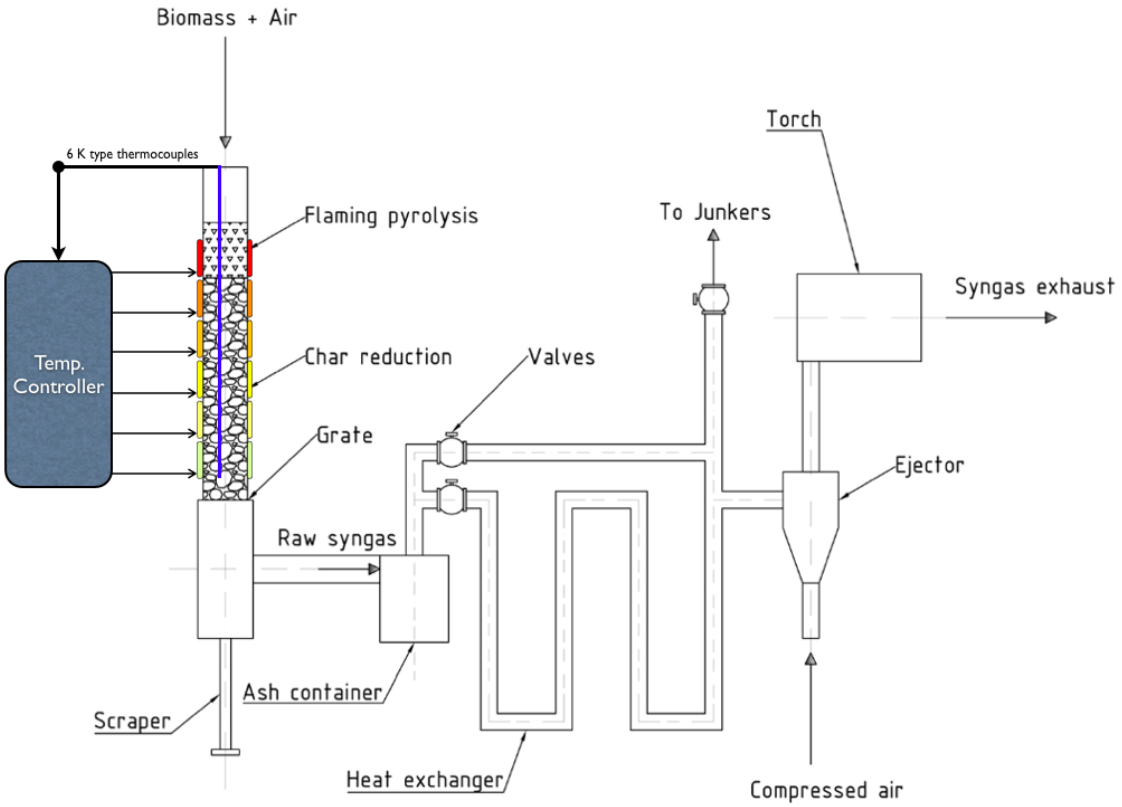

Figure 8.5: Upgraded lab-scale (stratified) downdraft reactor

biomasses collected from forest nursery maintenance. The biomass was divided into fine and medium size, as reported in Figures 8.6 and 8.7.

Both the biomasses used for this study were completely characterized, results of the chemical and physical investigations are reported in Table 8.2.

The elemental analysis was obtained through EA 1110 CHNS-O analyzer, while the higher heating value was obtained experimentally testing two biomass samples in a Mahler Bomb calorimeter woking with oxygen atmosphere with pressure of 20-25 bar. Then the ash content was obtained with a 4 hour permanence of the biomass samples in lab stove with temperature set to 550^o C.

The two biomasses were tested in the stratified-modified G.E.K. reactor. Two tests were done for each biomass typology. After a start-up period of about 30 minutes, a cylinder of syngas was filled for every test. Results of the gas analysis are reported in Table 8.3

The gas analysis outlined an instability in gasification reactions, in fact the gas composition and heating values change considerably in the different tests. One of the major causes of these instabilities is the slagging and channelling in the reactor, as reported in Figures 8.11 and 8.10.

The melted ashes avoid a correct spreading of gas on the reaction bed. This causes instabilities related to position and dimension of the melted ashes. Without a scraper or a mixer able to demolish the conglomerates the reactor was able to process such a low quality biomass only for a limited time. After a few hours the reactor needed to be emptied and the conglomerates removed.

Figure 8.6: medium size biomass investigated in this section

Looking at the results obtained, the stratified reactor designed is able to process the biomasses studied but, more suitable fuel is required for a correct and continuous running of the system. These biomasses represent the lower level of fuel exploitable in such a reactor, in terms of dimensions, non-homogeneity and inert content.

Just for comparison, two tests with the original G.E.K. reactor with the proposed biomasses were proposed. The G.E.K. in 40 minutes of running never reached a steady condition of gasification and the tests were stopped.

8.5 Summary

Contrary to the model operation, gasifiers with different diameters behave very differently. Some advantages related to stratified reactors, such as low tar content or absence of channelling, are not characteristic of all the stratified gasifiers of every diameter. Small scale seems to be a good solution and is able to process low quality biomasses with few running issues that can be fixed by designing the reactor properly. In order to investigate the causes of these differences an experimental method has been proposed and consists of a feedback controlled stack of heating tapes used for nullifying the thermal dispersion in the reactor wall, simplifying the family of causes of behavioral differences.

Figure 8.7: Small size biomass investigated in this section

Figure 8.8: Stratified reactor obtained from G.E.K.

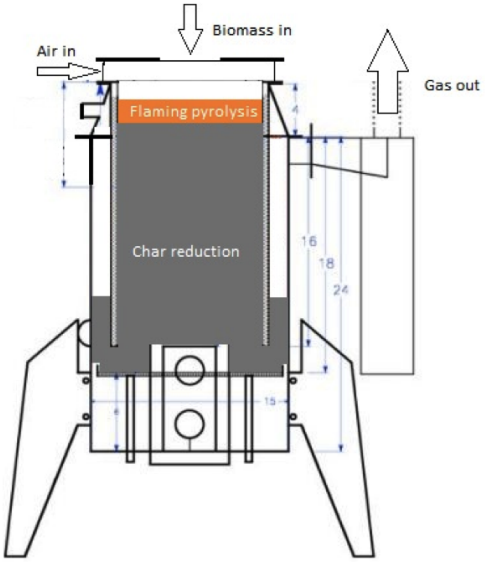

Figure 8.9: Stratified reactor obtained from G.E.K.; scheme of reactor length and gas flow

Table 8.2: Chemical, geometrical an physical properties of fine and medium biomasses from three nursery maintenance

Parameter	Medium size biomass	Small size biomass
Moisture content	4.79 % m/m	7.06 %
Carbon content	45.42 % m/m	46.912 % m/m
Hydrogen content	6.31 % m/m	7.32 % m/m
Nitrogen content	1.68 % m/m	1.71 % m/m
Oxygen content	30.41 % m/m	37.14 % m/m
HHV	14.4 MJ/kg	13.1 MJ/kg
Ash content	16.18 % m/m	6.91 % m/m

Table 8.3: Chemical, geometrical an physical properties of fine and medium biomasses from three nursery maintenance

Molar fraction %	H_2	CH_4	CO	CO_2	N_2	HHV [MJ/Nm^3]
Medium size test 1	7.6	2.6	15.7	17.1	56.9	4.00
Medium size test 2	4.7	1.0	17.8	14.0	62.5	3.24
Small size test 1	12.4	2.2	16.3	17.1	52.0	4.53
Small size test 2	6.2	2.1	11.9	21.5	58.4	3.12

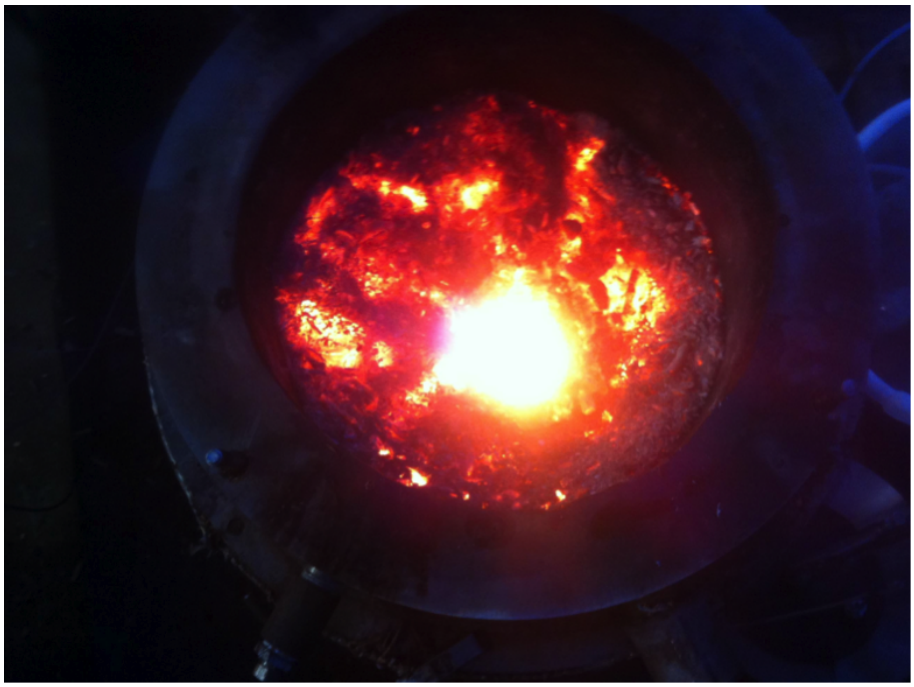

Figure 8.10: Channeling in stratified reactor

Figure 8.11: Melted ashes found in the stratified reactor

Chapter 9

Stratified reactors in industrial application

This thesis is focused on stratified downdraft reactors and related issues. The experimental and analytical investigation of these gasifiers is reviewed here together with the prevision for the industrialization of this technology.

9.1 Medium scale power plants

Since the first studies reported in Chapter 3, the gasifiers investigated were characterized by low efficiencies, high tar content in the gas and frequent stops due to extraordinary maintenance. Even with a complex gas cleaning system (cyclone, water scrubber, electrostatic filters) the fouling of engine turbines was frequent. All these factors rule against the use of stratified downdraft reactors for medium and large scale applications. Actually the study proposed in Chapter 4 resolved part of the problems working on control parameters of the power plant system. In view of industrial applications, some matters need to be taken into account in order to reach acceptable values of efficiency and reliability: the design of a downdraft open core reactor must be based on all the technical solutions that contribute to the stratification of the different zones in the reactor. In first place all the issues that row against a proper stratification have to be solved:

- The gas suction needs to take place form the whole bottom surface of the reactor without interferences. The gas suction point needs to be placed where it does not affect its own operation. If the gas suction point is too close to some part of the reactor bottom grid, the gas flowing path is disturbed. For this reason, some gasifiers use the same solution proposed for Imbert reactors where the gas is forced to pass between two layers of the reactor jacket. This solution gives more chances to the dust particles to be separated from the gas stream and, moreover, it increases the reactor efficiency reducing the thermal dispersion through the reactor surfaces.

- Similar to the previous point, as the gas flows through the gasifier, it needs to move uniformly during all its permanence in the reaction bed: first of all, the fuel and the gasification agent require a sufficient volume above the biomass bed in order to properly spread on the top surface of the reactor; moreover, in the whole reaction bed, biomass packing, bridging and channeling as well as slag formation must be

avoided. A scraper and a mixer can prevent these issues but they can also disturb the stratification as reported in the previous chapter (Chapter 8). But a proper design of the mixer starts from a proper knowledge of the reaction zones lengths, making modeling and preliminary tests vital for reactor design.

- Because these reactors start from low nominal efficiencies it is vital to properly design the insulation of the gasifier. As reported in the previous discussion, Chapter 8, especially when dry biomasses are processed, the flaming pyrolysis zone rises and major heat dispersions occur. Moreover these reactors are hardly ever equipped with a air pre-heating system, when possible it is best to practice by using the sensible heat of syngas or engine exhaust gases for air pre-heating. The gas-gas heat exchangers have low efficiencies and sometimes they are complex, but in these reactors the advantages of air pre-heating are payed in a higher energy conversion efficiency and less influence of environmental conditions on the gasification process.

On the basis of the previous discussion, two opposite scenarios are proposed:

1. Single biomass gasifier: a stratified reactor can operate for several thousands hours a year only under strict conditions. First of all the biomass needs to be uniform without sawdust or dirt. The moisture content of the biomass need to be controlled and limited to a fixed range. Once the biomass is defined the power plant can be designed. Models and experimental investigation define the zone lengths and the gas properties. This information permits to choose the engines, to design the mixer and the gas cleaning system. If the ash content is low and the preliminary tests do not outline slags formation, the power plant is able to work for a long time without maintenance.

2. A completely different approach consists in a design for flexibility. When it is not possible to control the quality of biomasses processed by the power plant, it is vital to design the reactor in order to facilitate maintenance operations. The slags can be broken by the mixer and the char scraper if they are properly designed. An IC engine can not be used in this scenario due to the low controls on gas cleaning process. An ORC system is a better solution because it is able to work with a gas characterized by high tar content and variable HHV. The solution outlined here is the opposite of the power plant described previously, the reactor needs to be high enough to guarantee the char reduction reactions to take place under very different conditions, moreover secondary air inlets may be necessary when the biomass particle size is too small or the reactor is too wide.

9.2 Small and micro scale power production

Stratified downdraft reactors can be produced in small and micro scale, an example is reported in Chapter 8. These reactors have the major advantage of being incredibly simple, the basic design consists of a cylinder, a scraper for char and ash removal, a cyclone and a bio-filter. If the purpose of the gasifier is heat production these components are sufficient. The system here outlined does not represent a power plant; for power production it is necessary to equip the gasifier with a feeder, but when air pre-heating is not required, the gasifier basically consists in an open top reactor and many feeding methods are suitable.

The simplicity of these small scale reactors allows to design and produce low cost systems with two major applications for the market:

- There is a big market niche composed of all the industries that have a considerable amount of biomasses waste available, but not enough to justify an investment such as a full-scale power plant because of the costs and the impossibility to run these system 24-7. Otherwise small scale power plants have costs that justify the investment even when they work for 3000-4000 hours a year. On the other hand the simplicity of these systems is payed by an incomplete autonomy: it is important to guarantee all the maintenance operations after every run (or few runs), moreover these simple systems rarely are designed for more than 5-6 hours of work with a batch of biomass.
- The second market that opens to small scale simple reactors is the underdeveloped countries market. In these countries agriculture is a predominant and widespread sector, producing a sufficient amount of by products for running a small power pant every few hectares of cultivations. Moreover in these countries gasifier-engine systems can partially cover the lack of electricity, ensuring a few hours of electrical power. The simple design allows to the manufacturing of these reactors directly on-site, importing only a few components, such as the engine or the instruments for process control.

9.3 Chapter summary

Downdraft stratified reactors are nowadays, in an unusual situation: on one hand they represent state of the art for the simplicity and flexibility in fuel choice without the high tar content of updraft reactors. On the other hand these gasifiers never rose the attention of the scientific and industrial communities and few attempts to industrialize these reactors were made. The recent interest in renewable energy is giving stratified reactors the possibility to take a market niche, but first of all few issues related to these gasifiers need to be fixed. For this reason, research will reinforce its key role in the next years.

Concluding Remarks

The aim of the presented research is to investigate the biomass gasification in downdraft stratified reactors when used for electrical energy production. The task was carried out starting with full-scale power plants investigation, then switching to pilot scale and lab scale reactors. In Chapter 2 a simple energy-based model was proposed and discussed. It is proven to be a useful tool for biomass-based power plant designs. Moreover, Chapter 2 shows that the gasifier-IC systems are the best solution for energy conversion due to their high efficiencies. Different results were obtained simulating and analyzing a gasifier with low efficiency. When the amount of tar increases, two major effects occur: systems such as IC-engines and gas turbines are not able to process gasses with high tar content, moreover, from an energy balance point of view, the higher energy leaves the gasifiers in the tar, the less energy remains in the gas. For these reasons the analytical analysis proposed in Chapter 2 suggests external combustion engines whenever it is not possible to adopt primary methods for tar reduction.

The first step that needs to be taken for a plant monitoring is reported in Chapter 3. The main goal of Chapter 3 was to define both a simple energy model and an experimental campaign able to monitor a full-scale gasifier-engine power plant. The proposed model is based on energy and mass balances, it is proven to be able to predict the behavior of the gasifier investigated with a maximum error of 19%. Errors in the models are caused by imprecisions in the experimental data acquisition and in the excessive simplicity of the model proposed in this chapter. The main errors in the experimental analysis were cased by the air and gas flow rate measurements. During the tests some parameters were evaluated by acquisition of few single values even when these variables were characterized by big fluctuations. For this reason this approach may have lead to considerable errors. Moreover, another source of imprecision was the biomass flow rate measurement due to the intermittent operation of the dryer. The dryer contained a volume of biomass several times greater than the amount used for the single tests. On the other hand, this preliminary approach has shown how a few simple equations can give a useful feedback on the performance of a power plant. During the first study reported here, the tar overproduction was related to the air excess and the non-homogeneous fuel. The biomass used in this work was characterized by a high content of very small pieces of wood similar to sawdust. This hypothesis is partially true, in fact a better understanding of the problem came only after the modeling analysis performed in Chapter 4.

The kinetic model proposed in Chapter 4 pointed out different issues of large reactors. Some of these peculiarities can be extended to other stratified reactors, giving important guidelines for gasifier design and operation. In particular the experimental campaigns and the model analysis have drawn attention to the extreme sensitivity of these reactors to loading operations. Subdividing the loading into small amounts, a consistent reduction

of tar and water production were observed. The approach reported in Chapter 4 has integrated the results obtained in Chapter 3: the "inception" model explained the effect of large loads on the reactions in terms of local choking and bridging phenomena enhancement. These observations demonstrate that precise parameters control is the very first method for tar reduction and efficiency increase in these reactors.

During the literature review and the experimental campaigns discussed in the first chapters of this thesis, it is possible to underline how the tar represents a major critical point of the gasification process. Tar affects the efficiency and avoids the use of IC engines or turbines. Moreover the measurement of the tar amount in the syngas stream is difficult. Power plants are provided with tar separation systems, but as discussed in Chapter 3 these methods have delays and inertias in tar disposal. These delays avoid a real-time monitoring of tar content in the gas. This issues about plant running and tar monitoring are reported in literature, where some tar measurement methods are proposed but, the complexity of these methods affect reactors of any size. Chapters 5 and 6 report two innovative methods for on-line tar measurement, the first method proposed here consists of a calorimetric analysis of the raw and clean gases, an equation set was developed in order to correlate the heating values of the two gas streams to the tar production. The second method, tested at the University of British Columbia, consists of a gas dilutor coupled with a light-scattering particle meter. The preliminary results from these two methods are encouraging, moreover, the second one, due to its compactness, is more suitable for multipoint measurements that can be used for cleaning processe control. The calorimetric method was also implemented with two equations set for gas composition analysis. The equations are promising, the method proposed can not substitute gas chromatography analysis but it represents a simple, cheap and robust tool for syngas composition investigation.

In Chapter 7 a new application for downdraft reactors was proposed. A micro scale reactor was modeled for on-site biodiesel production. The system proposed is a synergy of thermochemical and biochemical methods for conversion of biomasses. The approach proposed allows cutting all the costs and energy consumption related to transportation of products during all the steps of the industrial biodiesel production supply chain. The system discussed was proven to be innovative from an energetic and sociological point of view: in fact this method allows the complete energy use of all the organic matter from seeds, moreover the single plant centralizes all the passages of biodiesel production. The surface necessary for sustainability of the system is about 14 hectares for a pilot plant equipped with a 10 kW engine, therefore a farmer, or a union of farmers, can organize in order to purchase the equipment (gasifier, press, engine, biodiesel and methanol reactors) and gain all earnings from them.

The present study represents a limited, but nevertheless, significant contribution to the research in the field of gasification in stratified downdraft reactors. The studies proposed in this thesis have opened new paths for research, the reactor typology studied here represents a good compromise between flexibility in fuel restrictions and gas quality. The downdraft stratified, if properly designed, are able to feed IC or external combustion engines. Future work needs to focus on reduction of instabilities and other issues reported in this thesis in order to enable the downdraft reactors to be more competitive on the gasification market.

List of Figures

List of Tables

Bibliography

[1] T.C. Acharjee, C.J. Coronella, and V.R. Vasquez. Effect of thermal pretreatment on equilibrium moisture content of lignocellulosic biomass. *Bioresource Technology*, 102:4849–4854, 2011.

[2] M.J.C. van der Stelt, H. Gerhauser, J.H.A. Kiel, and K.J. Ptasinski. Biomass upgrading by torrefaction for the production of biofuels: a review. *Biomass and Bioenergy*, 35:3748–3762, 2011.

[3] ENEA. Energia dalle biomasse, tecnologie e prospettive. Technical report, Ente per le Nuove tecnologie, l'Energia e l'Ambiente - Regione Siciliana, assessorato industria, 2008.

[4] John E. White, W. James Catallo, and Benjamin L. Legendre. Biomass pyrolysis kinetics: A comparative critical review with relevant agricultural residue case studies. *Journal of Analytical and Applied Pyrolysis*, 91(1):1–33, 2011.

[5] Ozlem Onay and O.Mete Kockar. Slow, fast and flash pyrolysis of rapeseed. *Renewable Energy*, 28(15):2417–2433, 2003.

[6] Thomas B. Reed and Agua Das. *Handbook of Biomass Downdraft Gasifier Engine Systems*. The biomass energy foundation press, 1988.

[7] FAO Forestry Department Mechanical Wood Products Branch. *Woodgas as engine fuel*, volume ISBN 92-5-102436-7. F.A.O., 1986.

[8] H.A.M. Knoef. *Handbook of Biomass Gasification*. BTG, 2005.

[9] Prabir Basu. *Biomass Gasification and Pyrolysis: Practical Design and Theory*. Academic Press, Elsevier, 2010.

[10] SERI. *Generator Gas: The Swedish Experience from 1939-1945, Di Ingenjörsvetenskapsakademien (Sweden)*. Solar Energy Research Institute, United States. Dept. of Energy,, Golden, Colorado, 1979.

[11] A. M. Squires. Clean fuels from coal gasification. *Science*, 184(4134):330–346, 1974.

[12] H.A.M. Knoef. *Handbook of Biomass Gasification, Second Edition*. BTG, 2012.

[13] B. Goldman and C. Jones. The modern portable gas-producer. *Journal of institute of fuel*, 63(12), 1939.

[14] T. B. Reed and S. Gaur. *A survey of biomass gasification*. NREL, 2001.

[15] R. Rauch. Biomass gasification to produce synthesis gas for fuels and chemicals. Technical report, IEA Bioenergy Agreement, 2003.

[16] Z.A Zainal, Ali Rifau, G.A Quadir, and K.N Seetharamu. Experimental investigation of a downdraft biomass gasifier. *Biomass and Bioenergy*, 23(4):283–289, 2002.

[17] Yan Cao, Yang Wang, John T. Riley, and Wei-Ping Pan. A novel biomass air gasification process for producing tar-free higher heating value fuel gas. *Fuel Processing Technology*, 87(4):343–353, 2006.

[18] X.T. Li, J.R. Grace, C.J. Lim, A.P. Watkinson, H.P. Chen, and J.R. Kim. Biomass gasification in a circulating fluidized bed. *Biomass and Bioenergy*, 26(2):171–193, 2004.

[19] K.N. Sheeba, J. Sarat Chandra Babu, and S. Jaisankar. Air gasification characteristics of coir pith in a circulating fluidized bed gasifier. *Energy for sustainable development*, 13(3):166–173, 2009.

[20] Lopamudra Devi, Krzysztof J Ptasinski, and Frans J.J.G Janssen. A review of the primary measures for tar elimination in biomass gasification processes. *Biomass and Bioenergy*, 24(2):125–140, 2003.

[21] David Brown, Martin Gassner, Tetsuo Fuchino, and François Maréchal. Thermo-economic analysis for the optimal conceptual design of biomass gasification energy conversion systems. *Applied Thermal Engineering*, 29(11-12):2137–2152, 2009.

[22] T. B. Reed, R. Walt, S. Ellis, A. Das, and S. Deutch. Superficial velocity - the key to downdraft gasification. *4th Biomass Conference of the Americas; Oakland, CA*, 1999.

[23] Francisco V. Tinaut, Andrés Melgar, Juan F. Pérez, and Alfonso Horrillo. Effect of biomass particle size and air superficial velocity on the gasification process in a downdraft fixed bed gasifier. an experimental and modelling study. *Fuel Processing Technology*, 89(11):1076–1089, 2008.

[24] Juan Daniel Martínez, Electo Eduardo Silva Lora, Rubenildo Viera Andrade, and René Lesme Jaén. Experimental study on biomass gasification in a double air stage downdraft reactor. *Biomass and Bioenergy*, 35(8):3465–3480, 2011.

[25] L.C. Laurence and D. Ashenafi. Syngas treatment unit for small scale gasification-application to ic engine gas quality requirement. *Journal of Applied Fluid Mechanics*, 5(1):95–103, 2012.

[26] P. Hasler and Th. Nussbaumer. Gas cleaning for ic engine applications from fixed bed biomass gasification. *Biomass and Bioenergy*, 16(6):385–395, 1999.

[27] Z. Abu El-Rub, E. A. Bramer, and G. Brem. Review of catalysts for tar elimination in biomass gasification processes. *Ind. Eng. Chem. Res.*, 43:6911–6919, 2004.

[28] Kevin Jay Timmer. *Carbon conversion during bubbling fluidized bed gasification of biomasses.* PhD thesis, Iowa State University, 2008.

[29] Yi-Shun Chen, Shu-San Hsiau, Hsuan-Yi Lee, and Yau-Pin Chyou. Filtration of dust particulates using a new filter system with louvers and sublouvers. *Fuel*, 99:118.128, 2012.

[30] Thana Phuphuakrat, Tomoaki Namioka, and Kunio Yoshikawa. Absorptive removal of biomass tar using water and oily materials. *Bioresource Technology*, 102(2):543–549, 2011.

[31] R.S. Singh, S.S. Agnihotri, and S.N. Upadhyay. Removal of toluene vapour using agro-waste as biofilter media. *Bioresource Technology*, 97(18):2296–2301, 2006.

[32] R. Rameshkumar and K. Mayilsamy. A novel compact bio-filter system for a downdraft gasifier: An experimental study. *AASRI PROCEDIA*, 3:700–706, 2012.

[33] *Gasifier Experimental Kit, http://www.gekgasifier.com/*, 2013.

[34] S. Anis and Z.A Zainal. Tar reduction in biomass producer gas via mechanical, catalytic and thermal methods: A review. *Renewable and Sustainable Energy Reviews*, 15(5):2355–2377, 2011.

[35] Christopher Higman and Maarten van der Burgt. *Gasification*. GPP, 2008.

[36] C.C.P. Pian and K. Yoshikawa. Development of a high-temperature air-blown gasification system. *Bioresource Technology*, 79(3):231–241, 2001.

[37] J. Chen, X. Lu, H. Liu, and J. Liu. The effect of solid concentration on the secondary air-jetting penetration in a bubbling fluidized bed. *Power Technology*, 185(2):164–169, 2008.

[38] Scott Hurley, Chunbao (Charles) Xua, Fernando Preto, Yuanyuan Shao, Hanning Li, Jinsheng Wang, and Guy Tourigny. Catalytic gasification of woody biomass in an air-blown fluidized-bed reactor using canadian limonite iron ore as the bed material. *Fuel*, 91(1):170–176, 2012.

[39] Steve Lysenko, Samy Sadaka, and Robert C. Brown. Comparison of mass and energy balances for air blown and thermally ballasted fluidized bed gasifiers. *Biomass and Bioenergy*, 45:95–108, 2012.

[40] V. Belgiorno, G. De Feo, C. Della Rocca, and R.M.A. Energy from gasification of solid wastes. *Waste Management*, 23:1–15, 2003.

[41] Lath E. and P. Herbert. Make co from coke, co2, and o2. *Hydrocarbon Processing*, 64(8):55–58, 1986.

[42] P. Lv, Z. Yuan, L. Ma, C. Wu, T. Chen, and J. Zhu. Hydrogen-rich gas production from biomass air and oxygen/steam gasification in a downdraft gasifier. *Renewable Energy*, 32(13):2173–2185, 2007.

[43] B.O. Oboirien, A.D. Engelbrecht, B.C. North, V.M. du Cann, and R. Falcon. Textural properties of chars as determined by petrographic analysis: Comparison between air-blown, oxygen-blown and oxygen-enriched gasification. *Fuel*, 101:16–22, 2012.

[44] Gong Cheng, Pi wen He, Bo Xiao, Zhi quan Hu, Shi ming Liu, Le guan Zhang, and Lei Cai. Gasification of biomass micron fuel with oxygen-enriched air: Thermogravimetric analysis and gasification in a cyclone furnace. *Energy*, 43(1):329–333, 2012.

[45] G. Schuster, G. Löffler, K. Weigl, and H. Hofbauer. Biomass steam gasification – an extensive parametric modeling study. *Bioresource Technology*, 77(1):71–79, 2001.

[46] H. Hofbauer and R. Rauch. Hydrogen-rich gas from biomass steam gasification. Technical report, Institute of Chemical Engineering Fuel and Environmental Technology, 1998.

[47] Toshiaki Hanaoka, Seiichi Inoue, Seiji Uno, Tomoko Ogi, and Tomoaki Minowa. Effect of woody biomass components on air-steam gasification. *Biomass and Bioenergy*, 28(1):69–76, 2005.

[48] Yoshinori Tanaka, Tsuyoshi Yamaguchi, Kenji Yamasaki, Akifumi Ueno, and Yoshihide Kotera. Catalyst for steam gasification of wood to methanol synthesis gas. *Ind. Eng. Chem. Res.*, 23(2):225–229, 1984.

[49] E.G. Baker and M.D. Brown. Catalytic steam gasification of bagasse for the production of methanol. In *energy from biomass and wastes meeting*, 1983.

[50] I. Iliuta, A. Leclerc, and F. Larachi. Allothermal steam gasification of biomass in cyclic multi-compartment bubbling fluidized-bed gasifier/combustor – new reactor concept. *Bioresource Technology*, 101(9):3194–3208, 2010.

[51] Caecilia R. Vitasari, Martin Jurascik, and Krzysztof J. Ptasinski. Exergy analysis of biomass-to-synthetic natural gas (sng) process via indirect gasification of various biomass feedstock. *Energy*, 36(6):3825–3837, 2011.

[52] Matthias Mayerhofer, Panagiotis Mitsakis, Xiangmei Meng, Wiebren de Jong, Hartmut Spliethoff, and Matthias Gaderer. Influence of pressure, temperature and steam on tar and gas in allothermal fluidized bed gasification. *Fuel*, 99:204–209, 2012.

[53] Marcin Siedlecki, Wiebren de Jong, and Adrian H.M. Verkooijen. Fluidized bed gasification as a mature and reliable technology for the production of bio-syngas and applied in the production of liquid transportation fuels—a review. *Energies*, 4:389–434, 2011.

[54] Manuel Campoy, Alberto Gómez-Barea, Angel L. Villanueva, and Pedro Ollero. *Ind. Eng. Chem. Res.*, 47(16):5857–5965, 2008.

[55] F. Marini. *Monitoraggio e valutazione delle prestazioni di un impianto di cogenerazione a cippato di legno con gassificatore e motore Stirling.* CISA, http://www.centrocisa.it/ImpiantiRealizzati/stirlingCasteldaiano.php, 2012.

[56] D. Khummongkol and W. Arunlaksadamrong. Performance of an updraft mangrove-wood gasifier. *Energy*, 15(9):781–784, 1990.

[57] E. Kurkela, P. Ståhlberg, P. Simell, and J. Leppälahti. Updraft gasification of peat and biomass. *Biomass*, 19(1-2):37–46, 1989.

[58] J.G. Brammer and A.V. Bridgwater. The influence of feedstock drying on the performance and economics of a biomass gasifier–engine chp system. *Biomass and Bioenergy*, 22(4):271–281, 2002.

[59] Arjan F. Kirkels and Geert P.J. Verbong. Biomass gasification: Still promising? a 30-year global overview. *Renewable and Sustainable Energy Reviews*, 15(1):471–481, 2011.

[60] F.P. Nagel, S. Ghosh, C. Pitta, T.J. Schildhauer, and S. Biollaz. Biomass integrated gasification fuel cell systems–concept development and experimental results. *Biomass and Bioenergy*, 35(1):354–362, 2011.

[61] J.G. Brammer and A.V. Bridgwater. The influence of feedstock drying on the performance and economics of a biomass gasifier–engine chp system. *Biomass and Bioenergy*, 22(4):271–281, 2002.

[62] B.S. Pathak, S.R. Patel, A.G. Bhave, P.R. Bhoi, A.M. Sharma, and N.P. Shah. Performance evaluation of an agricultural residue-based modular throat-type downdraft gasifier for thermal application. *Biomass and Bioenergy*, 32(1):72–77, 2008.

[63] P. N. Sheth and B. V. Babu. Production of hydrogen energy through biomass (waste wood) gasification. *International journal of hydrogen energy*, 35(19):10803–10810, 2010.

[64] M. Ouadi, J.G. Brammer, M. Kay, and A. Hornung. Fixed bed downdraft gasification of paper industry wastes. *Applied Energy*, 103:692–699, 2013.

[65] T.H. Jayah, Lu Aye, R.J. Fuller, and D.F. Stewart. Computer simulation of a downdraft wood gasifier for tea drying. *Biomass and Bioenergy*, 25(4):459–469, 2003.

[66] Inna Rudakova. Use of biomass gasification for transport. Master's thesis, LAPPEENRANTA UNIVERSITY OF TECHNOLOGY, 2009.

[67] Prokash C. Roy, Amitava Datta, and Niladri Chakraborty. Assessment of cow dung as a supplementary fuel in a downdraft biomass gasifier. *Renewable Energy*, 35(2):379–386, 2010.

[68] A. Saravanakumara, T.M. Haridasanb, and Thomas B. Reed. Flaming pyrolysis model of the fixed bed cross draft long-stick wood gasifier. *Fuel Processing Technology*, 91(6):669–675, 2010.

[69] Er. Bhakta B. Ale, Nawaraj Bhattarai, Jitendra Gautam, Pradeep Chapagain, and Pushpa K.C. Institutional gasifier stove: A sustainable prospect for institutional cooking. *Journal of the institute of engineering*, 7(1):1–8, 2009.

[70] J. Hasan, D. R. Keshwani, S. F. Carter, and T. H. Treasure. Thermochemical conversion of biomass to power and fuels. *Biomass to Renewable Energy Processes*, pages 437–489, 2010.

[71] R. Warnecke. Gasification of biomass: comparison of fixed bed and fluidized bed gasifier. *Biomass and Bioenergy*, 18(6):489–497, 2000.

[72] W. Renzenbrink, R. Wischnewski, J. Engelhard, A. Mittelstadt, and Rheinbraun-AG. High temperature winkler (htw) coal gasfiction – a fully developed process for methanol and electricity production. In *Gasification technology conference*, San Francisco, 1998.

[73] Christoph Pfeifer, Reinhard Rauch, and Hermann Hofbauer. In-bed catalytic tar reduction in a dual fluidized bed biomass steam gasifier. *Ind. Eng. Chem. Res.*, 43:1634–1640, 2004.

[74] Scott Hurley, Chunbao (Charles) Xu, Fernando Preto, Yuanyuan Shao, Hanning Li, and Jinsheng Wang amdand Guy Tourigny. Catalytic gasification of woody biomass in an air-blown fluidized-bed reactor using canadian limonite iron ore as the bed material. *Fuel*, 91:170–176, 2012.

[75] S. Rapagnà, N. Jand, and P.U. Foscolo. Catalytic gasification of biomass to produce hydrogen rich gas. *International journal of hydrogen energy*, 23(7):551–557, 1998.

[76] P. McKendry. Energy production from biomass (part 3): gasification technologies. *Bioresource Technology*, 83(1):55–63, 2002.

[77] E. Kurkela. Status of peat and biomass gasification in finland. *Biomass*, 18(3-4):287–292, 1989.

[78] Frank N. Reale and Tharam S. Dillon. Investigation into the use of large-scale total-energy systems in mild and warm climates. *Fuel*, 56(3):257–265, 1977.

[79] K.N Patil, R.N Singh, and S.U Saiyed. Case study of spreri natural draft gasifier installation at a ceramic industry case study of spreri natural draft gasifier installation at a ceramic industry. *Biomass and Bioenergy*, 22(6):497–504, 2002.

[80] Juan Daniel Martínez, Khamid Mahkamov, Rubenildo V. Andrade, and Electo E. Silva Lora. Syngas production in downdraft biomass gasifiers and its application using internal combustion engines. *Renewable Energy*, 38(1):1–9, 2012.

[81] Ulugbek Azimov, Eiji Tomita, Nobuyuki Kawahara, and Yuji Harada. Effect of syngas composition on combustion and exhaust emission characteristics in a pilot-ignited dual-fuel engine operated in premier combustion mode. *International journal of hydrogen energy*, 36(18):11985–11996, 2011.

[82] Bibhuti B. Sahoo, Niranjan Sahoo, and Ujjwal K. Saha. Effect of h2:co ratio in syngas on the performance of a dual fuel diesel engine operation. *Applied Thermal Engineering*, 49:139–146, 2012.

[83] Felipe Centeno, Khamid Mahkamov, Electo E. Silva Lora, and Rubenildo V. Andrade. Theoretical and experimental investigations of a downdraft biomass gasifier-spark ignition engine power system. *Renewable Energy*, 37(1):97–108, 2012.

[84] S. B. Ferreira and P. Pilidis. Comparison of externally fired and internal combustion gas turbines using biomass fuel. *Journal of energy resources technology*, 123(4):291–296, 2001.

[85] R. H. Williams and E. D. Larson. Biomass gasifier gas turbine power generating technology. *Biomass and Bioenergy*, 10(2-3):149–166, 1996.

[86] E. D. Larson, R. H. Williams, M. Leal, and L. V. Regis. A review of biomass integrated-gasifier/gas turbine combined cycle technology and its application in sugarcane industries, with an analysis for cuba. *Energy for sustainable development*, 5(1):54–76, 2001.

[87] J. Kalina. Integrated biomass gasification combined cycle distributed generation plant with reciprocating gas engine and orc. *Applied Thermal Engineering*, 31(14-15):2829–2840, 2011.

[88] L. Dong, H. Liu, and S. Riffat. Development of small-scale and micro-scale biomass-fuelled chp systems – a literature review. *Applied Thermal Engineering*, 29(11-12):2119–2126, 2009.

[89] M. Kautz and U. Hansen. The externally-fired gas-turbine (efgt-cycle) for decentralized use of biomass. *Applied Energy*, 84(7-8):795–805, 2007.

[90] H. Tan. Development of distributed heat and power cogeneration system integrated by gasifier, stirling engine and absorption cooler. *Applied mechanics and materials*, 66-68:1634–1641, 2011.

[91] Bios-bioenergiesysteme, H. Carlsen, and F. Biedermann. State-of-the-art and future developments regarding small-scale biomass chp systems with a special focus on orc and stirling engine technologies. *International nordic bioenergy conference*, 2003.

[92] J. De Ruyck, F. Delattin, and S. Bram. Co-utilization of biomass and natural gas in combined cycles through primary steam reforming of the natural gas. *Energy*, 32(4):371–377, 2007.

[93] Vladimir M. Zubtsov, Carlson C.P. Pian, and Kunio Yoshikawa. Potential applications of high-temperature air/steam-blown gasification and pyrolysis systems. *Energy*, 30(11-12):2229–2242, 2005.

[94] K. C. Waugh. Methanol synthesis. *Catalysis today*, 15(1):51–75, 1992.

[95] T. B. Reed, B.Levie, and M. S. Graboski. Fundamentals, development and scaleup of the air=oxygen stratified downdraft gasifier. Technical report, Pacific Northwest Lab., 1988.

[96] Michael Stöcker. Biofuels and biomass-to-liquid fuels in the biorefinery: Catalytic conversion of lignocellulosic biomass using porous materials. *Angewandte Chemie International Edition*, 47(48):9200–9211, 2008.

[97] Blanca Antizar-Ladislao and Juan L. Turrion-Gomez. Second-generation biofuels and local bioenergy systems. *Biofuels, Bioproducts and Biorefining*, 2(5):455–469, 2008.

[98] Ayhan Demirbas. Competitive liquid biofuels from biomass. *Applied Energy*, 88(1):17–28, 2011.

[99] B. G. Miller. *Coal Energy Systems*. Elsevier academic press, 2005.

[100] P. Upham and S. Shackley. Local public opinion of a proposed 21.5 mw(e) biomass gasifier in devon: Questionnaire survey results. *Biomass and Bioenergy*, 31(6):433–441, 2007.

[101] Isabella Aigner, Christoph Pfeifer, and Hermann Hofbauer. Co-gasification of coal and wood in a dual fluidized bed gasifier. *Fuel*, 90(7):2404–2412, 2011.

[102] J. S. Brar, K. Singh, J. Wang, and S. Kumar. Cogasification of coal and biomass: A review. *International Journal of Forestry Research*, 2012.

[103] K. Sjöström, G. Chen, Q. Yu, C. Brage, and C. Rosén. Promoted reactivity of char in co-gasification of biomass and coal: synergies in the thermochemical process. *Fuel*, 78(10):1189–1194, 1999.

[104] Daniele Fiaschi and Riccardo Carta. Co2 abatement by co-firing of natural gas and biomass-derived gas in a gas turbine. *Energy*, 32(4):549–567, 2007.

[105] Nexterra corporation. Nexterra systems corp. project. Technical report, BC Bioenergy Network, 2011.

[106] LTD HENAN JIEBANG ELECTRIC TECHNOLOGY CO. 2mw power plant proposal. Technical report, Great POwer, 2011.

[107] C. Z. Wu, H. Huang, S. P. Zheng, and X. L. Yin. An economic analysis of biomass gasification and power generation in china. *Bioresource Technology*, 83(1):65–70, 2002.

[108] Bram van der Drift. Status of biomass gasification. Technical report, ECN, 2008.

[109] I. Obernberger and G. Thek. Combustion and gasification of solid biomass for heat and power production in europe-state-of-the-art and relevant future developments. *8th European conference on industrial furnaces and boilrs*, 2008.

[110] Septimus van der Linden, Mark Wiley, Gary Williams, and Roel Swart. Syngas fuel hybrid 45 mw gtcc/orc power plant using modular 500 tpd coal/biomass modular pyrolytic gasification. *ASME Conference Proceedings*, 2010.

[111] C.M. van der Meijden, W. Sierhuis, and A. van der Drift. Waste wood fueled gasification demonstration project. *European Biomass conference and exhibition*, 2011.

[112] *Victory Gasifier, http://gasifier.wpengine.com/*, feb 2013.

[113] Stak-Gasifier. http://www.stakproperties.com. *Stak*, feb 2013.

[114] Leilei Dong, Hao Liu, and Saffa Riffat. Development of small-scale and micro-scale biomass-fuelled chp systems – a literature review. *Applied Thermal Engineering*, 29(11-12):2119–2126, 2009.

[115] Ronney Arismel Mancebo Boloy, Jose Luz Silveira, Celso Eduardo Tuna, Christian R. Coronado, and Julio Santana Antunes. Ecological impacts from syngas burning in internal combustion engine: Technical and economic aspects. *Renewable and Sustainable Energy Reviews*, 15(9):5194–5201, 2011.

[116] Marianne Salomón, Tuula Savola, Andrew Martin, Carl-Johan Fogelholm, and Torsten Fransson. Small-scale biomass chp plants in sweden and finland. *Renewable and Sustainable Energy Reviews*, 15(9):4451–4465, 2011.

[117] Kantawan Sarasuk and Boonrod Sajjakulnukit. Design of a lab-scale two-stage rice husk gasifier. *Energy Procedia*, 9:178–185, 2011.

[118] Malte Bartels, Weigang Lin, John Nijenhuis, Freek Kapteijn, and J. Ruud van Ommen. Agglomeration in fluidized beds at high temperatures: Mechanisms, detection and prevention. *Progress in energy combustion science*, 34(5):633–666, 2008.

[119] Filomena Pinto, Rui Neto André, Carlos Franco, Helena Lopes, Carlos Carolino, Ricardo Costa, and Ibrahim Gulyurtlu. Co-gasification of coal and wastes in a pilot-scale installation. 2: Effect of catalysts in syngas treatment to achieve sulphur and nitrogen compounds abatement. *Fuel*, 89(11):3340–3351, 2010.

[120] T.B. Reed and M.L. Markson. A predictive model for stratified downdraft stratified. *Progress in Biomass COnversion*, 4:219–254, 1983.

[121] J. Herguido, J. Corella, and J. González-Saiz. Steam gasification of lignocellulosic residues in a fluidized bed at small pilot scale. effect of the type of feedstock. *Ind. Eng. Chem. Res.*, 31(5):1274–1282, 1992.

[122] Debyani Ghosha, Ambuj D Sagara, and V.V.N. Kishore. Scaling up biomass gasifier use: an application-specific approach. *Energy Policy*, 34(13):1566–1582, 2006.

[123] Robert P. Ma, Richard M. Felder, and James K. Ferrell. Modeling a pilot-scale fluidized bed coal gasification reactor. *Fuel Processing Technology*, 19(3):265–290, 1988.

[124] Y. Wang and C. Kinoshita. Kinetic model of biomass gasification. *Solar Energy*, 51(1):19–25, 1993.

[125] T.B. Reed, B. Levie, M.L. Markson, and M.S. Graboski. A mathematical model for stratified downdraft gasifier. *Symposium on Mathematical Modeling of Biomass Pirolysis Phenomena*, 1983.

[126] T.B. Reed and B. Levie. A simplified model of the stratified downdraft gasifier. *International Bio-Energy Directory and Handbook*, pages pag. 379–389, 1984.

[127] M.P. Arnavat, J. C. Bruno, and A. Coronas. Review and analysis of biomass gasification models. *Renewable and Sustainable Energy Reviews*, 14:2841–2851, 2010.

[128] Francisco Jurado, Antonio Cano, and José Carpio. Modelling of combined cycle power plants using biomass. *Renewable Energy*, 28(5):743–753, 2003.

[129] Victoria Maxim, Calin-Cristian Cormos, and Paul Serban Agachi. Design of integrated gasification combined cycle plant with carbon capture and storage based on co-gasification of coal and biomass. *Computer aided chemical engineering*, 29:1904–1908, 2011.

[130] F. Casella and P. Colonna. Dynamic modeling of igcc power plants. *Applied Thermal Engineering*, 35:91–111, 2012.

[131] C. Mandl, I. Obernberger, and F. Biedermann. Modelling of an updraft fixed-bed gasifier operated with softwood pellets. *Fuel*, 89(12):3795–3806, 2010.

[132] Niladri Sekhar Barman, Sudip Ghosh, and Sudipta De. Gasification of biomass in a fixed bed downdraft gasifier – a realistic model including tar. *Bioresource Technology*, 107:505–511, 2012.

[133] C. Di Blasi. Dynamic behaviour of stratified downdraft gasifiers. *Chemical Engineering Science*, 55(15):2931–2944, 2000.

[134] A. Gómez-Barea and B. Leckner. Modeling of biomass gasification in fluidized bed. *Progress in energy combustion science*, 36(4):444–509, 2010.

[135] Susanna Nilsson, Alberto Gómez-Barea, Diego Fuentes-Cano, and Pedro Ollero. Gasification of biomass and waste in a staged fluidized bed gasifier: Modeling and comparison with one-stage units. *Fuel*, 97:730–740, 2012.

[136] Qi Miao, Jesse Zhu, Shahzad Barghi, Chuangzhi Wu, Xiuli Yin, and Zhaoqiu Zhou. Modeling biomass gasification in circulating fluidized beds. *Renewable Energy*, 50:655–661, 2013.

[137] Yurany Camacho Ardila, Jaiver Efren Jaimes Figueroa, Betânia Hoss Lunelli, Rubens Maciel Filho, and Maria Regina Wolf Maciel. Syngas production from sugar cane bagasse in a circulating fluidized bed gasifier using aspen plus^{TM}: Modelling and simulation. *Computer aided chemical engineering*, (2012):1093–1097, 30.

[138] Wayne Doherty, Anthony Reynolds, and David Kennedy. The effect of air preheating in a biomass cfb gasifier using aspen plus simulation. *Biomass and Bioenergy*, 33(9):1158–1167, 2009.

[139] Naveed Ramzan, Asma Ashraf, Shahid Naveed, and Abdullah Malik. Simulation of hybrid biomass gasification using aspen plus: A comparative performance analysis for food, municipal solid and poultry waste. *Biomass and Bioenergy*, 35(9):3962–3969, 2011.

[140] A. K. Sharma. Equilibrium and kinetic modeling of char reduction reactions in a downdraft biomass gasifier: A comparison. *Solar Energy*, 82(10):918–928, October 2008.

[141] Prokash C. Roy, Amitava Datta, and Niladri Chakraborty. Modelling of a downdraft biomass gasifier with finite rate kinetics in the reduction zone. *International journal of energy research*, 33(9):833–851, 2009.

[142] H. Molintas and A.K. Gupta. Kinetic study for the reduction of residual char particles using oxygen and air. *Applied Energy*, 88(1):306–315, 2011.

[143] B.V. Babu and Pratik N. Sheth. Modeling and simulation of reduction zone of downdraft biomass gasifier: Effect of char reactivity factor. *Energy Conversion and Management*, 47:2602–2611, 2006.

[144] K. Jaojaruek and S. Kumar. Numerical simulation of the pyrolysis zone in a downdraft gasification process. *Bioresource Technology*, 100(23):6052–6058, 2009.

[145] Nicolas Piatkowski and Aldo Steinfeld. Reaction kinetics of the combined pyrolysis and steam-gasification of carbonaceous waste materials. *Fuel*, 89(5):1133–1140, 2010.

[146] N. Gao and A. Li. Modeling and simulation of combined pyrolysis and reduction zone for a downdraft biomass gasifier. *Energy Conversion and Management*, 49(12):3483–3490, 2008.

[147] A. Kr. Sharma. Modeling fluid and heat transport in the reactive, porous bed of downdraft (biomass) gasifier. *International Journal of Heat and Fluid Flow*, 28(6):1518–1530, 2007.

[148] S. Murgia, M. Vascellari, and G. Cau. Comprehensive cfd model of an air-blown coal-fired updraft gasifier. *Fuel*, 101:129–138, 2012.

[149] Alireza Abbasi, Paul E. Ege, and Hugo I. de Lasa. Cpfd simulation of a fast fluidized bed steam coal gasifier feeding section. *Chemical Engineering Journal*, 174(1):341–350, 2011.

[150] I. Petersen and J. Werther. Three-dimensional modeling of a circulating fluidized bed gasifier for sewage sludge. *Chemical Engineering Science*, 60(16):4469–4484, 2005.

[151] Carlos R. Altafini, Paulo R. Wander, and Ronaldo M. Barreto. Prediction of the working parameters of a wood waste gasifier through an equilibrium model. *Energy Conversion and Management*, 44:2763–2777, 2003.

[152] Jin-Shi Chen and Wesley W. Gunkel. Modeling and simulation of co-current moving bed gasification reactors -part i. a non-isothermal particle model. *Biomass*, 14:51–72, 1987.

[153] Jin-Shi Chen and Wesley W. Gunkel. Modeling and simulation of co-current moving bed gasification reactors – part ii. a detailed gasifier model. *Biomass*, 14:75–98, 1987.

[154] C. Di Blasi and C. Branca. Modeling a stratified downdraft wood gasifier with primary and secondary air entry. *Fuel*, 104:847–860, 2013.

[155] P. De Filippis, M. Scarsella, B. De Caprariis, and G. Belotti. Tecniche di campionamento e rimozione di tar e particolato contenuti nel syngas da gassificazione del carbone. Technical report, Enea, Università la Sapienza, 2010.

[156] Saran Sohi, Elisa Lopez-Capel, Evelyn Krull, and Roland Bol. Biochar, climate change and soil: A review to guide future research. Technical report, CSIRO Land and Water Science, 2009.

[157] Johannes Lehmann and Stephen Joseph. *Biochar for Environmental Management: science and technology*. Routledge, 2009.

[158] Guido Galeno. *MODELLIZZAZIONE DI UN MICRO COGENERATORE BASATO SULLA TECNOLOGIA MCFC ACCOPPIATA AD UN GASSIFICATORE DI BIOMASSA*. PhD thesis, University of Cassino, Italy, 2006-2007.

[159] A. Duvia and M. Gaia. Cogenerazione a biomassa mediante turbogeneratori orc turboden: tecnologia, efficienza, esperienze pratiche ed economia. *Congress: Cogenerazione a biomassa mediante Turbogeneratori ORC Turboden: tecnologia, efficienza, esperienze pratiche ed economia.*, 2004.

[160] F. Martelli, G. Riccio, S. Maltagliati, and D. Chiaramonti. Technical study and environmental impact of an external fired gas turbine power plant fed by solid fuel. *1st world Conference of Biomass, Sevilla*, 2000.

[161] V. Naso. *La macchina di Stirling.* CEA, 1991.

[162] S. Compaore. *MOTORI A COMBUSTIONE INTERNA E TURBINE A GAS DI PICCOLA TAGLIA PER GAS DI SINTESI.* PhD thesis, University of Padova, bachelor thesis, 2011-2012.

[163] A. Sarvi and R. Zevenhoven. Large-scale diesel engine emission control parameters. *Energy*, 35(2):1139–1145, 2010.

[164] A. Kr. Sharma. Modeling and simulation of global reduction reactions for downdraft (biomass) gasifier. *Energy Conversion and Management*, 52:1386–1396, 2011.

[165] Bernardo Hellrigl. Il potere calorifico del legno. *Congress: Le biomasse agricole e forestali nello scenario energetico nazionale, Progetto Fuoco*, 2004.

[166] S.A. Channiwala and P.P. Parikh. A unified correlation for estimating hhv of solid, liquid and gaseous fuels. *Fuel*, 81(8):1051–1063, May 2002.

[167] Y. A. Cengel. *Introduction to thermodynamics and heat transfer.* McGraw-Hill, 1997.

[168] L. Waldheim and T. Nilsson. Heating value of gases from biomass gasification. Technical report, IEA Bioenergy Agreement, Task 20 - Thermal Gasification of Biomass, 2001.

[169] Beedie D., P.J. Bowen, T. O'Dohery, and N. Syred. Cyclic variations and control of a batch biomass gasifier-combustor. *Combustion Science and Technology*, 1(113):529–556, 1996.

[170] H V Sridhar, G Sridhar, S Dasappa, N K S Rajan, and P J Paul. Experience of using various biomass briquettes in ibg (iisc bioresidue gasifier). Technical report, Advanced Bio-residue Energy Technologies Society Combustion Gasification and Propulsion Laboratory Department of Aerospace Engineering, Indian Institute of Science, Bangalore, India, -.

[171] S. Dasappa, H. V. Sridhar, G. Sridhar, and P. J. Paul. Science and technology aspects of bio-residue gasification. *Biomass Conversion and Biorefinery*, 1(3):121–131, September 2011.

[172] E.R. Huff. Effect of size, shape, density, moisture and furnace wall temperature on burning time of wood pieces. *Fundamentals of thermo-chemical biomass conversion: An international conference, Estes Park, CO*, 1982.

[173] K. J. Laidler. *Chemical kinetics.* Harper sRow Publishers, New York, 1987.

[174] R. C. Everson, H. V. J. P. Neomagus, H. Kasaini, and D. Njapha. Reaction kinetics of pulverized coal-chars derived from inertinite-rich coal discards: Gasification with carbon dioxide and steam. *Fuel*, 85:1076–82., 2006.

[175] Vytenis Babrauskas. Ignition of wood: A review of the state of the art. In *Interflam*. Interscience Communications Ltd., London, 2001.

[176] Mark J. Prins, Krzysztof J. Ptasinski, and Frans J.J.G. Janssen. Torrefaction of wood: Part 1. weight loss kinetics. *Journal of Analytical and Applied Pyrolysis*, 77(1):28–34, 2006.

[177] Michele Battistoni. Dispense di macchine, 2008.

[178] J.P.A. Neeft, H.A.M. Knoef, U. Zielke, K. Sjöström, P. Hasler, P.A. Simell, M.A. Dorrington, L. Thomas, N. Abatzoglou, S. Deutch, C.Greil, G.J. Buffinga, C. Brage, and M. Suomalainen. Guideline for sampling and analysis of tar and particles in biomass producer gases. Technical report, European Commission (DGXII) Netherlands Agency for Energy and the Environment (NOVEM) Swiss Federal Office of Education and Science Danish Energy Agency (Energistyrelsen) US Department of Energy (DoE) National Resources Canada, 2002.

[179] Peter Ulbig and Detlev Hoburg. Determination of the calorific value of natural gas by different methods. *Thermochimica Acta*, 382(1-2), 2002.

[180] A.P.C. Faaij. Bio-energy in europe: changing technology choices. *Energy Policy*, 34(3):322–342, 2006.

[181] Walter Zegada-Lizarazu and Andrea Monti. Energy crops in rotation. a review. *Biomass and Bioenergy*, 35(12-25), 2011.

[182] A. Innocenti, M. Poli, and L. Dal Re. Coltivazione della colza: Esperienze nel ravennate. *Rivista Agricoltura*, (11):77–79, 2008.

[183] ISMEA. Commodity: Semi oleosi: Prezzi: Mercato internazionale. Technical report, Istituto di servizi per il mercato agricolo alimentare, 2013.

[184] ISTAT Istituto Nazionale di Statistica. Consultazione dati: Navigazione tra i dati: Coltivazioni: Seminativi: Coltivazioni industriali: Tav. c14/2012 – superficie (ettari) e produzione (quintali): arachide colza girasole. Technical report, http://agri.istat.it, feb 2013.

[185] Istruzione Agraria online. Atlante delle coltivazioni erbacee – piante industriali: Girasole – helianthus annuus l. Technical report, http://www.agraria.org/coltivazionierbacee/girasole.htm, feb 2013.

[186] ISMEA. Commodity: Semi oleosi: Prezzi: News mercati n. 32/2012 – settimana n.47. Technical report, ISMEA, feb 2013.

[187] R. Colombo and M. Poli. Lino da olio, le varietà e la tecnica culturale. *Rivista Agricoltura*, (5):33–35, 2000.

[188] Istruzione Agraria online. Atlante delle coltivazioni erbacee – piante industriali: Linolinum usitatissimum l. Technical report, Istruzione Agraria online, feb 2013.

[189] ECN. Database for biomass and waste; www.ecn.nl/phyllis.

[190] J. Van Gerpen, B. Shanks, R. Pruszko, D. Clements, and G. Knothe. Biodiesel production technology. Technical report, NREL, Colorado, 2004.

[191] G. A. Foulds N. Dave. Comparative assessment of catalytic partial oxidation and steam reforming for the production of methanol from natural gas. *Industrial and Engineering Chemistry Research*, 34:1037–1043, 1995.

[192] Unione Petrolifera Italiana; http://www.unionepetrolifera.it. Databook 2012 p. 103.

[193] www.sviluppoeconomico.gov.it Ministero dello Sviluppo Economico. D.m. 16/07/2012.

[194] Europe's Energy Portal. Electricity – industry (italy), http://www.energy.eu.

[195] Seeds press cost. model clb-500-em, http://www.croplandbiodiesel.com, feb 2013.

Ringraziamenti

Prima di concludere questa tesi vorrei cogliere l'occasione per ringraziare alcune persone,

Il primo doveroso ringraziamento va al professor Paolo Tartarini ed all'ing. Alberto Muscio. Loro mi hanno dato l'opportunitá di portare avanti il mio dottorato presso il loro gruppo di ricerca, hanno sempre ascoltato pazientemente le mi proposte, anche quanto queste erano poco 'ordinarie'. Mi hanno lasciato sbagliare e percorrere strade diverse e mi hanno saputo guidare grazie al loro esempio di straordinaria professionalitá.

Vorrei poi ringraziare i miei compagni e colleghi. Parto dai piú navigati: Antonio e Diego che sono stati dei veri senpai, si sono sempre confrontati con me insegnandomi il mestiere e rassicurandomi nei momenti di bonaccia o di sconforto. Grazie davvero. Poi un grazie a tutti i miei compagni di (dis)avventure: Simone, Luca, Fabio e Chiara. Spero di poter continuare a lavorare con voi per tanto tempo.

Infine vorrei ringraziare la mia famiglia, vecchia e nuova e quella non ancora formata. I nuovi arrivati cosí come chi se ne é giá andato. Grazie per il supporto la serenitá e l'esempio in tutti questi anni.